

Efficacy of Novel Antisense Oligonucleotides for the Treatment of Spinal Muscular Atrophy

By

Aleksander Touznik

A thesis submitted in partial fulfillment of the requirements for the degree of

Master of Science

Medical Sciences – Medical Genetics

University of Alberta

Abstract

Spinal muscular atrophy (SMA) is one of the most common autosomal recessive neuromuscular disorders affecting the motor neurons, which usually has an early onset resulting in a rapid progression of muscle weakness, leading to death at a young age. SMA is caused by a homozygous mutation of survival of motor neuron 1 (*SMN1*) gene, which is the primary producer of the survival of motor neuron (SMN) protein. An *SMN1* paralog, *SMN2*, is capable of producing approximately 10% functional full-length SMN protein. *SMN2* is a duplicate gene of *SMN1*, however due to a new C-to-T transition, a new silencer is created which promotes the exclusion of the seventh exon in the post-transcriptional mRNA. Antisense therapy technology uses synthetic RNA-like molecules to target splice silencer sites along the *SMN2* gene via Watson-Crick complementation. Once the antisense oligonucleotide (ASO) is bound, it represses the silencer function, resulting in an increase of exon 7 inclusion in the final splice form. Increased levels of full-length mRNA transcripts lead to a “knock-up” of functional SMN protein. We will evaluate several ASO-based strategies for splicing correction in SMA patient cell lines and investigate ASO efficacy in the phosphorodiamidate morpholino oligomer (PMO), and locked nucleic acid (LNA) chemistries. Novel ASOs identified in this study will potentially offer improvement for the treatment of SMA in the future.

Preface

This thesis is an original work by Aleksander Touznik. Permission was obtained to test PMO 9 sequence (patented) from the Singed group. Data in Chapter 4 was obtained with the help of Biology 499 student Nicole McRorie (University of Alberta).

Dedication

This thesis is dedicated to my mother and father, who have always been there supporting me throughout my academic career. None of this would have been possible without them.

Acknowledgements

I would like to first and foremost thank my supervisor, Dr. Toshifumi Yokota, and my committee members, Dr. Ted Allison and Dr. Rachel Wevrick, for their continuous wisdom, support and direction throughout my degree. Thanks to Dr. Michael Walter, Dr. Sarah Hughes, and Dr. Sherryl Taylor for their time and guidance.

Thank you to our postdoctoral fellows, Dr. Yusuke Echigoya for training me, and Dr. Kana Hosoki who will be taking over the SMA project after I graduate.

Thanks to our funding sources for making this work possible: Women and Children's Health Research Institute, Slipchuk SMA Research Fund, the Faculty of Medicine and Dentistry, and the Government of Alberta.

Thank you to all my friends and colleagues in the department who have been there to support me. Particular thanks to my lab mates Ashley Guncay and Joshua Lee who worked with me on a daily basis, and our technician Nhu Trieu.

Thank you to our summer students Bo Bao, Xinran Yu, Justin Elliot and Baily Nichols.

Thanks to our Biology 499 student Nicole McRorie for all her work on the LNA project.

A special thank you to my mother Nina, my father Mikhail, and my sister Jessica for their support and encouragement throughout both my undergraduate and my graduate studies.

Table of Contents

CHAPTER 1

Introduction.....	1
Clinical representation and epidemiology.....	2
Genetic cause of Spinal muscular atrophy.....	5
SMN protein function, interactions and complexes.....	6
Effect of reduced SMN levels on motor neurons.....	12
Introduction to antisense therapy.....	15
Antisense therapy in Spinal muscular atrophy.....	18
Moving towards a cure.....	22
Purpose of this study.....	26

CHAPTER 2

Materials and Methods	27
Antisense drug design.....	28
Cell stock and management.....	28
Cell counting and seeding.....	33
PMO preparation	35
LNA preparation.....	35
PMO transfection.....	35

LNA transfection	36
RNA collection.....	36
RNA purification.....	36
Protein collection.....	37
Reverse transcription polymerase chain reaction	39
Western blotting.....	40
Immunostaining.....	43
cDNA sequencing.....	43
Immunocytochemistry.....	44
Statistical analysis	44

CHAPTER 3

Efficacy of novel PMO based antisense oligonucleotides in SMA patient cell lines	46
3.1 Background	47
3.2 Results: PMO screening	48
Semi-quantitative RT-PCR PMO screens targeting various silencer sites along <i>SMN2</i> pre-mRNA.....	48
Cocktail and semi-complementary PMO screening using quantitative RT-PCR.	50
Screening for hybrid PMOs simultaneously targeting Element-1 and ISS-N1 using semi-quantitative RT-PCR.....	50

Protein expression analysis of PMO screens targeting various silencer sites along <i>SMN2</i> pre-mRNA.....	53
Analysis of PMOs targeting the ISS-N1 silencer site at reduced transfection concentrations.	53
cDNA sequencing of bands differentiated by electrophoresis.	57
3.3 Results: PMO efficacy in multiple SMA cell lines	57
Dose-dependent analysis of PMOs in patient fibroblasts (GM03813)	57
Dose-dependent analysis of PMOs in patient fibroblasts (GM09677)	59
Dose-dependent analysis of PMOs in patient fibroblasts (GM00232)	64
PMO 7 rescues nuclear gem phenotype in SMA patient fibroblasts	64
 CHAPTER 4	
Effect of novel splice-switching LNA based antisense oligonucleotides in SMA patient.....	69
4.1 Background	70
4.2 Results: Novel LNA based ASO screening.....	71
LNAs screening at multiple transfection concentrations.....	71

Screening for the optimal LNA using semi-quantitative RT-PCR	71
Western blot analysis reveals importance of transfection concentration in patient SMA fibroblasts.	72
Effect of LNAs of patient SMA fibroblasts nuclear gem phenotype	77

CHAPTER 5

Discussion	79
The application of antisense therapy in SMA	80
Initial PMO screening shows ISS-N1 is the most suitable target site for PMOs.	81
Hybrid and cocktail PMO screening	83
Identifying efficacy of SMN protein “knock-up” at varying transfection concentrations.....	84
PMO 7, 8 and 9 induce exon 7 inclusion and increased SMN production in multiple SMA patient cell lines	85
Evaluation of novel splice-switching LNA/DNA mixmers targeting ISS-N1.....	88
Restoring the nuclear gem phenotype in SMA fibroblasts	89
Conclusions and future directions	91
REFERENCES.....	94

List of Tables

Table 2-1: PMOs targeting various silencers designed for screening	29
Table 2-2: Cocktail and semi-complementary PMOs.....	30
Table 2-3: Hybrid PMO design.....	31
Table 2-4: Phosphorothioated LNA/DNA mixmers	32
Table 2-5: Cell line characteristics	34
Table 2-6: Primers for RT-PCR and Sequencing.....	42

List of Figures

Figure 1-1: Summary of Spinal muscular atrophy phenotype	4
Figure 1-2: <i>SMN1</i> and <i>SMN2</i> genes, and the subsequent protein production in healthy and affected individuals	7
Figure 1-3: SMN complex interactions and functions.....	11
Figure 1-4: Role of the SMN protein complex in motor neurons	13
Figure 1-5: Mechanism of antisense therapy in Spinal muscular atrophy	21
Figure 1-6: Molecular structure of the PMO and LNA antisense oligonucleotides	25
Figure 2-1: Timeline for PMO and LNA transfections	38
Figure 2-2: Primer design for <i>SMN2</i> detection	41
Figure 3-1: Effect of novel PMO screening along <i>SMN2</i> pre-mRNA indicates PMO 7, 8, and 9 may be effective candidates for restoring protein levels in SMA patient cells	49

Figure 3-2: Effect of cocktail and semi-complementary PMOs in SMA patient fibroblasts.....51

Figure 3-3: Effect of hybrid PMOs simultaneously targeting Element-1 and ISS-N1 splice silencers in SMA patient fibroblasts..... 52

Figure 3-4: Protein “knock-up” screening using PMOs targeting various Targets on *SMN2* pre-mRNA54

Figure 3-5: PMOs targeting the intronic repressor ISS-N1 with reduced transfection concentrations 56

Figure 3-6: cDNA sequence analysis of *SMN2*.....58

Figure 3-7: Dose-dependent analysis showing exon 7 inclusion efficacy of ISS-N1 targeting PMOs in the GM03813 SMA patient fibroblasts.....60

Figure 3-8: Dose-dependent analysis testing the ability of PMOs targeting ISS-N1 to promote SMN protein production in GM03813 SMA patient fibroblasts..... 61

Figure 3-9: Dose-dependent analysis showing exon 7 inclusion efficacy of ISS-N1 targeting PMOs in the GM09677 SMA patient fibroblasts.....62

Figure 3-10: Dose-dependent analysis testing the ability of PMOs targeting ISS-N1 to promote SMN protein production in GM09677 SMA patient fibroblasts..... 63

Figure 3-11: Dose-dependent analysis showing exon 7 inclusion efficacy of ISS-N1 targeting PMOs in the GM00232 SMA patient fibroblasts.....	65
Figure 3-12: Dose-dependent analysis testing the ability of PMOs targeting ISS-N1 to promote SMN protein production in GM00232 SMA patient fibroblasts.....	66
Figure 3-13: Antisense therapy using PMO chemistry recovers nuclear gem phenotype in SMA patient cell lines.....	68
Figure 4-1: Novel LNAs screened across multiple concentration levels.....	73
Figure 4-2: Efficacy of novel LNA antisense oligonucleotides to induce exon 7 inclusion in SMA patient cells.....	74
Figure 4-3: Efficacy of novel LNA antisense oligonucleotides to promote full-length SMN protein production in SMA patient cells.....	75
Figure 4-4: 25 nM transfections reduce efficacy of LNAs to produce SMN protein production in SMA patient cells.....	76
Figure 4-5: LNAs 1, 3 and 5 fail to restore nuclear gem phenotype in patient SMA fibroblasts.....	78

List of Abbreviations

2'MOE – 2'-methoxyethoxy

2'O-MePS – 2'O-methylphosphorothioate

AAV – Adeno-associated virus

ANOVA – Analysis of variance

ASO – Antisense oligonucleotide

ASO – Antisense oligonucleotide

ATP – Adenosine triphosphate

BBB – Blood brain barrier

BCL-2 - B-cell lymphoma 2

BMD – Becker muscular dystrophy

cDNA – Complementary DNA

CLNS1A – Chloride channel, nucleotide sensitive, 1A

CNS – Central nervous system

DAPI – 4',6-Diamidino-2-Phenylindole, Dihydrochloride

DMD – Duchenne muscular dystrophy

DNA – Deoxyribonucleic acid

EDTA - Ethylenediaminetetraacetic acid

ESE – Exonic splice enhancer

ESS – Exonic splice silencer

FBS – Fetal bovine serum

HEPES – 4-(2-hydroxyethyl)-1-piperazineethanesulfonic acid

ICC – Immunocytochemistry

ICV – intracerebroventricular

ISS – Intronic splice silencer
ISS-N1 – Intronic splice silencer N1
IV – Intravenous
LNA – Locked nucleic acid
LSm – Sm-like
m₃G – 2,2,7-trimethyl guanosine cap
m⁷G – 7-monomethyl guanosine cap
mRBP – mRNA binding proteins
mRNA – Messenger ribonucleic acid
mRNP – axonal mRNA
PBS – Phosphate buffered saline
PBSTr – Phosphate buffered saline (Triton-X)
PBSTw – Phosphate buffered saline (Tween 20)
PMO – Phosphorodiamidate morpholino oligomer
PVDF – Polyvinylidene difluoride
RBP – RNA binding protein
RG-rich – Arginine-Glycine rich
RNA – Ribonucleic acid
RNP – Ribonucleoprotein
rRNA – Ribosomal RNA
SC – Subcutaneous
Sm – snRNP component proteins
SMA – Spinal muscular atrophy
SMN – Survival of motor neuron (human)
Smn – Survival of motor neuron (mouse)
SMN1 – Survival of motor neuron 1

SMN2 – Survival of motor neuron 2

snoRNA – Small nucleolar RNA

snRNA – Small nuclear ribonucleic acid

snRNP – Small nuclear ribonuclear protein

SSO – Splice-switching oligonucleotide

CHAPTER 1

Introduction

Clinical representation and epidemiology

Spinal muscular atrophy (SMA) is a recessive autosomal neuromuscular disorder characterized by degradation of motor neurons within the anterior horn of the spinal cord and brain stem, resulting in progressive trunk and limb muscle paralysis (Cali *et al.* 2014; Moosa *et al.* 1973). SMA is currently the most common cause of infant mortality, estimated to affect somewhere between 1 in 6000 to 1 in 11000 live births. Patients show variation in the age of onset and disease progression based on described clinical types, with the most severe form (SMA type I) accounting for approximately 60% of all cases. Life expectancy in milder SMA (types II and III) is only slightly increased, and patients are still not expected to survive to reach teenage years (Darras *et al.* 2015).

SMA is a result of a homozygous, loss of function mutation of the survival of motor neuron 1 (*SMN1*) gene. The survival of motor neuron 2 (*SMN2*) duplicate gene is capable of producing functional transcripts of the *SMN1* protein product (although not nearly as efficiently), which makes the gene a major modifier of the SMA phenotype. With a higher copy number of *SMN2*, less severe clinical presentations are expected (Osman *et al.* 2014; Brkusanin *et al.* 2015). Type I SMA (Werdnig-Hoffmann disease), the acute infantile form of the disease, is the most common and most severe. Infants usually manifest symptoms between birth to six months of age, are never able to sit up without aid, and have difficulty swallowing amongst other complications. SMA was originally described as a motor neuron disorder, but it is now known that the *SMN1* gene is ubiquitously expressed, and any deficiency in expression can have aberrant effects in various organs, vasculature, cardiac, and sensory systems. This knowledge is driving researchers to study treatments by focusing on systemic approaches (Darras *et al.* 2015;

Gray *et al.* 2013; Menke *et al.* 2008). Type II SMA (Dubowitz disease) is the intermediate, chronic infantile, form of the disease. Age of onset ranges from 6 to 18 months, where patients begin to present proximal weakness in the extremities, which later progresses to central muscles such as the intercostal muscles, resulting in severe respiratory problems with age. No cognitive dysfunction has been observed. In fact, patients usually present above average verbal intelligence (Zerres *et al.* 1995; Wirth *et al.* 2006; von Gontard *et al.* 2002).

Type III (Kugelberg-Welander disease) is the chronic juvenile form of SMA, with symptoms usually manifesting between 18 months to 3 years. Progressive weakness of arms and legs usually begins after the child is ambulatory. Patients are usually wheelchair bound at a young age, however development of respiratory problems is rare. Life expectancy of these patients is variable, ranging from normal to death before age twelve (Wang *et al.* 2013; Darras *et al.* 2014; Zerres *et al.* 1997). Type IV SMA is the adult onset form, with symptoms not showing up until adulthood. Patients generally show minor symptoms, most able to walk unaided in later years with only mild signs of muscle weakness. SMA type is determined based on clinical milestones, however patients with milder phenotypes are expected with more copies of *SMN2*. Severity based on the genetic level alone is not fully understood, as some patients with as many as 3 *SMN2* copies can still have SMA type I symptoms (Russman *et al.* 2007; Harada *et al.* 2002).

It has been estimated that 1 in 38 to 1 in 70 people worldwide are carriers of *SMN1* mutations that lead to non-functional protein products. Based on these predictions, the

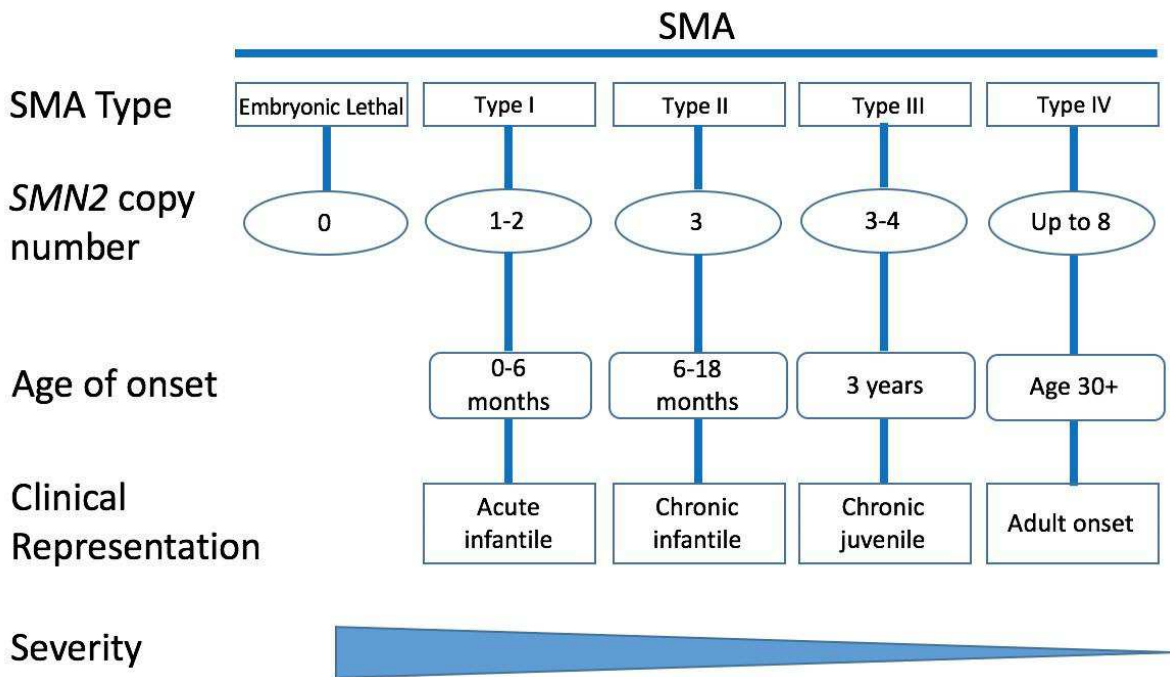


Figure 1-1: Summary of Spinal muscular atrophy phenotype

SMA phenotype has a wide spectrum, and may vary greatly between patients. SMA type is assigned based on clinical representation and motor milestones, and does not directly correlate with how many *SMN2* copies are present.

incidence of SMA manifestation is lower than one would expect, despite such a high carrier frequency. There is a hypothesis that the rate of incidence may be a result of some fetuses having a genotype where no functional copies of either the *SMN1* or *SMN2* gene (leading to no functional full-length protein product being present), which is known to be embryonic lethal in other species such as mice (Darras *et al* 2015; Prior *et al.* 2010).

Genetic cause of Spinal muscular atrophy

SMA is the result of reduced levels of the survival of motor neuron (SMN) protein, particularly in the motor neurons, rather than a complete loss. SMN protein can be produced by two ubiquitously expressed *SMN1* (telomeric) and *SMN2* (centromeric) genes, both located on chromosome 5 (5q13). The *SMN1* gene is the primary producer of SMN protein, and one copy is sufficient for maintaining a healthy phenotype. A homozygous mutation in the *SMN1* gene is required for the onset of SMA. (Fischer *et al.* 1997). Approximately 94% of SMA is due to a deletion of the *SMN1* gene (or exons within the gene). The with the remaining cases are *de novo* mutations or compound heterozygotes with a single deleted copy of the *SMN1* gene and a point mutation in the other (Carré *et al.* 2015; Ganji *et al.* 2015). The *SMN2* gene is an inverted duplication of a 500 Kb inverted repeat containing a nearly identical sequence to the *SMN1* gene with only a five base pair difference. Amongst those changes lies a C-to-T transition on intron 7 that converts a splicing enhancer into an intronic silencer site, which results in the spliceosomal machinery excluding the 7th exon in *SMN2* post-transcriptional mRNA. Most of these aberrantly spliced *SMN2* transcripts lead to an unstable protein which is degraded rapidly, as the absence of the 7th exon disrupts SMN protein oligomerization. Approximately

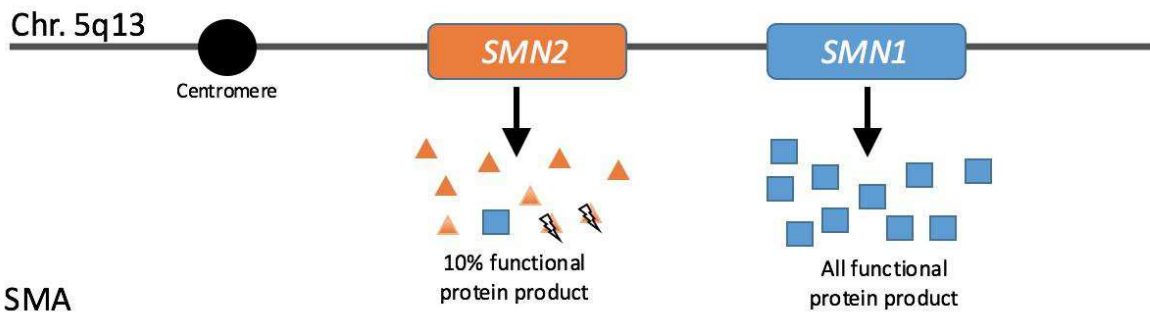
10% of transcripts are able to escape the silencing effect and include exon 7 in during spliceosomal processing, allowing the *SMN2* gene to produce a functional, full-length SMN protein product (identical to that of *SMN1*) (Rochette *et al.* 2001; Touznik *et al.* 2014).

SMN protein function, interactions and complexes

SMN is a 38 kDa protein, composed of 294 amino acids. While expressed in all cell types in vertebrates, the quantity of SMN expression varies between tissue types, with greater amounts seen in highly innervated areas such as the brain, liver and kidney, along with skeletal and smooth muscles to a smaller extent. SMN protein is primarily localized in the cytoplasm, but can also be found in the nucleus as part of a nuclear gem complex, also referred to as Gemini of coiled bodies (Liu *et al.* 1996; Gubitz *et al.* 2002). Though the exact function of SMN still unknown, extensive ongoing research shows evidence that SMN works as part of a complex with functions ranging from small nuclear ribonuclear protein (snRNP) assembly to ribosome production (Terns *et al.* 2001; Paushkin *et al.* 2002). No biochemical evidence has shown SMN function independently of other interacting molecules. SMN is known to be an essential part of the part of the SMN complex, where it associates with eight other proteins known as gemins (2-8), and the Unr-binding protein Unrip. When bound together, they form discrete nuclear bodies called gems, which can be seen in the cytoplasm, and in the nucleus of healthy, non-SMA cells (Charroux *et al.* 1999; Baccon *et al.* 2002; Kolb *et al.* 2007).

The best defined role on the SMN complex is in its interactions with Sm, LSm (Sm-like) proteins and small nuclear ribonucleic acids (snRNA), where it plays a catalytic role in assembling the snRNPs which are the building blocks of spliceosomes (Fischer *et al.* 1997). Sm

A) Healthy



B) SMA

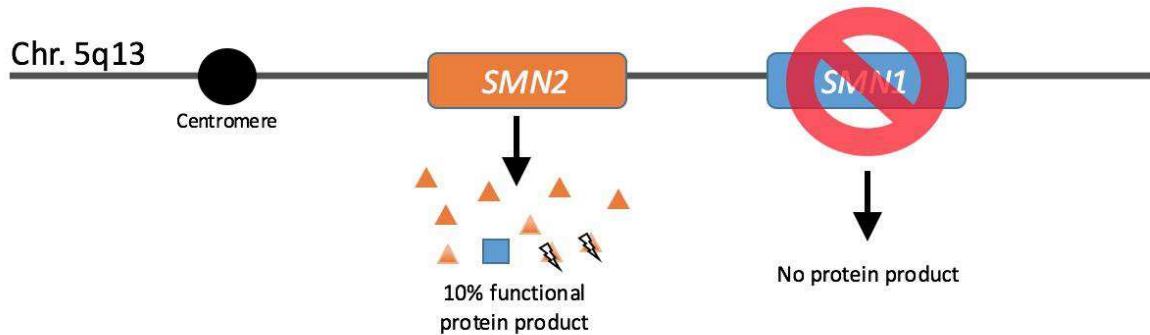


Figure 1-2: *SMN1* and *SMN2* genes, and the subsequent protein production in healthy and affected individuals

A) Representative gene function in a healthy individual. If at least 1 copy of *SMN1* is present that person will not be afflicted with SMA. B) Individuals with SMA do not a functional *SMN1* copy either through inheritance or mutation. *SMN2* is only capable of producing ~10% functional full-length protein (blue square), which is insufficient to sustain a healthy phenotype. Non-functional SMN protein (orange triangle) gets degraded rapidly in the cytoplasm.

proteins are essential to spliceosomal development (SNRPB/B', SNRPD1, D2 and D3, SNRPE, F, and G). They are made in the cytosol, and are protected by the chaperone protein CLNS1A (chloride channel, nucleotide-sensitive, 1A) where they remain inactive as part of a 6S pCLn-Sm complex (Meister *et al.* 2001). SMN complexes in the cytoplasm are able to recognize the dormant complex containing Sm proteins and force them to dissociate from the chaperones. The Sm proteins then become attached to the SMN complex until all components for snRNP assembly are gathered. The SMN complex takes on the role of a chaperone, protecting them from binding with non-RNP nucleic constructs, as Sm proteins lack intrinsic specificity to RNA-based substrates. This proofreading type role of the SMN complex is highly conserved in evolution (Raker *et al.* 1999; Kroiss *et al.* 2008; Li *et al.* 2014).

Another essential component of the snRNP is the U class of snRNAs (U1, U2, U4/6, and U5). These snRNAs ultimately become the one of the primary functional units in the catalytic center on the spliceosome during post-transcriptional modification of messenger ribonucleic acids (mRNA) (Buhler *et al.* 1999). U snRNAs are transcribed by RNA polymerase II, fold into a hairpin structure, and are finished off with a 5'-terminal 7-monomethyl guanosine cap (m⁷G). This final modification allows for bidirectional transport of the U snRNAs across the nuclear envelope which is necessary for localization of assembled snRNPs in the nucleus (Etzerodt *et al.* 1988). A uridine-rich motif sequence 5'-AUUUUUG-3' is located along the snRNA near the hairpin loop. This sequence is recognized by the SMN-Sm complex assembly, and through a catalytic process, the Sm proteins form a ring around the uridine motif. Once the new complex is formed, the 7-monomethyl guanosine cap is altered, changing into a 2,2,7-trimethyl guanosine cap (m₃G), signaling for the complex to be transported into the nucleus (Hamm *et al.*

1990; Fischer *et al.* 1997; Kolb *et al.* 2007). Once in the nucleus, these constructs may bind with several other ribonucleoprotein-specific proteins to form functional spliceosomal components capable of catalyzing the post-transcriptional modification reaction of mRNA (Mattaj *et al.* 1993; Will *et al.* 2001).

SMN complex function is strongly tied to its interactions with specific target proteins, particularly ones with arginine and glycine (RG)-rich domains such as Sm and LSm proteins that allow for snRNP complex assembly and ultimately pre-mRNA splicing (Selenko *et al.* 2001). The RG-rich regions are identified by the SMN complex through its tudor domain. Similar to the mRNA processing, the SMN complex plays a major role in processing ribosomal RNA (rRNA). Small nucleolar RNA (snoRNA) are a large family of transacting small RNA molecules, which have a role in ribosome biogenesis in the nucleus by acting as a guide for protein localization, as well as assist in modification and cleavage of rRNAs (Weinstein *et al.* 1999). GAR1 and fibrillarin are two target proteins for the SMN complex in the nucleus associated with snoRNA regulation. GAR1 ribonucleoprotein is a core protein component of the Box C/D snoRNA which have a role in methylation, and fibrillarin is a core component of the Box H/ACA snoRNA, which functions to pseudouridylate critical regions in rRNA modification. SMN complex association with the RG-rich regions of GAR1 and fibrillarin leads to activation of snoRNA, which play a role in pre-rRNA processing and ribosome production (Samarsky *et al.* 1998; Liang *et al.* 2001).

Regulation of transcription by the SMN complex is defined to a lesser extent, but there is evidence based on its interaction with helicase A. Helicase A is a DEATH-box RNA helicase which contains an RG-rich domain that is recognized and bound to by the SMN complex. SMN is thought to interact directly with the adenosine triphosphate (ATP) dependent RNA helicase A,

which can then form a transcriptosome complex with polymerase II and regulate transcription. In an *in vivo* study, a dominant negative SMN mutant resulted in transcriptional inhibition of polymerase I, II and III, which indicates SMN may have a larger role in transcriptional maintenance through its role in assembly of these three main transcription units (Pellizzoni *et al.* 2001; Terns *et al.* 2001).

Although first described in 1903 by Santiago Cajal, little progress has been made as to what exactly the function of Cajal bodies are (Lafarga *et al.* 2009). These small spherical sub-organelles found in the nucleus of proliferative cells remained a mystery until several processes that seemed to be regulated by these units were linked to SMN. Cajal bodies are held together by its primary scaffold protein coilin. Coilin contains an RG-rich domain which recruits SMN protein to the Cajal bodies, which can be visualized as nuclear gems. Current studies indicate that perhaps the most important role of these nuclear sub-organelles is transcription regulation, and with knowledge that SMN is an important component of the system, we may soon know the answer to the century of question (Gall *et al.* 1999; Ogg *et al.* 2002; Jády *et al.* 2006).

Since its discovery, the main focus of SMA research has been looking at the classical function of SMN in snRNP assembly, and other interactions of the SMN complex through the tudor domain (Fallini *et al.* 2012). A newer branch of SMA research focuses on SMN function within the axon of the motor neurons, where it acts as a chaperone and guide for mRNA through interactions with mRNA binding proteins (mRBPs). As a result of that function, several labs were able to show that reduction in SMN leads to defects in the cytoplasmic fate of some

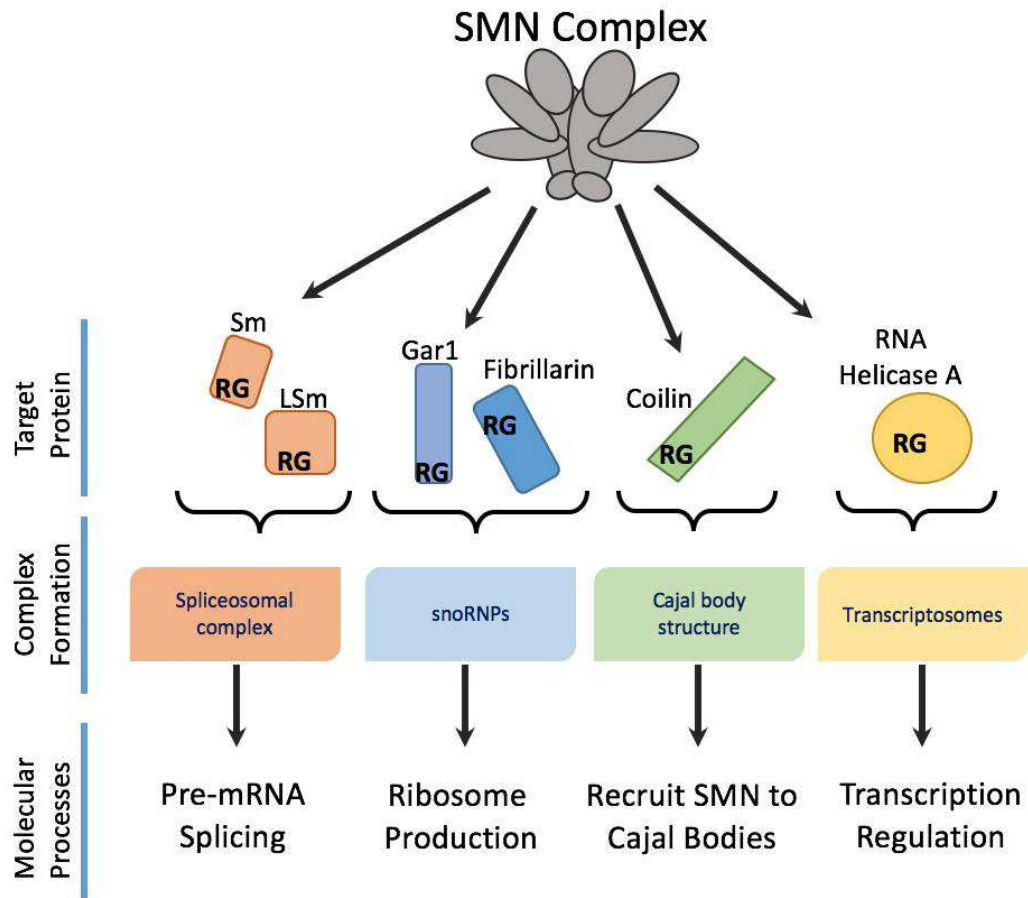


Figure 1-3: SMN complex interactions and functions

SMN protein interacts with many other proteins to form the SMN complex, which has roles both outside and inside the nucleus. The SMN complex targets proteins with an arginine-glycine (RG)-rich motif via its tudor domain. Depending on the substrate bound, the SMN complex plays various roles ranging from pre-mRNA splicing to ribosome production.

axonal mRNAs (mRNPs) in motor neurons (Akten *et al.* 2011; Hubers *et al.* 2011). SMA patients have lower levels of mRBPs, which play a significant role in mRNA transport along the motor neuron axon. The role of SMN in developing the mRBP complex formation may be similar to its role in snRNP assembly, which leads to the speculation that that SMN is a necessity for transport, and even local translation of mRNPs (Rossoll *et al.* 2009; Fallini *et al.* 2011). As motor neurons are some of the longest cells, there is demand for a dedicated mRNA transport system for mRNPs which need to be translated in the distal part of the axon. Localization of mRNPs and local protein synthesis are two key processes required for proper synaptic development and function (Wang *et al.* 2010; Swanger *et al.* 2011). The structure of the motor neurons alone hints as to why SMA is characterized as a neurodegenerative disorder.

Effect of reduced SMN levels on motor neurons

Recent publications have been describing SMA as a systemic disease rather than one specific to motor neuron degeneration. Researchers testing new drugs in SMA animal models have also begun systemic administration. Classic *in vivo* trials usually involved intracerebroventricular (ICV) injections, which administer the treatment directly into the central nervous system (CNS). Recent pre-clinical studies have shown that injections into the CNS, combined simultaneous systemic administration using intravenous (IV) or subcutaneous (SC) techniques, resulted in longer life spans and recovery of healthy phenotype in murine models (Hua *et al.* 2011; Nizzardo *et al.* 2014). Nonetheless, it is clear that motor neuron degeneration is a critical result of low SMN levels. The basis for cell selectivity in SMA is not entirely understood.

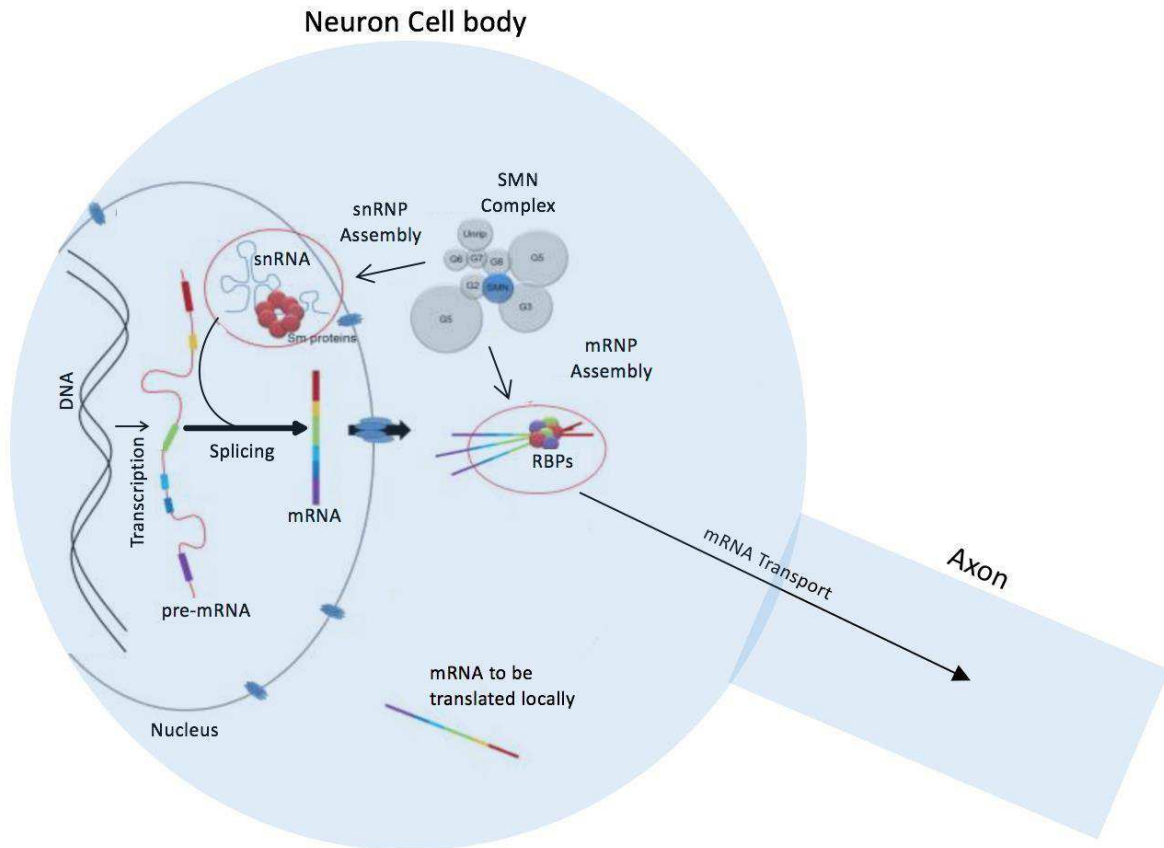


Figure 1-4: Role of the SMN protein complex in motor neurons

Motor neurons are the most critically affected cells when SMN levels are low. Along with the general functions of the SMN complex in the motor neurons, there is new evidence the SMN complex also functions in RBP assembly and transport of mRNA across the axon. As some mRNAs need to be translated at the dendrites, this process is getting a lot of focus in current research. Figure adapted from Fallini *et al.* 2012.

Pathogenesis of SMA is described by motor neuron specific cell degeneration when there is a relative reduction of SMN protein quantity throughout the body. As SMN appears to be mandatory for cell viability, regardless of cell type, one would expect a more severe phenotypic outcome (Kolb *et al.* 2007). It is interesting to investigate why a reduction in SMN has such a detrimental effect on motor neurons. Two hypotheses have been proposed as to why this is the case, each with its line of reasoning. The first hypothesis proposes that “the loss of SMN’s well-known function in snRNP assembly causes an alteration in the splicing of a specific gene or genes [specific to the motor neurons].” The second hypothesis claims that “SMN is critical for the transport of mRNA in neurons, and the disruption of [mRNA transport along the axon] results in SMA.” (Burghes *et al.* 2009).

The first hypothesis takes into account the role that the SMN complex plays in pre-mRNA splicing. Reduced SMN concentrations cause alterations in snRNP assembly. Without proper formation of the snRNP (as a result of lower SMN concentration), or even reduced amounts of snRNP, certain transcripts in the cell may not be spliced correctly or may not be spliced at all (Wan *et al.* 2005; Zhang *et al.* 2008). Aberrant splicing of motor neuron-specific genes may lead to neurodegeneration of motor neurons (Shpargel *et al.* 2005). Another cause may be through transcript down-regulation of motor neuron-specific proteins, as reduced amounts of SMN may decrease RNA helicase A and polymerase II interaction causing the transcriptional machinery to ignore essential promoter sites.

The second hypothesis suggests that SMN’s role in mRNP translocation is critical to the development and integrity of motor neurons. As previously described, null SMN genotypes are embryonic lethal. With at least one *SMN2* copy, live births with fully functional motor neurons

are possible, although this phenomenon is short lived as the onset of motor neuron degeneration soon occurs. The function of SMN in axons is disrupted when there are insufficient levels of the protein. A similar effect may not be observed in other cell types because they are either smaller or spherical by nature, so diffusion of mRNA in the cytoplasm may be sufficient for proper distribution. Without proper mRNA localization, the integrity of the motor neurons in early life is jeopardized, and neurodegeneration is the consequence (Fan *et al.* 2002; Rossoll *et al.* 2003; McWhorter *et al.* 2003).

Even though both hypotheses focus on different molecular mechanisms, nothing indicates that they cannot be linked. In one case, aberrant splicing of genes critical to the axon may be a result of reduced snRNP assembly. On the other hand, abnormal SMN function in the cytoplasm of neurons may interfere with snRNP assembly. Though the evidence for both exists, there is no definitive proof that either (or both) of the hypotheses are responsible for the disease onset (Burghes *et al.* 2009). One thing is for certain, that regardless of the mechanism or role of SMN, there is a direct link between SMN levels and the SMA phenotype. Thus, many treatments are focused on upregulation of SMN protein production.

Introduction to antisense therapy

Antisense oligonucleotides (ASOs) are short (usually 8-30 bp) single-stranded RNA-like analogs that target complementary mRNA via Watson-Crick base pairing in a sequence specific manner. ASOs act at their target location, and depending on their chemistry and area of hybridization, will have a different result on the target transcript. Knockdown of target mRNA is one of the most common uses of ASOs, which is usually achieved via RNase H endonuclease

activity which can cleave many RNA/ASO heteroduplexes (Crooke *et al.* 2004.; Wu *et al.* 2004). Another way ASOs can affect expression is through interference of mRNA maturation during post-transcriptional modification. This can be done by destabilizing mRNA in the nucleus, promoting different splicing patterns or complete splicing inhibition. ASOs may also prevent translation of already processed mRNA by binding to the transcript in the cytoplasm, causing steric hindrance which results in the translational arrest of ribosomal activity (Kurreck *et al.* 2003).

Historically, designing a good ASO has been challenging, as the original optimization techniques such as mRNA walking and RNase H mapping were both labor intensive and very expensive. Today there are several publically available programs, such as TargetFinder, that are able to develop and predict the binding efficacy of ASOs using computational algorithms. These algorithms take into account three main parameters when predicting the effectiveness of the ASO: 1) secondary RNA structure, 2) GC content and 3) binding energies (Bo *et al.* 2004; Chan *et al.* 2006). Sequence alone is not sufficient to produce effective antisense function in a biological setting, as the ASOs can be susceptible to nuclease degradation, and may have difficulty crossing biological barriers such as the blood-brain barrier (BBB), as well as cellular and nuclear membranes.

Over time, chemical alterations to ASOs have been developed to not only be immune to nuclease breakdown, but also increase affinity to its targets while reducing off-target effects, and improving construct stability *in vivo*. One of the first and most notable chemical alterations is phosphorothioation of the ASO sequence backbone, where a sulfur atom replaces the negatively charged oxygen atom in the phosphodiester bond that links the two nucleotides.

This modification leads to more bioavailability of the ASO, as it establishes higher resistance to nuclease degradation (Eckstein *et al.* 2000; Crooke *et al.* 2000). Other modification such as addition of alkyl groups to the 2'-Carbon in the ribose ring, or changing the structure of the sugar ring completely further contribute to the efficacy of modified ASOs, but not without a cost as they incur higher levels of toxicity when tested *in vivo* (Altmann *et al.* 1996; Yu *et al.* 2004).

There are some notable clinical trials that have taken place using ASOs. Genta Inc. is testing a new phosphorothioated 18-mer ASO (18 nucleotides long) that may increase the success of chemotherapy for cancer patients. Their ASO targets the gene B-cell lymphoma 2 (*BCL-2*), which is overexpressed in several types of cancer. Overexpression of *BCL-2* aids tumors in resisting chemotherapy treatments, as it contributes to halting apoptotic processes. Using antisense therapy Genta is hoping to knock down *BCL-2* product, and in turn increasing the effectiveness of cytotoxic agents during chemotherapy in cancers where *BCL-2* is overexpressed such as lymphocytic leukemia and multiple myeloma (Badros *et al.* 2005).

New applications of antisense therapy are being investigated in Duchenne muscular dystrophy (DMD) studies. Sarepta Therapeutics is currently holding phase III clinical trials for their antisense drug eteplirsen. In many cases in DMD, patients show a severe phenotype due to premature stop codon found within a mutation hotspot in the *dystrophin* gene, which results in a truncated protein product. Many times these premature stop codons arise due to out of frame mutations. Eteplirsen targets exon 51 on the *dystrophin* gene pre-mRNA, inducing a mechanism known as exon skipping. By skipping exon 51, the mRNA is put back in frame, and the premature stop codon is eliminated. This alteration allows for a shorter, yet functional

dystrophin protein to be made, alleviating the severe DMD phenotype allowing the patient to live with the much less severe Becker muscular dystrophy (BMD) (Lee *et al.* 2013; Mendell *et al.* 2016).

Antisense therapy in Spinal muscular atrophy

Several experimental therapies have been developed for treating SMA. Self-complementary adeno-associated virus (AAV) therapies have been used to correct for the SMA phenotype in mice. This method is used to transduce long-term expression of specific transgenes *in vivo*, by having the viral genome incorporate in a site-specific manner (Deyle *et al.* 2009). In mice, successful integration of the human *SMN1* gene was achieved by injecting the AAV both systemically (IV) and locally (ICV), both improving motor function and longevity of the mice. Though a promising approach, challenges such as tissues remaining refractory to transduction, and immune-related complications remain major hurdles in viral therapy (Passini *et al.* 2010; Dominguez *et al.* 2011). Small drug therapies have also been conducted targeting the cell's natural methylation mechanisms to promote more protein product from the *SMN2* gene. Drugs such as trichostatin A were shown to increase SMN expression levels in mice which lead to longer life spans (Avila *et al.* 2007). LB598, a histone deacetylase, tested in SMA patient cell lines was able to increase SMN protein production ten times (Garbes *et al.* 2009). At the protein level, one group had success stabilizing present SMN protein in an SMA mouse model using aminoglycosides (antibacterial therapeutic agents), which resulted in a less severe phenotype (Mattis *et al.* 2006). In a more recent study by Naryshkin *et al.*, an ambitious attempt was made to develop an oral drug targeting polymerases to increase SMN levels both

in patient cells, and in mice (Naryshkin *et al.* 2014). Although each report showed promising results, a major concern that was not accounted for in each study was the systemic off-target effect of the treatments. The mechanisms of each drug may have been able to increase in functional SMN, but aberrant side effects of the drugs remain uninvestigated.

Perhaps one of the most promising methods to treat SMA is antisense therapy. Using splice switching antisense oligonucleotides (SSOs), many publications have shown promising results in increasing SMN protein concentrations by targeting the *SMN2* gene (Porensky *et al.* 2012). SMA provides medical genetics research with a unique case where the gene (or lack of) is responsible for the disease phenotype, but treatment is not focused around it. The *SMN2* gene is unique to *Homo sapiens*, and provides us with a promising therapeutic target to develop a cure for SMA (Rochette *et al.* 2001). Antisense therapy for SMA uses a “knock-up” approach, where splice-switching ASOs target silencing motifs along the *SMN2* pre-mRNA to overcome the C-to-T transition mutation that introduced a new exonic splice silencer (ESS). Using systematic tiling (wide ASO screen followed by an antisense microwalk), three prominent silencers were discovered (Hua *et al.* 2007; Singh *et al.* 2010).

Element-1 is a 45 bp long intronic splice silencer (ISS) on intron 6 of *SMN2* pre-mRNA. It is located 67 base pairs upstream of exon 7. This cis-regulatory element was discovered in 2002 by the Imaizumi group using 2'-O-methyl ASOs with phosphorothioated backbone (2'O-MePS) modifications, where they showed increased SMN levels *in vitro* when targeting this region (Miyajima *et al.* 2002; Baughan *et al.* 2009). Osman *et al.* have shown that flanking the repressor region results in increased SMN protein and motor function in SMA mice (Osman *et*

al. 2014). Having a cell and an animal model to back up the role of Element-1 as an intronic splice silencer, there is potential that it may be a suitable therapeutic target to treat SMA.

A logical location to examine is the site of the mutation that causes the abnormal splicing pattern in *SMN2*. In 2003 Kashima *et al.* showed that the region of the C-to-T transition is in fact a novel exonic splice silencer (ESS), whereas it was previously accepted to be a mutated exonic splice enhancer (ESE) that was no longer able to recruit spliceosomal machinery to include exon 7 due to the point mutation (Cartegni *et al.* 2002; Kashima *et al.* 2003).

Although it seems like a likely therapeutic antisense target, recent research suggests that the new ISS is bound by the splicing regulator Sam68 which promotes the exclusion of exon 7. This interaction may make it impossible for ASOs to bind to their respective target (Pedrotti *et al.* 2010). Although some groups attempted to target this region using ASOs, the feasibility of this region as a therapeutic target remains limited (Hua *et al.* 2007).

Perhaps the most studied silencer site in SMA research is the intronic splice silencer N1 (ISS-N1). Discovered in 2006 by the Singh group while investigating the effect of spot deletions along *SMN2*, it is now the primary focus of antisense therapy (Singh *et al.* 2006). Currently, the majority of antisense therapy in SMA focuses on targeting the ISS-N1 silencer motif, specifically beginning at the cytosine at the -10 position downstream from exon 7. Several antisense microwalk studies support that targeting this position enhances the percentage of exon 7 inclusion. In the same studies, it is also important to note that the length of the ASO contributes to treatment efficacy. Specifically, longer ASOs show greater exon 7 inclusion in *SMN2* post-transcriptional mRNA (Singh *et al.* 2009; Singh *et al.* 2010).

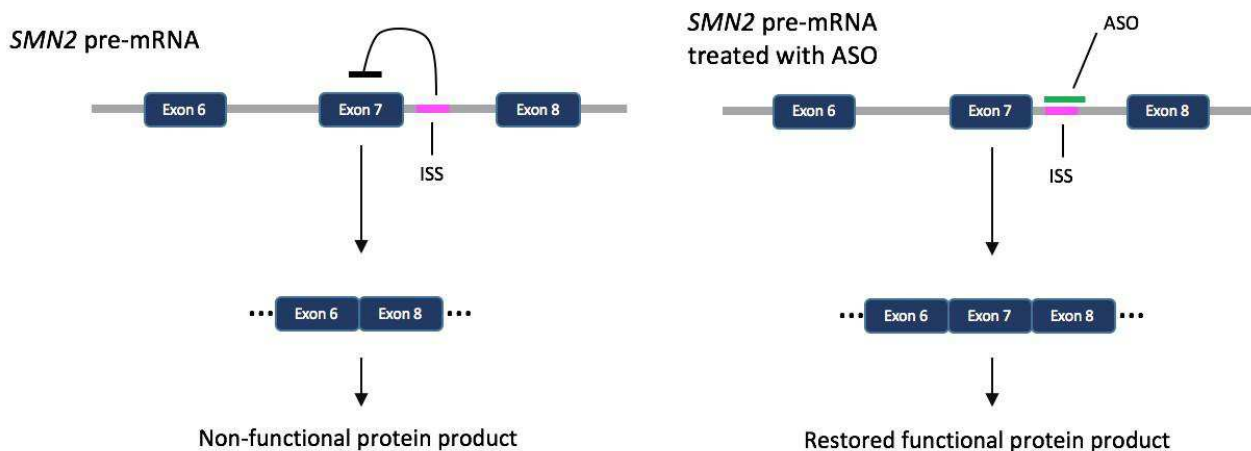


Figure 1-5: Mechanism of antisense therapy in Spinal muscular atrophy

The majority of *SMN2* mRNA is spliced so that exon 7 is not included in the final transcript. Multiple silencers and enhancers interact to mediate proper splicing. Due to the C-to-T transition on exon 7 of *SMN2* pre-mRNA, a splice enhancer was switched into a splice silencer. Antisense therapy works by binding to splice silencers that contribute to the exclusion of exon 7, and promote production of proper full length mRNA. Figure adapted from Touznik *et al.* 2014.

The search for a cure for SMA had its share of hurdles and promises. From gene conversion using antisense therapy to gene replacement with viral vectors, many advances have been made in correcting for SMA at the genetic level (Baioni *et al.* 2010). Beyond that, gene activation strategies using histone deacetylase and drugs such as trichostatin A and vorinostat to target methylation pathways have been investigated to promote *SMN2* transcription (Narver *et al.* 2008; Riessland *et al.* 2010). A new strategy termed “neuroprotection” aims to prolong the survival of motor neurons even with low SMN levels. By using antibody constructs or an activin-binding protein such as follistatin, motor neuron protection in low SMN environments has been observed, however, the success is currently limited to *in vitro* studies (Rose *et al.* 2009; Hedlund *et al.* 2011). Of all the proposed strategies, antisense therapy stands alone as the most promising therapeutic approach for SMA. Current ongoing clinical and pre-clinical trials are trying to make this prospect a reality.

Moving towards a cure

A significant step towards clinical trials for SMA therapies was the establishment of the transgenic SMA mouse lines. Mice can have up to two copies (paternal and maternal) of the *Smn* gene (equivalent to the human *SMN1*), however there is no equivalent gene for *SMN2*. *Smn* null mice exhibit an embryonic lethal phenotype. To create a viable mouse line with no copies of *Smn*, the human *SMN2* transgene was introduced into the mouse genome (Hsieh-Li *et al.* 2000; Monani (1) *et al.* 2000; Monani (2) *et al.* 2000). These transgenic mice provide antisense therapy research targeting *SMN2* with a target gene identical to that in humans, allowing therapies to transition into human trials more easily than when studying other

diseases. In DMD, prior to the development of humanized mouse models containing a human version of the *dystrophin* gene, ASOs used in pre-clinical trials needed to be altered prior to application in humans (Mann *et al.* 2002; Fletcher *et al.* 2007).

Recent work in mice showed that a single administration of ASO was sufficient to rescue SMA phenotype, and that SMA mice with as little as 50% SMN protein levels had normal muscle function (Porensky *et al.* 2012; Iyer *et al.* 2015). Many ASO drugs have been tested using transgenic models, some of which have gone on to human clinical trials. Ionis Pharmaceuticals (formerly ISIS Pharmaceuticals) is currently holding two separate phase III clinical trials with their antisense drug Nusinersen. The first test group is in children ages 2-12, the second group is composed of newborn infants. Nusinersen, is an 18 base pair long 2'-methoxyethoxy (2'MOE) chemistry ASO (www.ionispharma.com/pipeline; February 2016). Although there is much hope for further development of this drug, many complications have been known since the pre-clinical phase. Nusinersen has poor cell uptake, and cannot easily cross the blood-brain barrier. Toxicity, particularly in the kidney, is also quite high as there is drug accumulation in that area (Hua *et al.* 2011). With the current complications, the latest research is trying to identify better antisense chemistries to overcome these problems.

Two chemistries that may be leading candidates for future clinically tested ASOs are the phosphorodiamidate morpholino oligomers (PMOs) and locked nucleic acids (LNAs). PMOs are neutrally charged RNA analogs which contain a phosphorodiamidate linkage in place of the phosphodiester bond, and a morpholine ring takes the place of the ribose sugar (Chan *et al.* 2006). The benefits gained from these chemical modifications include increased stability, high target specificity, and resistance to nucleases. PMO effects are mediated by steric interference,

as the six-membered morpholine ring does not allow RNase H activity (Amantana *et al.* 2005; Nelson *et al.* 2005). *In vivo* evidence supports the use of PMO chemistries targeting various ISS sites in mouse models; however, more support is needed before PMOs can be translated in human SMA trials (Porensky *et al.* 2012; Osman *et al.* 2014). LNAs are nucleic acid analogs that contain a methylene bridge that “locks” the ribose ring in place by creating a bond between the 4'-carbon atom and the 2'-oxygen atom. This modification makes them resistant to nucleases, increases affinity and specificity towards its complementary target, and enhances thermal stability once the duplexes are formed. The most common use of the LNA chemistry is to form chimeric LNA/DNA hybrids known as GapmeRs, where a stretch of DNA is flanked by several LNA base pairs. This modification allows for all the benefits offered by LNAs, in addition to RNase H function due to the DNA insertion (Kurreck *et al.* 2002; Vester *et al.* 2004). As it is important that the *SMN2* mRNA be kept intact, RNase H activity is not favored. Splice switching LNA/DNA mixmers (ASO composed of alternating LNA and DNA nucleotides) have been developed to avoid RNase H activity by not allowing a sufficient stretch of DNA for the cleavage to occur (Shimo *et al.* 2014).

When investigating SMA at the genetic level, it is evident that antisense therapy is at the forefront for finding a cure. The groundwork has already been laid out, and now the challenges lay in identifying the optimal chemistry and sequence to induce the highest amount of exon 7 inclusion, while utilizing the least amount of ASO. Other important factors include transfection efficiency, toxicity, and understanding how much exon 7 inclusion is translated into full-length, functional SMN protein. Understanding the fundamentals of SMA genetics, antisense therapy, and the progress that has been made form the platform for this thesis project.

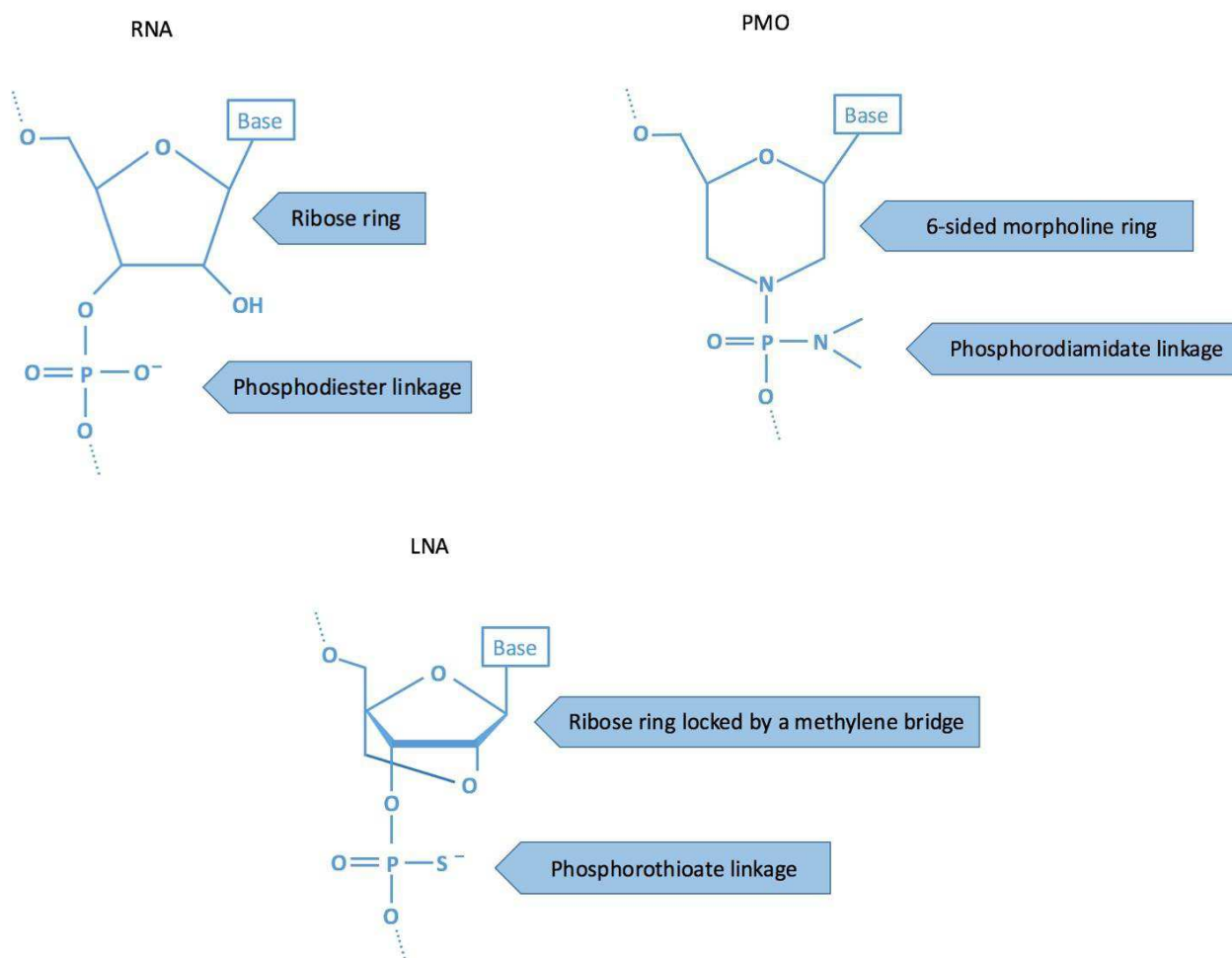


Figure 1-6: Molecular structure of the PMO and LNA antisense oligonucleotides

PMOs and LNAs have a relatively similar structure to RNA. PMOs contain a 6-sided morpholine ring in place of the ribose ring, along with a change in the backbone where the phosphodiester bond is replaced with a phosphorodiamidate linkage. LNAs retain the ribose ring, however it is locked in place by a methylene bridge between the bridge 4'-carbon atom and the 2'-oxygen atom. The phosphorothioate linkage is an optional characteristic, however it greatly improves stability of the LNA oligomer.

Purpose of this study

The purpose of this study is to design and evaluate the efficacy of novel antisense drugs. The sequences designed by my colleagues and myself target various silencer regions within the *SMN2* gene, which may potentially induce measurable levels of exon 7 inclusion, leading to a “knock-up” of functional SMN protein. Currently, amongst the most promising ASO chemistries are PMOs and LNAs. My hypothesis for this project is that ASOs designed in these two chemistries will be more efficient and less toxic than those currently in clinical trials, and that longer ASOs may be more effective for exon 7 inclusion as they target more of the silencer region. Another benefit to longer ASOs is that they may reduce the potential for off-target effects. In the data chapters ahead I will screen various newly designed ASO drugs in human SMA patient cell lines, and determine ones most suitable for further study, potentially taking some to pre-clinical stages. My objective is to determine the optimal ASO candidate for treatment based on sequence, position, and chemistry. The ultimate goal is to create a safe drug that may one day be a therapeutic option for treating SMA.

CHAPTER 2

Materials and Methods

Antisense drug design

The foundation of PMO design was based on silencer position and splice acceptor sites positioned on *SMN2* pre-mRNA. Antisense microwalk results contributed to primary oligo starting positions for the ISS-N1 ASO design (Singh *et al.* 2009; Singh *et al.* 2010). All PMOs were designed as 30-mers (30 nucleotide bases) except those used as comparison sequence to ones currently being investigated in clinical trials, or where the length was not feasible [Table 2-1]. PMO cocktails were designed based on screening results observed in the original PMO screen [Table 2-2]. The second set of PMOs were designed to test a new strategy for targeting Element-1 (Osman *et al.* 2014) and the ISS-N1 silencer simultaneously [Table 2-3]. *In silico* analysis was performed using the online BLAST software (<http://blast.ncbi.nlm.nih.gov/Blast.cgi>) to determine if our sequences may be targeting any other critical genes that may cause aberrant off target effects. LNAs were designed based on PMO results targeting the ISS-N1 silencer site. LNA-based SSOs were constructed by inserting DNA nucleotides in between LNAs or between every two LNAs as described by Shimo *et al.* (2014). LNA design also took into account the length of the oligomer, ranging from 8 to 30 bases in length [Table 2-4].

Cell stock and management

SMA cell lines were purchased from the Coriell NIGMS human genetic cell repository. All cells used were fibroblasts containing the same mutation pattern in the *SMN1* gene – an exon 7 and 8 deletion. Cell lines GM03813 and GM09677 contain 2 copies of the *SMN2* gene.

Table 2-1: PMOs targeting various silencers designed for screening

Splicing regulatory element	Positions bps	PMO #	Name	PMO Sequence
Intron 6 Element 1 (-112,-68)	-97,-68	1	hSMN_Int6_-97_30mer	TTTATATGGATGTTAAAAAGCATTGTGTTT
	-112, -83	2	hSMN_Int6_-112_30mer	AAAAGCATTGTGTTCCACAAGACATTTTAC
	-89,-74 from 5'end of ex7	3	hSMN_Int6_-89_16mer	TGGATGTTAAAAAGCA
Splicing regulatory element	Positions bps		Name	PMO Sequence
Exon7	30-53	4	hSMN_Ex7_30_24mer	CCTTAATTTAAGGAATGTGAGCAC
	34-53	5	hSMN_Ex7_34_20mer	CCTTAATTTAAGGAATGTGA
	34-48	6	hSMN_Ex7_34_15mer	ATTTAAGGAATGTGA
Splicing regulatory element	Positions bps		Name	PMO Sequence
Intron7 ISS-N1	-10,-39 from Ex7 3'end	7	hSMN_Int7_-10_30mer	CAAAAGTAAGATTCACITTCATAATGCTGG
	-9,-38	8	hSMN_Int7_-9_30mer	AAAAGTAAGATTCACITTCATAATGCTGGC
	-10,-27	9	hSMN_Int7_-10_18mer	TCACITTCATAATGCTGG
Splicing regulatory element	Positions bps		Name	PMO Sequence
3'UTR of Int7 & 5' start of exon 8	-1,+17	10	hSMN_Ex8_-1_18mer	CTCTATGCCAGCATTTC
	-5 to 12	11	hSMN_Ex8_-5_17mer	TGCCAGCATTTCCTGCA

Table 2-2: Cocktail and semi-complementary PMOs

Positions bps	PMO #	Name	PMO Sequence
-8 to -17	12	hSMN_Int7_-7_12mer	TAATGCTGGCAG
-18 to -39	13	hSMN_Int7_-19_21mer	CAAAAGTAAGATTCAC TTCA
-1 to -10 & -25 to -39	14	hSMN_Int7_-1/-25_29mer	CAAAAGTAAGATTCAGCTGGCAGACTTAC
-1 to -10	15	hSMN_Int7_-1_14mer	GCTGGCAGACTTAC
-25 to -39	16	hSMN_Int7_-25_15mer	CAAAAGTAAGATTCA

Table 2-3: Hybrid PMO design

Splicing regulatory element	Positions bps	PMO #	Name	PMO Sequence	Comments
Element 1 and IS- N1	N1: -10; DnE1: -67	17	SMN2_PMO_N1-DnE1	TTCATAATGCTGGCTATATAGATA	ISS-N1/DOWN-E1
Element 1 and IS- N1	N1: -10; DnE1: -68	18	SMN2_PMO_N1-UpE1	TTCATAATGCTGGTTATTCAACAAA	ISS-N1/UP-E1
Element 1 and IS- N1	N1: -10; DnE1: -69	19	SMN2_PMO_DnE1-N1	CTATATATAGATATTCATAATGCTGG	DOWN-E1/ISS-N1
Element 1 and IS- N1	N1: -10; DnE1: -70	20	SMN2_PMO_UpE1-N1	GTTATTCAACAAATTCATAATGCTGG	UP-E1/ISS-N1
Element 1	N1: -10; DnE1: -71	21	SMN2_PMO_DnE1-UpE1	CTATATATAGATAGITATTCAACAAA	Lorsons
Element 1	N1: -10; DnE1: -72	22	SMN2_PMO_DnE1_13m	CTATATATAGATA	DOWN-E1
Element 1	N1: -10; DnE1: -73	23	SMN2_PMO_UpE1_13m	GTTATTCAACAAA	UP-E1

N1 --> ISS-N1
DnE1 --> Downstream Element 1
UpE1 --> Upstream Element 1

Table 2-4: Phosphorothioated LNA/DNA mixmers

Positions bps (from Ex7_3'end)	LNA #	Name	AO seq. 5' to 3' <u>Bold/Underlined</u> letter indicates a base for core C-10	Length (bp)	# of LNAs	Comments
-10,-39	1	SMN2ln7_C10PS1L30m	C*+A*A*+A*A*+G*T*+A*A*+G*A*+T*T*+C*A*+C*T*+T*T*+C*A*+T*A*+A*T*+G*C*+T*G*+G	30_mer	15	Alternating DNA/LNA.
-10,-27	2	SMN2ln7_C10PS1L18m	T*+C*A*+C*T*+T*T*+C*A*+T*A*+A*T*+G*C*+T*G*+G	18_mer	9	Alternating DNA/LNA.
-10,-27	3	SMN2ln7_C10PS2L18m	T*+C*A*+C*T*+T*T*+C*A*+T*A*+A*T*+G*C*+T*G*+G	18_mer	12	2 LNA between DNA
-10,-22	4	SMN2ln7_C10PS1L13m	+T*T*+C*A*+T*A*+A*T*+G*C*+T*G*+G	13_mer	7	Alternating DNA/LNA.
-10,-22	5	SMN2ln7_C10PS2L13m	+T*T*+C*A*+T*A*+A*T*+G*C*+T*G*+G	13_mer	9	2 LNA between DNA
-10,-17	6	SMN2ln7_C10PS1L8m	A*+A*T*+G*C*+T*G*+G	8_mer	4	Alternating DNA/LNA.
-10,-17	7	SMN2ln7_C10PS2L8m	+A*+A*T*+G*+C*T*+G*+G	8_mer	6	2 LNA between DNA
-10,-17	8	SMN2ln7_C10PSaL8m	+A*+A*+T*+G*+C*+T*+G*+G	8_mer	8	all LNA

Blue = DNA
 Red = LNA
 Phosphorothioate linkage indicated by *
 LNA base: +G, +A, +T, +C, DNA base: G, A, T, C

GM00232 contains 1 copy of the *SMN2* gene. All SMA cell lines were from patients diagnosed with Type I SMA. GM23815 fibroblasts were used as healthy controls. No information was available on *SMN2* copy number of GM23815 cells [Table 2-5]. Cells were passaged overnight in Nunc™ Cell Culture Treated EasYFlasks™ (T225) using Gibco® DMEM (Dulbecco's modified Eagle medium 1:1 F-12 (Ham)) + 10% fetal bovine serum (FBS). Cells were washed with sterilized 1x phosphate buffered saline (PBS) and detached using Gibco® 0.05% Trypsin-EDTA (1x) for 5 minutes at 37°C. Cells were frozen in Gibco® Recovery™ Cell culture freezing media via Nalgene™ Cryo 1°C Freezing Container (Cat. No. 5100-0001) at -80°C overnight. Long term storage in liquid nitrogen (-196°C) in a sealed Nunc™ 1.8 mL Cryovial.

Cell counting and seeding

Cells were thawed by swirling in a 37°C hot water bath, and immediately transferred to growth media: Gibco® DMEM (Dulbecco's modified Eagle medium 1:1 F-12 (Ham)) + 10% FBS. Growth media contains 0.5% Gibco® Pen-Strep antibiotic (Penicillin (10,000 Units/mL) Streptomycin (10,000 µg/mL)). After overnight incubation in a Nunc™ T225 flask at 37°C in a CO₂ incubator, cells were washed with sterilized 1x phosphate buffered saline (PBS) and detached using Gibco® 0.05% Trypsin-EDTA (1x) for 5 minutes at 37°C. Growth serum containing 10% FBS was used to stop the trypsin reaction. Cells were spun down in a mini-centrifuge at 300 rcf for 5 minutes. The pellet was resuspended in 10 mL growth media. 10 µL was taken and diluted 1:1 with Gibco® 0.4% Trypan blue (Cat. No. 15250061), 10 µL of the diluted solution was used for counting on a commercial hemocytometer. Cells were diluted to

Table 2-5: Cell line characteristics

Cell line ID	Species	Sex	Race	Age at sampling	Cell type	SMN1 Mutation	Clinically affected	SMN2 copy number
GM03813	Homo sapiens	Male	Caucasian	3 years	Fibroblasts	Exon 7&8 Deletion	Yes	2
GM09677	Homo sapiens	Male	Caucasian	2 years	Fibroblasts	Exon 7&8 Deletion	Yes	2
GM00232	Homo sapiens	Male	Caucasian	7 months	Fibroblasts	Exon 7&8 Deletion	Yes	1
GM23815	Homo sapiens	Male	Caucasian	22 years	Fibroblasts	N/A	No	Unknown

1x10⁵ cells/mL and seeded on appropriate plate (500 µL for a 24 well plate; 1000 µL for a 12 well plate).

PMO preparation

PMOs were synthesized by Gene Tools, LLC. PMOs were delivered in powdered form at 300 nmol. Vials were spun down at 2000 rpm for 5 minutes. To make 1 mM stocks, the PMO powder was resuspended in 300 µL of UltraPure™ RNase/DNase-free distilled water (Invitrogen). PMOs were left for 24 hours after resuspension prior to use. Storage containers were sealed with Parafilm and stored at room temperature.

LNA preparation

LNAs were synthesized by Exiqon. LNAs were delivered in powdered form at varying weights listed on the product order form. LNAs were to be spun down briefly in a micro-centrifuge and resuspended with UltraPure™ RNase/DNase-free distilled water (Invitrogen) to reach a 100 µM concentration. LNAs were further diluted to 10 µM (minimum concentration allowed for storage), and aliquoted at 50 µL. LNAs were to be stored at -20°C. No more than 3 freeze/thaw cycles are permitted per aliquot.

PMO transfection

Prior to transfecting, PMOs were heated for 15 minutes at 70°C. PMOs were diluted in growth media made from OPTI-MEM® Reduced Serum Media (+HEPES; 2.4 g/L sodium bicarbonate; L-glutamine)(Gibco®), 5% FBS, and 0.6% of the co-transfection reagent Endo-

Porter (Gene Tools). The transfection mixture replaces growth media used in seeding.

Transfected cells were incubated for 48 hours at 37°C in a CO₂ incubator.

LNA Transfection

LNAs were thawed and kept on ice until ready for use. LNAs first need to be incubated for 10 minutes at room temperature with the co-transfection reagent Lipofectamine® RNAiMAX (Invitrogen). A 100 µL solution containing required amount of LNA and RNAiMAX (2 µL per 498 µL transfection media), in OPTI-MEM® Reduced Serum Media. Once incubation was complete, the mixture was further diluted with OPTI-MEM® containing 5% FBS. Transfected cells were incubated for 48 hours at 37°C in a CO₂ incubator.

RNA Collection

Transfected cells were collected using TRIzol® reagent by Life Technologies. The procedure was done in a fume hood, as recommended by safety guidelines. Once transfection media was removed, 1 mL of TRIzol was added to each sample. After mixing by pipetting 3-4 times, TRIzol® solution was transferred to a clear 1.5 mL centrifuge tube and kept on ice. Each sample was mixed by vortexing for 10 seconds at maximum speed. The sample was purified right away or stored at -80°C for future use.

RNA purification

RNA purification was done using the TRIzol® protocol. The procedure was done in a fume hood, as recommended by safety guidelines. 200 µL chloroform was added to RNA

solution in 1 mL TRIzol[®]. The mixture was shaken vigorously for 15 seconds, and incubated at room temperature 3 minutes, then spun down in a mini-centrifuge at 12,000 g for 15 minutes at 4°C. The clear aqueous phase containing RNA was isolated. 500 µL of molecular grade isopropanol and 2 µL of RNA grade glycogen were added to the aqueous solution, vortexed for 5 seconds and incubated at room temperature for 10 minutes. Following incubation, the samples were centrifuged at 12,000 g for 10 minutes at 4°C. The supernatant was removed, and 1000 µL of 75% ethanol was used to wash the RNA pellet. After the wash, the sample was spun down at 7500 g for 5 minutes at 4°C. Ethanol was removed completely, and the pellet was allowed to dry for 5 minutes. The pellet was resuspended in 30 µL of UltraPure™ RNase/DNase-free distilled water (Invitrogen). RNA concentration was measured using a NanoDrop™ Lite Spectrophotometer (Thermo Scientific). RNA concentrations were adjusted to 50 ng/µL. Samples stored at -80°C.

Protein Collection

Protein was collected using Pierce[®] RIPA lysis buffer (Thermo Scientific) with 1x Roche cOmplete™ protease inhibitor. Cells were washed with PBS to remove transfection media. 100 µL of the lysis buffer was used per sample. Cells were detached from well using a sterile Falcon™ Cell Scraper (Fisher Scientific). Cell solution was collected into 1.5 mL mini centrifuge tubes and incubated for 30 minutes on ice. A 21-G needle was used to break up cells. Cells were spun down at 14,000 g for 15 minutes at 4°C. Supernatant containing the proteins was collected. Protein concentration was measured via Bradford assay. The protein sample was diluted with lysis buffer to 1.0 µg/µL. Samples stored at in the -80°C freezer.

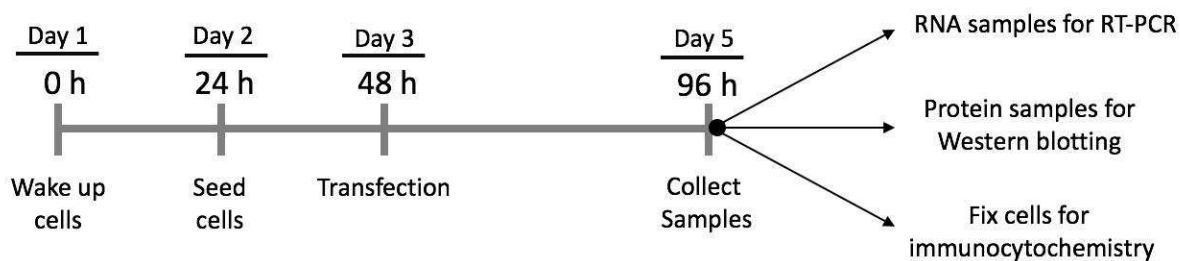


Figure 2-1: Timeline for PMO and LNA transfections.

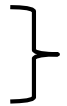
After cells are thawed and plated, they are given 24 hours to grow. After 24 hours, cells are ~80% confluent. Cells were counted and seeded on required plating, and given 24 hours to attach to the bottom of plate. Cells were then transfected for 48 hours in a 37°C CO₂ incubator.

Reverse transcription polymerase chain reaction

Reverse transcription polymerase chain reaction (RT-PCR) was performed using the SuperScript® III Reverse Transcriptase kit from Invitrogen. Total cell RNA was used for each PCR reaction. Primers were designed to only detect *SMN2* sequences in SMA cell lines. Total RNA was amplified using forward primer 5'- CTGCCTCCATTCCTTCTG-3' and reverse primer 5'- TGGTGTCATTTAGTGCTGCTC-3'. Primer set was specifically designed to detect only *SMN2* and not *SMN1* [Figure 2-2]. Each sample contained 12.5 µL of Invitrogen 2x RT-PCR reaction mix, 1.0 µL of SuperScript® III Taq polymerase, 0.5 µL of forward primer 2F, 0.5 µL of reverse primer 2R, 8.5 µL of UltraPure RNase/DNase-free distilled water (Invitrogen), and 2.0 µL total RNA template at 50 ng/µL. Thermo-cycler settings were as follows:

Temperature	Time
50°C	5 min.
94°C	2 min.
94°C	15 sec.
60°C	30 sec.
68°C	25 sec.
68°C	5 min.
4°C	5 min.
20°C	-----

30x



DNA Gel loading dye (Thermo Scientific) loading dye was added to the PCR cDNA products. 5 µL of each sample was run on a 2% agarose gel (0.5% Tris-borate-EDTA buffer) for 2 minutes at 135 V followed by 30 minutes at 100 V. The cDNA was stained with SYBR® safe DNA gel stain (Life Technologies) for 30 minutes under agitation. Images were taken using the Kodak scientific imager. ImageJ software (National Institutes of Health) was used to quantify the intensity of each band. Percentage of exon inclusion was calculated by dividing the intensity of the top

band by the total intensity of both bands. The internal control used was Glyceraldehyde-3-phosphate dehydrogenase (*GAPDH*). *GAPDH* forward primer was 5'- TCCCTGAGCTGAACGGGAAG-3' and the reverse primer was 5'-GGAGGAGTTTGGTCGCTGT-3' [Table 2-6].

Western blotting

Western blotting was done using a semi-dry system. XCell4 SureLock™ Midi-Cell electrophoresis system (Invitrogen) was used to run the gel, and the Novex® Semi-Dry Blotter was used to transfer protein onto polyvinylidene difluoride (PVDF) membrane. Protein samples were diluted in 2x sodium dodecyl sulfate (SDS) sample buffer (10% SDS; 14% 0.5M Tris-HCl solution, pH 6.7; 1% 0.5M EDTA-2Na stock solution, pH 8.0; 20% Glycerol; 0.004% bromophenol blue (BPB) loading dye; 5% β-mercaptoethanol). Samples were incubated at 70°C for 10 minutes in a hot water bath. 5 µg of protein was loaded onto 20-well NuPAGE™ Novex™ 4-12% Bis-Tris Midi Protein Gels (Life Technologies). Spectra™ Multicolor Broad Range protein ladder (Thermo Scientific) was used to mark protein size. Samples were run for 1 hour at 150V. Proteins were transferred onto PVDF membrane (pore size 0.45µm) via extra thick blotting sheets soaked in transfer buffers. Layers from anode: concentrated anode buffer (0.3 M Tris, 20% methanol)/anode buffer (0.03 M Tris, 20% methanol)/PVDF membrane/midi gel/cathode buffer (25 mM Tris, 20% methanol, 40 mM 6-amino-n-hexanoic acid, 0.01 % SDS). Transfers were run for 30 minutes at 20V. PVDF membrane blocked overnight at 4°C with 5% skim milk in 0.05% Tween 20 detergent in PBS (PBSTw).

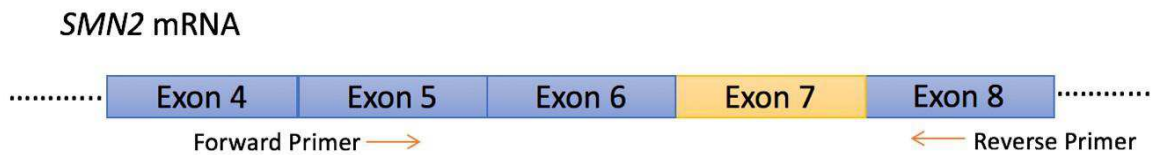


Figure 2-2: Primer design for *SMN2* detection

The forward and reverse primers were designed to detect spliced *SMN2* mRNA transcripts, while avoiding *SMN1* mRNA. To do this the reverse primer was put on exon 8, which has been deleted in the *SMN1* gene. The forward primer was placed along exon 5 to avoid detecting isoforms where exon 5 is not present. Note: 90% of *SMN2* post-transcriptional mRNA does not contain exon 7.

Table 2-6: Primers for RT-PCR and Sequencing

Gene	Type	Primer ID	Sequence [5'→3']	Length (bp)	Annealing temp.	GC %	Amplicon size
<i>SMN2</i>	Forward	Ex5_70-88_hSMN_F	CTGCCTCCATTTCCTTCTG	19	58.4°C	52.6	227 bp with exon 7 173 bp without exon 7
	Reverse	Ex8_15-35_hSMN_R	TGGTGTCATTAGTGCTGCTC	21	58.9°C	47.6	
<i>GAPDH</i>	Forward	hGAPDH_662-81_Fwd1	TCCCTGAGCTGAACGGGAAG	20	65°C	60.0	218 bp
	Reverse	hGAPDH_860-79_Rv1	GGAGGAGTTTGGTCGCTGT	19	65°C	57.9	

Immunostaining

PVDF membrane was cut to separate target proteins. SMN primary antibodies (BD Biosciences Purified mouse anti-SMN) were diluted 1 in 10,000 times in 5% skim milk blocking solution. For the original PMO screening experiments, anti-alpha-tubulin primary antibodies (Abcam MS mAB to alpha tubulin [DMA1]) were used diluted 1 in 10,000 times. Loading control Cofilin primary antibodies (New England BioLabs Cofilin (D3F9) XP[®] Rabbit mAb) were diluted 1 in 10,000 times in 5% skim milk blocking solution. Primary antibody staining was done under agitation for 1 hour at room temperature. Primary antibodies were removed by three 10 minute washes using PBS with 0.05% Tween 20 detergent (PBSTw). Secondary antibodies (HRP conjugated goat anti-mouse IgG (H+L) for SMN and alpha tubulin (Bio-Rad); HRP conjugated goat anti-rabbit IgG (H+L) for Cofilin (Bio-Rad)). Both were diluted in PBSTw 1 in 10,000 times. Secondary antibody staining was done under agitation for 1 hour at room temperature in the dark. Secondary antibodies were removed with three 10 minute washes using PBSTw. The Amersham ECL Select Western blotting detection kit (GE Healthcare) was used for band detection. Detection reagents were mixed in a 1:1 ratio, and covered the PVDF membrane for 5 minutes in the dark. Images were taken using the Kodak scientific imager. ImageJ software was used to quantify the intensity of the bands.

cDNA Sequencing

Wizard[®]SV Gel and PCR Clean-Up System (Promega) were used to purify cDNA from the agarose gel. Gel slices were vortexed and incubated in membrane binding solution at 65°C until the gel was completely dissolved. Dissolved gel mixture was placed into the SVMinicolumn

attached to the collection tube and incubated for 1 minute at room temperature. Minicolumn was centrifuged at 16,000 g for 1 minute, and flow through was discarded. 700 μ L of Membrane Wash Solution (containing ethanol) was added to the Minicolumn and was centrifuged again at 16,000 g for 1 minute. A second wash with 500 μ L Membrane Wash Solution was spun down at 16,000 g for 5 minutes. Minicolumn was transferred into now 1.5 mL microcentrifuge tube. 35 μ L of UltraPure™ RNase/DNase-free distilled water (Invitrogen) was added to Minicolumn and incubated at room temperature for 1 minute. Minicolumn was then centrifuged at 16,000 g for 1 minute. cDNA samples were diluted to 0.3 ng/ μ L and stored at 4°C. Samples were sent off to the University of Alberta Sanger sequencing facility at the Katz Center for Pharmacy and Health Research facility. Sequenced results were analyzed using FinchTV (Geospiza).

Immunocytochemistry

Cells were seeded at 2.5×10^4 cells/well onto the Nunc™ Lab-Tek™ II Chamber Slide™ System. After transfections were complete, cells were washed with twice with 1x PBS and fixed with 300 μ L of 4% paraformaldehyde (PFA) for 5 minutes. Following fixation, each well was washed 3 times for 5 minutes with 1x PBS containing 0.1% Triton X-100 detergent (PBSTr). Cells were blocked for 20 minutes with 300 μ L goat serum based blocking solution (PBS; 0.5% Triton X-100 detergent; 10% goat serum (Sigma-Aldrich)). SMN primary antibodies (Developmental Studies Hybridoma Bank; MANSMA1) were diluted 1 in 8 times in the goat serum blocking solution. After chambers had been removed, the glass slide was covered with primary antibody solution and covered with Parafilm. Slides were incubated for 24 hours at 4°C. Primary antibody was washed off with three 5 minute washes using PBSTr. The secondary antibody (Alexa Fluor

594 goat anti-mouse IgG H+L (Life Technologies)) was diluted 1 in 500 times in PBSTr. Secondary antibodies incubated for 1 hour at room temperature in the dark. The secondary antibody was washed off with three 5 minute washes using PBSTr. Slides were then treated with ProLong® Gold Antifade Mountant with DAPI (Life Technologies) and stored at 4°C away from light. Immunocytochemistry (ICC) images were taken with a Zeiss LSM 710 confocal microscope.

Statistical analysis

Statistical analysis was done using Microsoft Excel, R software (<https://www.r-project.org>), and GraphPad Prism software. Data was tested for normality using the Shapiro-Wilk test. Statistical significance of treatment results was tested using one-way ANOVA analysis for parametric data and Kruskal-Wallis analysis for non-parametric data. Error bars on all histograms represent the standard deviation of three independent biological rounds.

CHAPTER 3

Efficacy of novel PMO-based antisense oligonucleotides in SMA patient cell lines

3.1 Background

Applications of PMOs have been studied extensively, ranging from hereditary disease treatment such as Huntington's to developing gene-specific countermeasures to fight against the Ebola virus (Warfield *et al.* 2006; Sun *et al.* 2014). SMA researchers have also looked into the possibility of using PMOs to develop a treatment. Recently, one group has published *in vivo* results testing their PMO sequences in a mild transgenic mouse model containing two copies of *SMN2* with promising results (Zhou *et al.* 2015). The first aim covered of this section was to design novel PMOs to effectively induce exon 7 inclusion in *SMN2* mRNA, and ultimately restore SMN levels in SMA patient cell lines. The initial PMO screening assessed various target locations and PMO design strategies. The second aim was to statistically demonstrate the effectiveness of the most promising PMOs from my initial screen in multiple SMA patient cell lines. Several of the PMOs designed by my colleagues and I contain 30 base pairs, as one of the core hypothesis of this project is that longer ASO sequences may be more effective for exon 7 inclusion than shorter ones for treating SMA. Two of the reasons behind this idea is that longer ASOs cover more of the splicing silencer and that more base pairs increases binding strength. Another benefit is that higher specificity of long ASOs could reduce potential off-target effects. A benefit of the PMO specificity is their extremely low toxicity. All PMO sequences were tested using the online BLAST (<http://blast.ncbi.nlm.nih.gov/Blast.cgi>) software to check for potential negative off-target effects, none of which presented any reason for concern.

3.2: Results: PMO screening

Semi-quantitative RT-PCR PMO screening targeting various silencer sites along *SMN2*

pre-mRNA

Semi-quantitative RT-PCR results indicated various levels of exon 7 inclusion efficiency in the SMA patient cell line GM03813 when treated with PMOs 1-11 at a 10 μ M concentration [Figure 3-1]. Each lane represents an independent treatment, where the top band indicates full-length *SMN2* mRNA that includes exon 7. The bottom band represents mRNA transcripts that failed to include exon 7, and would ultimately lead to the non-functional protein product. The PMO treatments aimed at converting the non-functional products into the functional full-length products by suppressing silencer regions on the *SMN2* pre-mRNA transcript that promote non-functional splice form. PMOs 1-3 targeted the ISS Element-1 directly. Results showed that targeting these areas resulted in less exon 7 inclusion than in the mock and non-treated control samples. PMOs 4-6, which targeted exon 7 directly, also failed to show any improvement in exon 7 inclusion. PMO 4 (along with PMO 1-3) results strongly indicate a reverse effect, where their sequence may, in fact, play a role in hindering the natural exon 7 inclusion process. PMO 7-9 (indicated by the white arrows), which targets the ISS-N1 silencer on intron 7, indicated complete exon 7 inclusion, as no lower bands were detected using Image J software. PMO 10 and 11, which targeted exon 8 acceptor sites, failed to show any difference from the mock and non-treated controls.

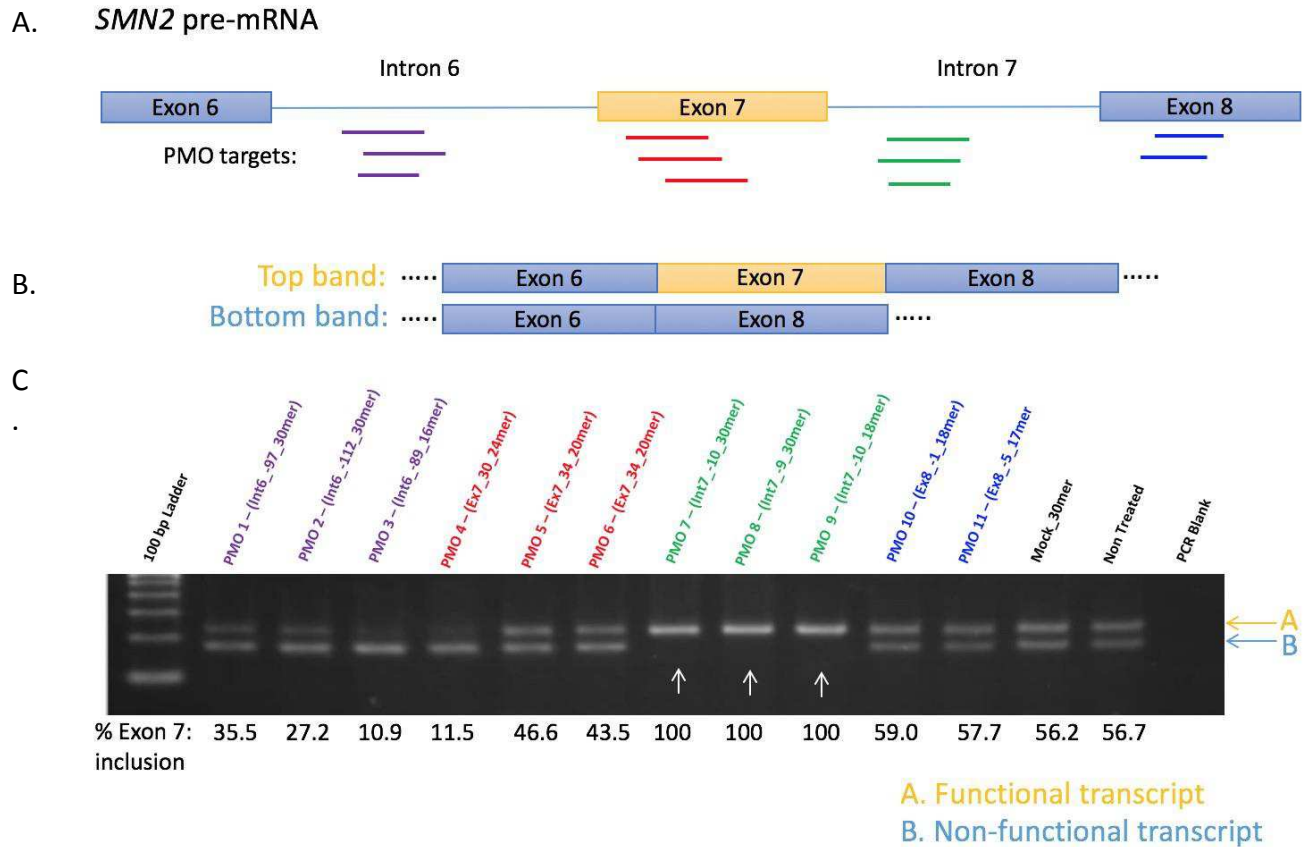


Figure 3-1: Effect of novel PMO screening along *SMN2* pre-mRNA indicates PMO 7, 8, and 9 may be effective candidates for restoring protein levels in SMA patient cells.

(A) Diagrammatic representation of PMO annealing positions along the *SMN2* pre-mRNA transcript. (B) Summary diagram describing band positions on an agarose gel. (C) Semi-quantitative RT-PCR analysis of exon 7 incorporation in post-transcriptional *SMN2* mRNA. SMA patient fibroblasts (Cell ID: GM03813) were treated with 10 μ M of each PMO (co-transfected with Endo-Porter™). Splicing effect was determined 48 hours after transfection. Total RNA was amplified with *SMN2* specific primers.

Cocktail and semi-complementary PMO screening using quantitative RT-PCR

A follow-up strategy based on the initial screening results was to test PMO cocktails targeting the ISS-N1 silencer site. Two sets of PMO cocktails were designed and tested in the SMA patient cell line GM03813 [Figure 3-2]. Each cocktail candidate was tested individually (PMO 12,13,15,16), as well as in combinations with its counterpart. Both individual components and combination cocktails (containing 10 μ M of each component) failed to induce exon 7 inclusion levels comparable to the PMO 8 positive control. Semi-complementary PMO 14 sequence also failed to improve inclusion of exon 7. PMO 14 and 15, whose sequences target the mRNA close to the exon 7/intron 7 junction promoted splice forms that exclude exon 7.

Screening for hybrid PMOs simultaneously targeting Element-1 and ISS-N1 using semi-quantitative RT-PCR

Based on the success of the PMOs targeting the ISS-N1 silencer, and new data suggesting that targeting the flanking regions of Element-1 leads to improved splicing inclusion of exon 7, I designed a new set of PMOs to simultaneously target ISS-N1 and Element-1. PMOs 17-20 did not show complete exon 7 inclusion previously seen with a single oligo only targeting the ISS-N1 region. PMO 21 targeting both regions flanking Element-1 showed results comparable to that of the mock and non-treated samples [Figure 3-3].

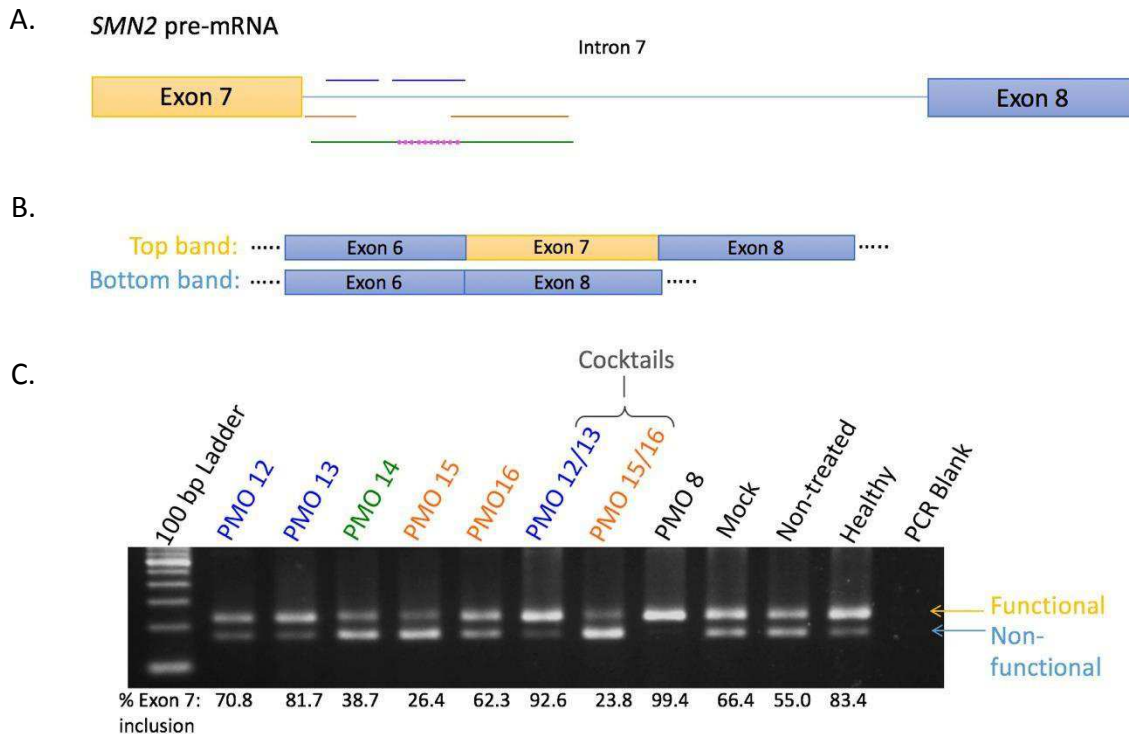


Figure 3-2: Effect of cocktail and semi-complementary PMOs in SMA patient fibroblasts

(A) Diagrammatic representation of cocktail and dual targeting PMO annealing positions along the *SMN2* pre-mRNA transcript. Dotted region on the semi-complementary PMO (represented by a green line) represents the non-targeting (skipped) region. (B) Summary diagram describing band positions on an agarose gel. (C) Semi-quantitative RT-PCR analysis showing exon 7 incorporation in post-transcriptional *SMN2* mRNA induced by cocktail and semi-complementary PMOs. SMA patient fibroblasts (Cell ID: GM03813) were treated with 10 μ M of each PMO (co-transfected with Endo-Porter™). The splicing effect was determined 48 hours after transfection. PMO 8 was used as a positive control to compare results to a single oligo. Total RNA was amplified with *SMN2* specific primers.

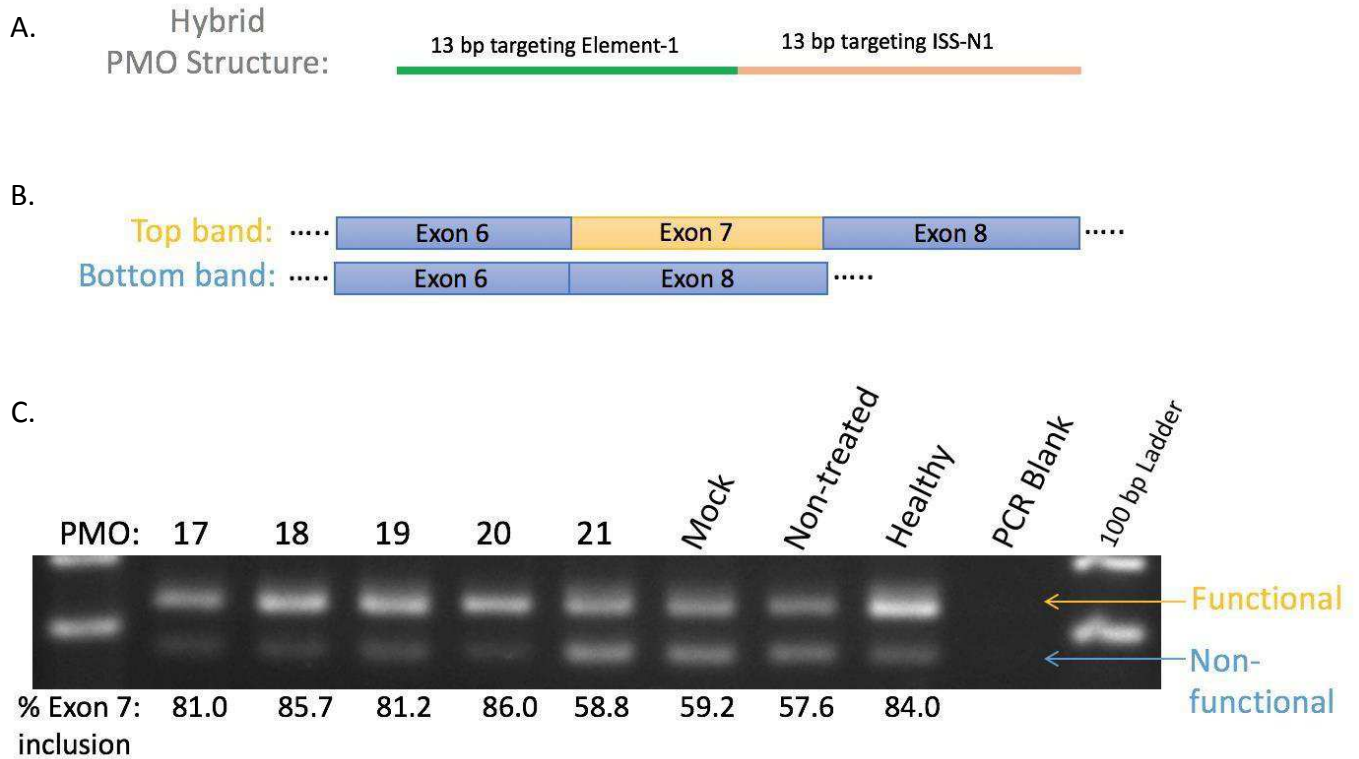


Figure 3-3: Effect of hybrid PMOs simultaneously targeting Element-1 and ISS-N1 splice silencers in SMA patient fibroblasts

(A) A schematic representing structural design of novel hybrid PMOs. (B) Summary diagram describing band positions on an agarose gel. (C) RT-PCR analysis of exon 7 incorporation in post-transcriptional *SMN2* mRNA induced by hybrid PMOs. PMO 21 structure (used as a positive control) flanks both outer regions of Element-1. SMA patient fibroblasts (Cell ID: GM03813) were treated with 10 μ m of each PMO (co-transfected with Endo-Porter™). The splicing effect was determined 48 hours after transfection. Total RNA was amplified with *SMN2* specific primers.

Protein expression analysis of PMO screens targeting various silencer sites along *SMN2* pre-MRNA

After the initial screening analysis of total mRNA product, I followed up with an equivalent protein screen to see in change if exon 7 inclusion translates into production of functional full-length SMN protein. Western blot analysis results show the ability of PMOs 1-11 to “knock-up” full-length SMN protein quantity in SMA patient cells (Cell ID: GM03813) [Figure 3-4]. Patient fibroblasts were treated with 10 μ M of each respective PMO. PMOs targeting Element-1 and exon 7 (PMO 1-6) resulted in an overall lower SMN band intensity relative to the mock and non-treated control, while PMOs 10 and 11 showed similar results. PMO 7, 8 and 9 which target the ISS-N1 silencer site produced a higher level of full-length SMN protein product.

Analysis of PMOs targeting the ISS-N1 silencer site at reduced transfection concentrations

To follow up on the work from the initial screening results, PMO 7, 8 and 9 were transfected at 1 μ M, 3 μ M, and 5 μ M. RT-PCR and Western blotting results can be seen in Figure 3-5. RT-PCR data shows that at lower concentrations these PMOs are still capable of promoting exon 7 inclusion in the *SMN2* mRNA. At 1 μ M none of the PMOs are able to achieve the 100% levels of exon 7 inclusion. PMO 7 and 9 had relatively similar efficacy, while PMO 8 began to decrease as transfection concentration amount decreased. The RT-PCR results are supported by protein analysis data. SMN protein quantity was reduced as the PMO concentrations used in the transfection was lowered. PMO 8 had the lowest amount of SMN protein produced. Treatment with PMO 7 had slightly higher levels of SMN protein levels, however, this difference increased with transfection concentration. The higher the PMO

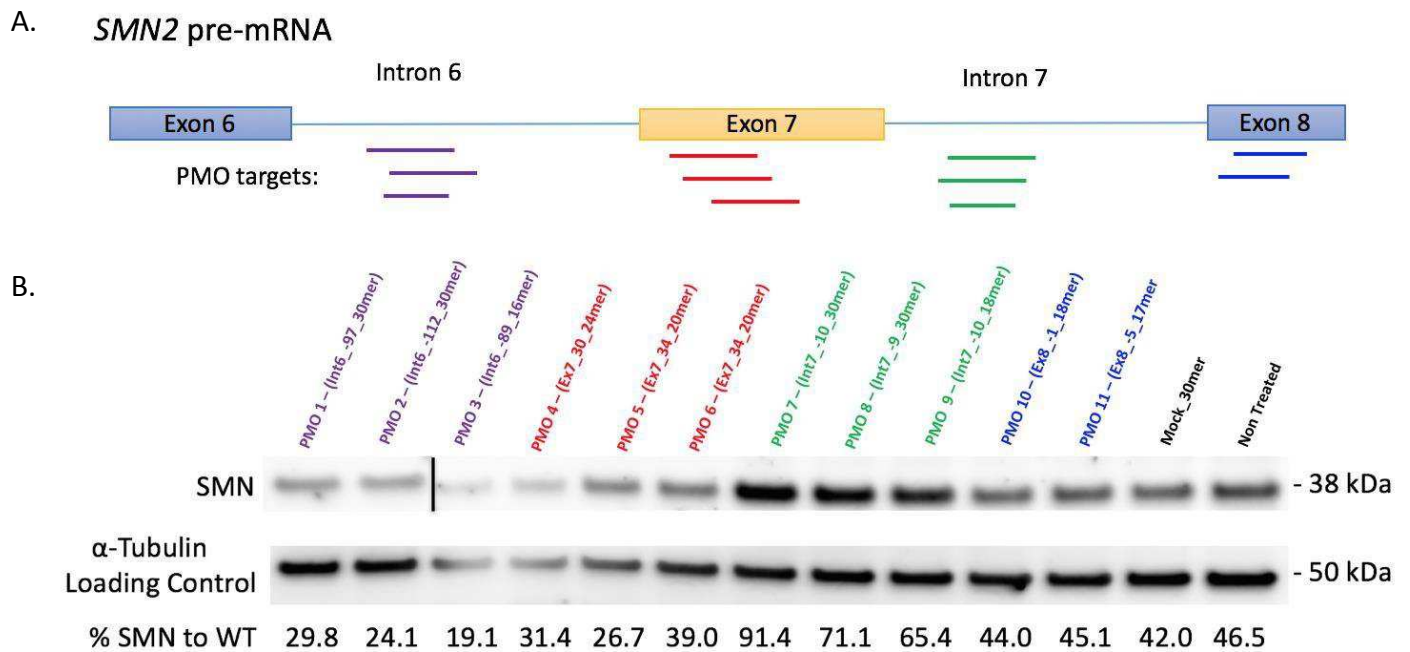
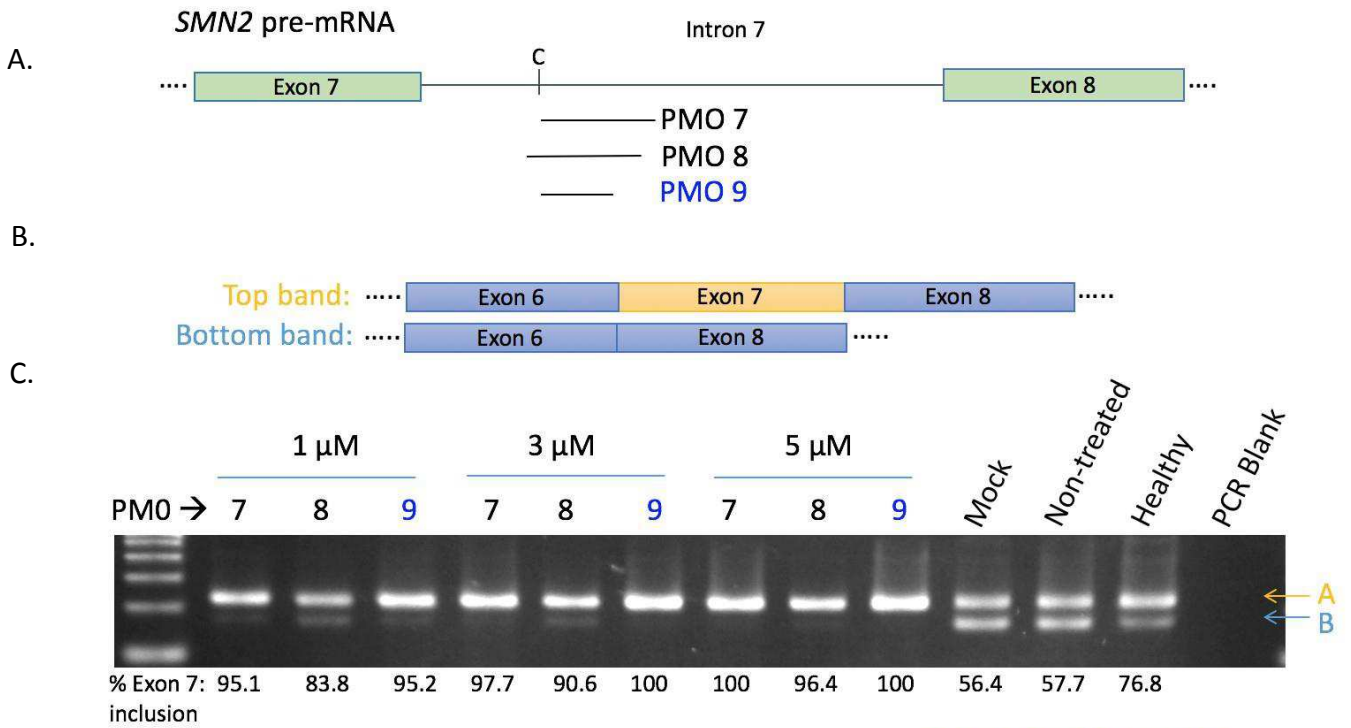


Figure 3-4: Protein “knock-up” screening using PMOs targeting various targets on *SMN2* pre-mRNA

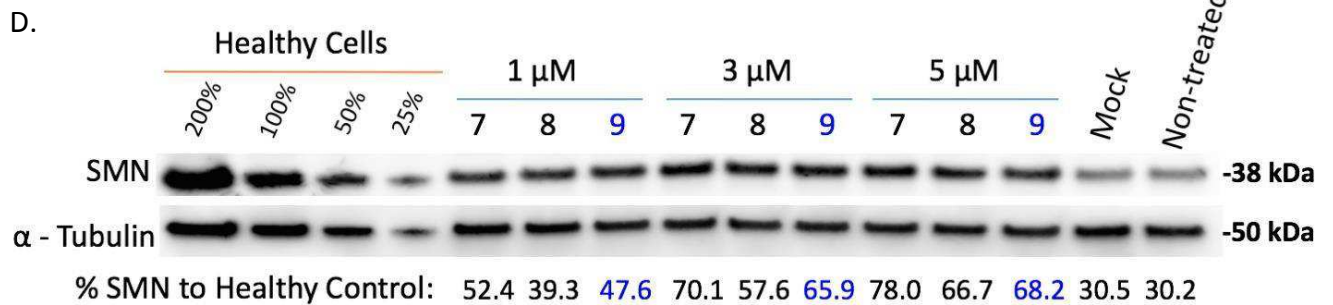
(A) Diagrammatic representation of PMO annealing positions along the *SMN2* pre-mRNA transcript. (B) Western blot analysis of SMN protein production in SMA patient fibroblasts (Cell ID: GM03813). Cells were treated with 10 μ M of each PMO (co-transfected with Endo-Porter™). Protein levels were determined 48 hours after transfection. Note: vertical black line on between PMO 2 and 3 treatments represents a break in the gel.

Figure 3-5: PMOs targeting the intronic repressor ISS-N1 with reduced transfection concentrations

(A) Diagrammatic representation of PMO annealing positions along the *SMN2* pre-mRNA transcript. (B) Summary diagram describing band positions on an agarose gel in RT-PCR analysis. (C) Semi-quantitative RT-PCR analysis showing exon 7 inclusion in post-transcriptional *SMN2* mRNA. SMA patient fibroblasts (Cell ID: GM03813) were treated with 1 μ M, 3 μ M and μ M of each PMO (co-transfected with Endo-Porter™). Total RNA was amplified with *SMN2* specific primers. The splicing effect was determined 48 hours after transfection. (D) Corresponding western blot analysis supporting RT-PCR data. Transfection was done simultaneously for RNA and Protein samples. The sequence in blue (PMO 9) is currently being tested in human clinical trials in the 2'MOE antisense chemistry.



A. Functional transcript



*Sequence currently in clinical trials in blue

concentration used in the transfections, the greater the difference in efficacy between PMO 7 and 9.

cDNA sequencing of bands differentiated by electrophoresis.

To analyze the identity of the two differentiated bands seen in RT-PCR analysis, I isolated samples of the top and bottom band, and submit the samples for Sanger sequencing. Results confirmed that the top band represents the *SMN2* transcript with exon 7, as the whole exon is included in the sequence. Bottom band result showed *SMN2* transcripts without exon 7. In this transcript there is an exon 6 and exon 8 junction [Figure 3-6].

3.3 Results: PMO efficacy in multiple SMA cell lines

Dose-dependent analysis of PMOs in patient fibroblasts (GM03813)

The screening results led to the identification of two novel PMO sequences (PMO 7 and 8), and also confirm the effectiveness of a sequence currently in clinical trials (PMO 9) in the PMO chemistry. Once the most promising PMO sequences were identified, I set out to show their efficacy across three different concentrations, and determine if the PMO effect is replicable across three different commercially available SMA patient cell lines. First I showed statistical data for cells used in PMO screening. SMA patient GM03813 fibroblasts (two *SMN2* copies) were treated with PMO 7, 8 and 9 at 0.1 μM , 1.0 μM and 10 μM each. Semi-quantitative RT-PCR analysis [Figure 3-7] showed that at 0.1 μM , all three PMOs fail to produce a statistically significant level of exon 7 inclusion. Increasing the concentrations ten times to 1.0 μM showed a significant increase ($p < 0.05$) in PMO 7, 8 and 9, with high early levels of exon 7 inclusion.

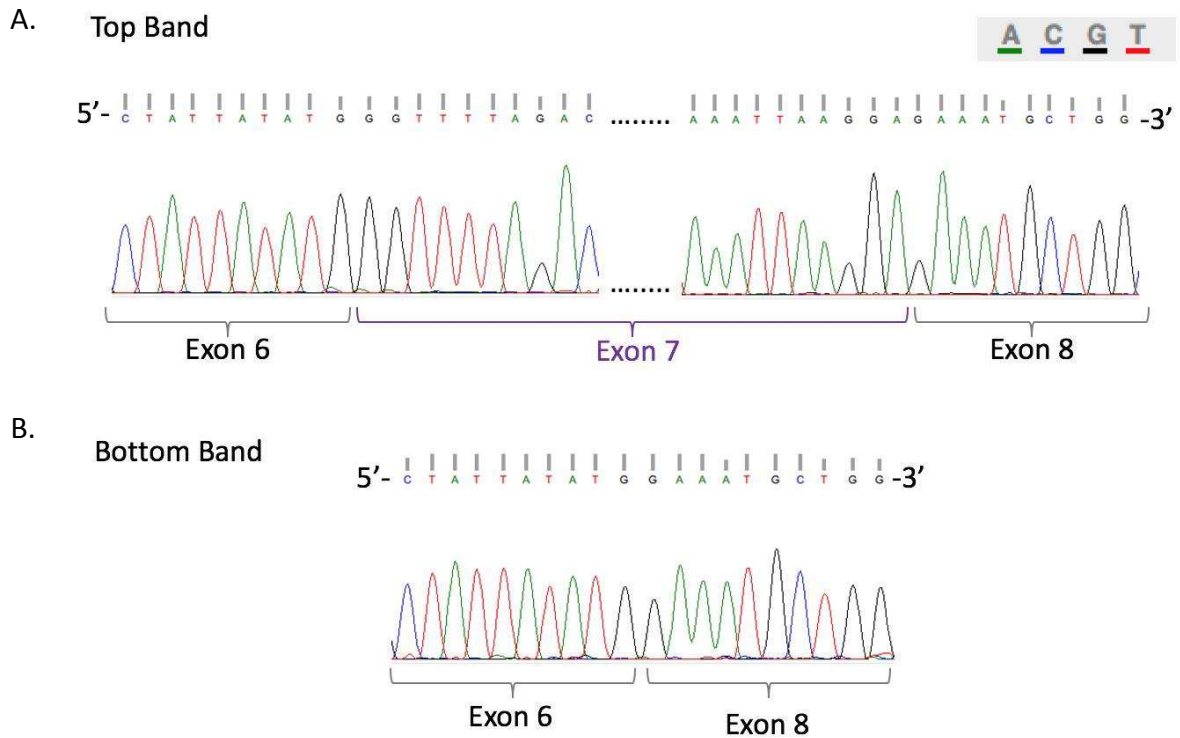


Figure 3-6: cDNA sequence analysis of *SMN2*

(A) cDNA sequence of the top band. *SMN2* transcript contain exon 7 in its natural position. (B) cDNA sequence of the bottom band. *SMN2* is missing exon 7. The exon 6/exon 8 junction is present in the sequence data sequence of the bottom band.

At the highest concentration of 10 μ M, all three PMOs show a statistical increase in exon 7 inclusion ($p < 0.05$). Western blotting analysis [Figure 3-8] showed a significant increase in SMN protein production in the 10 μ M treatments ($p < 0.01$), however, no significant increase was observed at the 1.0 μ M concentration. Statistical significance was determined using the one-way ANOVA analysis. Data distribution was confirmed to be normal via Shapiro–Wilk test.

Dose-dependent analysis of PMOs in patient fibroblasts (GM09677)

Human SMA fibroblasts GM09677 were chosen to be tested because they also have two copies of the *SMN2* gene. My goal was to see if similar conclusions can be reached using cells with the same phenotype. SMA patient GM09677 fibroblasts were treated with PMO 7, 8 and 9 at 0.1 μ M, 1.0 μ M and 10 μ M each. Semi-quantitative RT-PCR analysis [Figure 3-9] shows that fibroblasts treated with 0.1 μ M PMOs did not have a significantly increased amount of exon 7 inclusion. Treatment of fibroblasts with 1.0 μ M and 10 μ M significantly increased the amount of full-length *SMN2* transcript relative to the mock treatment ($p < 0.05$). Western blot analysis [Figure 3-10] showed that this cell line was more susceptible to PMO treatment at the 1.0 μ M concentration, as both PMO 7 and 9 significantly increased SMN protein production ($p < 0.05$). At the 10 μ M concentration, significant increases were also seen using PMOs 8 and 9 ($p < 0.05$), as well as PMO 7 ($p < 0.01$). As seen with the GM03813 fibroblasts, treatments at 0.1 μ M with any of the PMOs failed to produce statistically significant results.

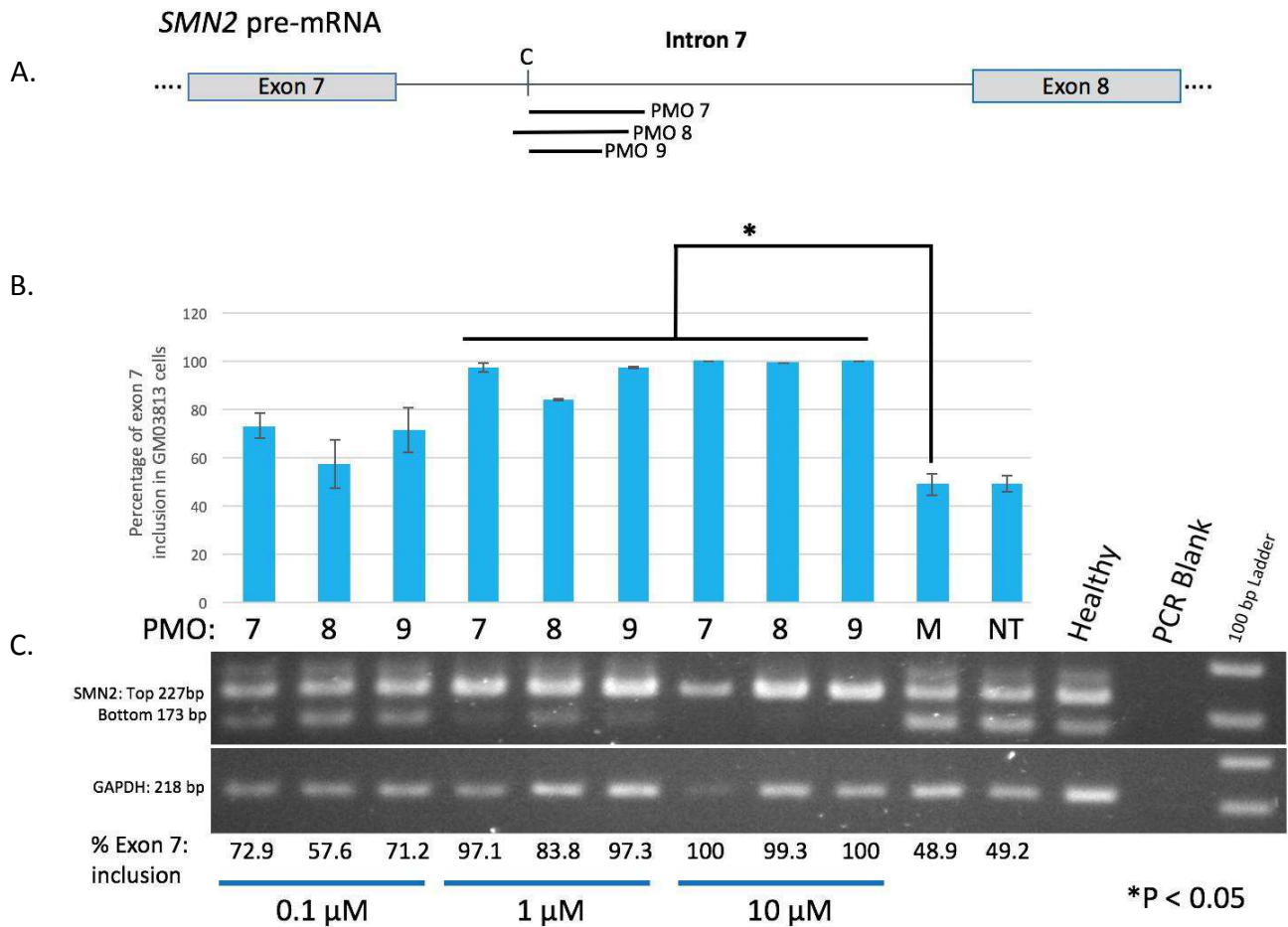


Figure 3-7: Dose-dependent analysis showing exon 7 inclusion efficacy of ISS-N1 targeting PMOs in the GM03813 SMA patient fibroblasts

(A) Diagrammatic representation of PMO annealing positions along the *SMN2* pre-mRNA transcript. (B) Histogram representing percentage of exon 7 inclusion in GM03813 cells following a 48 hour PMO transfection period. Treatments were normalized to the non-treated control, and compared to the mock sample using one-way ANOVA analysis. Data was shown to be normal via the Shapiro-Wilk test. (C) Semi-quantitative RT-PCR analysis depicting the percentage of exon 7 inclusion post transfection. (M: mock control; NT: non-treated control).

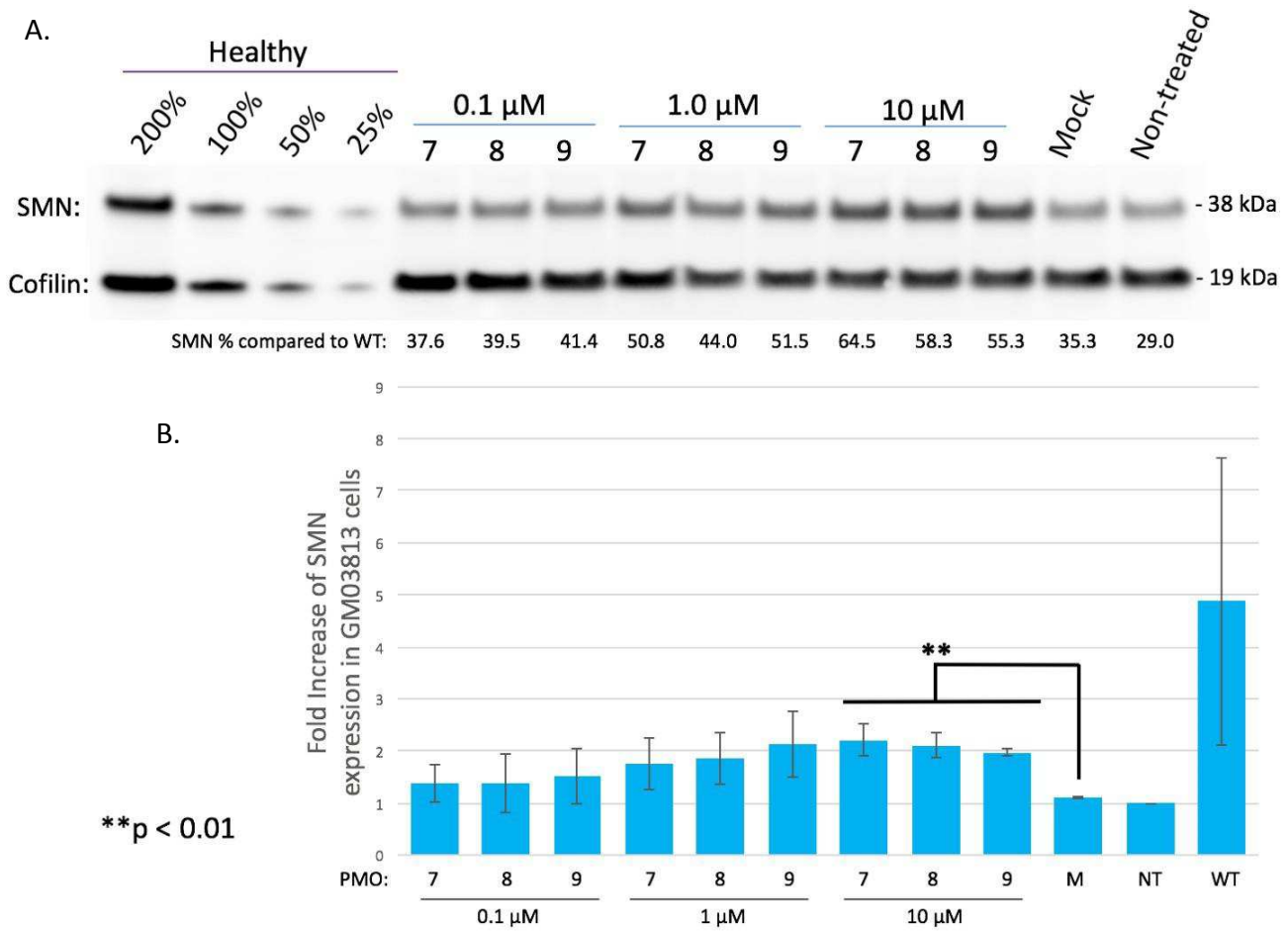


Figure 3-8: Dose-dependent analysis testing the ability of PMOs targeting ISS-N1 to promote SMN protein production in GM03813 SMA patient fibroblasts

(A) Western blot analysis of SMN protein quantity relative to healthy controls. (B) Histogram representing fold increase of SMN protein production in GM03813 fibroblasts following a 48 hour PMO transfection period. Treatments were normalized to the non-treated control, and compared to the mock sample using one-way ANOVA analysis. Data was shown to be normal via the Shapiro-Wilk test. (M: mock control; NT: non-treated control; WT: healthy control).

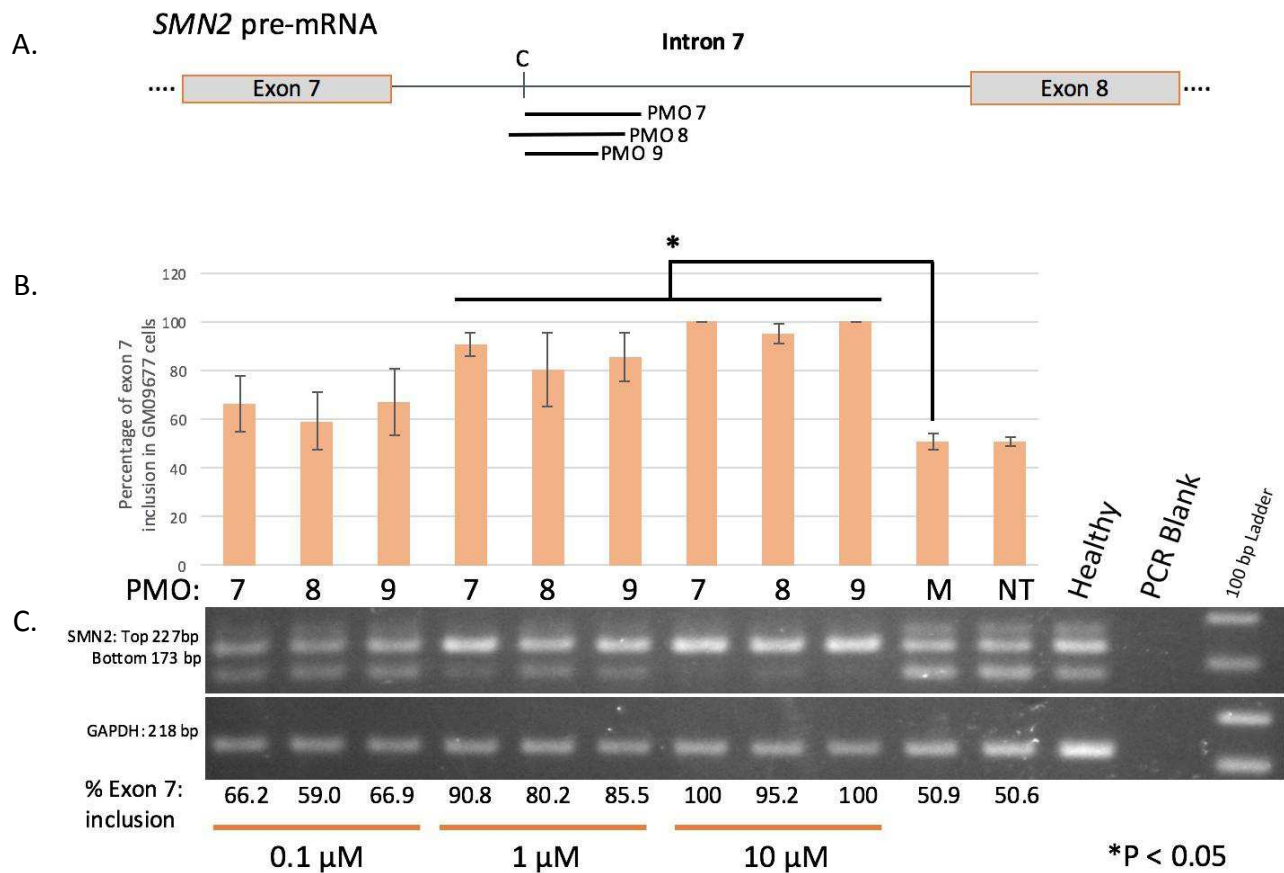


Figure 3-9: Dose-dependent analysis showing exon 7 inclusion efficacy of ISS-N1 targeting PMOs in the GM09677 SMA patient fibroblasts

(A) Diagrammatic representation of PMO annealing positions along the *SMN2* pre-mRNA transcript. (B) Histogram representing representing percentage of exon 7 inclusion in GM09677 cells following a 48 hour PMO transfection period. Treatments were normalized to the non-treated control, and compared to the mock sample using one-way ANOVA analysis. Data was shown to be normal via the Shapiro-Wilk test. (C) Semi-quantitative RT-PCR analysis depicting percentage of exon 7 inclusion post transfection. (M: mock control; NT: non-treated control samples).

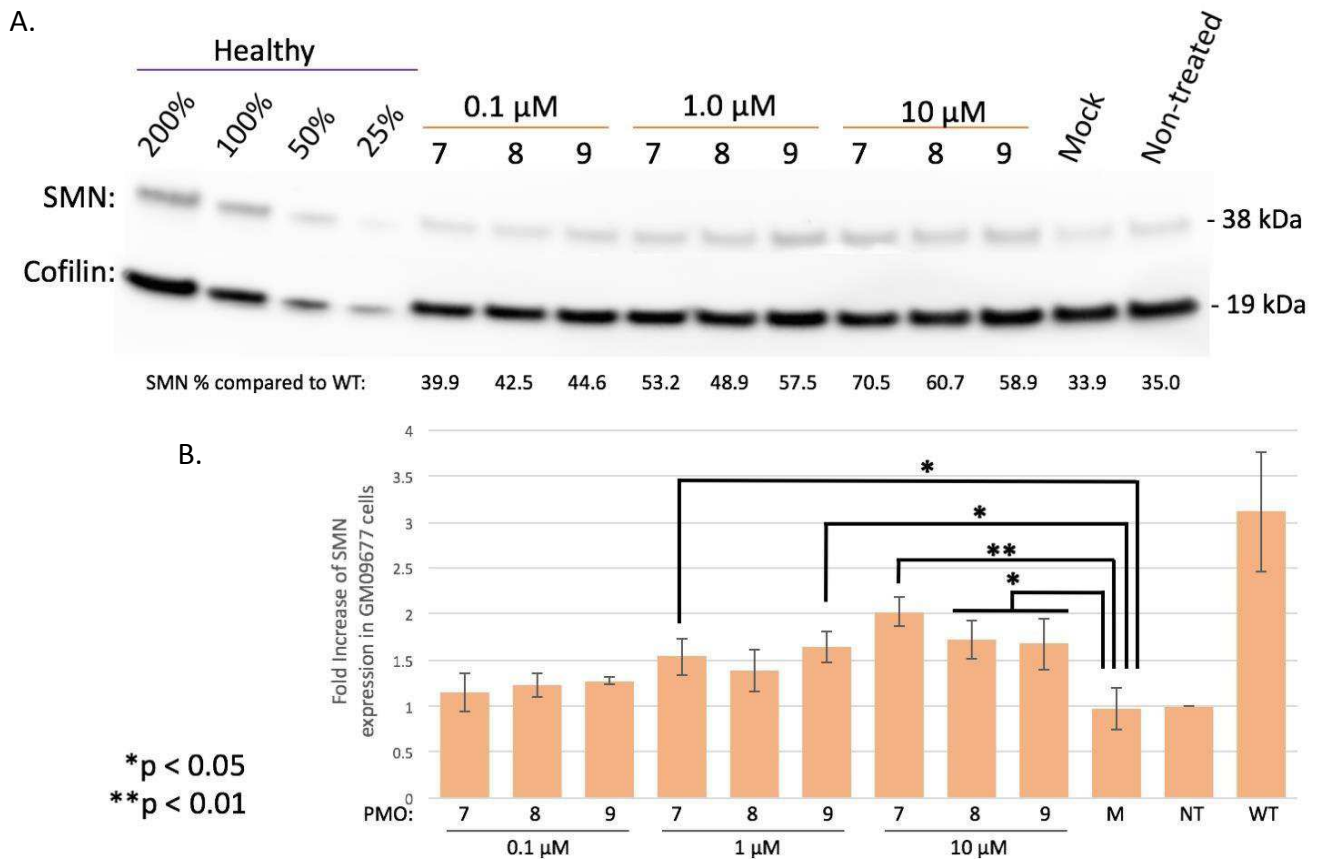


Figure 3-10: Dose-dependent analysis testing the ability of PMOs targeting ISS-

N1 to promote SMN protein production in GM09677 SMA patient fibroblasts

(A) Western blot analysis of SMN protein quantity relative to healthy controls. (B) Histogram representing fold increase of SMN protein production in GM09677 fibroblasts following a 48 hour PMO transfection period. Treatments were normalized to the non-treated control, and compared to the mock sample using one-way ANOVA analysis. Data was shown to be normal via the Shapiro-Wilk test. (M: mock control; NT: non-treated control; WT: healthy control).

Dose-dependent analysis of PMOs in patient fibroblasts (GM00232)

Human SMA fibroblast cell line GM00232 was the final cell line tested. It was chosen because it has only one copy of the *SMN2* gene. SMA patient GM00232 fibroblasts were treated with PMO 7, 8 and 9 at 0.1 μM , 1.0 μM and 10 μM each. Semi-quantitative RT-PCR analysis [Figure 3-11] showed that fibroblasts treated with 0.1 μM PMOs did not significantly increase amount of exon 7 inclusion, results that were consistent with the other two cell lines. Fibroblasts treated with 1.0 μM and 10 μM resulted in a significant increase in the amount of full-length *SMN2* transcript relative to the mock treatment ($p < 0.05$). Western blot analysis [Figure 3-12] showed that only the 10 μM PMO 7 treatment resulted in a significant increase in SMN protein ($p < 0.05$). All other treatments did not reach a statistical level of significance. This result indicates that *SMN2* copy number may play an important role in the efficacy of antisense therapy.

PMO 7 rescues nuclear gem phenotype in SMA patient fibroblasts

As I previously tested to see if induction of exon 7 inclusion leads to higher SMN protein production, I wanted to examine if the increase in SMN protein leads to a recovery of nuclear gem phenotype. After testing the top three PMOs in three different cell lines, I chose PMO 7 for follow up immunocytochemistry experiments. GM03813 SMA patient fibroblasts were treated with 10 μM of PMO 7 for 48 hours. Preliminary data shows that antisense therapy is capable of rescuing the nuclear gem phenotype in SMA patient cells [Figure 3-13]. Nuclear gem localization can be seen in both healthy and PMO 7 treated cells, while absent in the mock

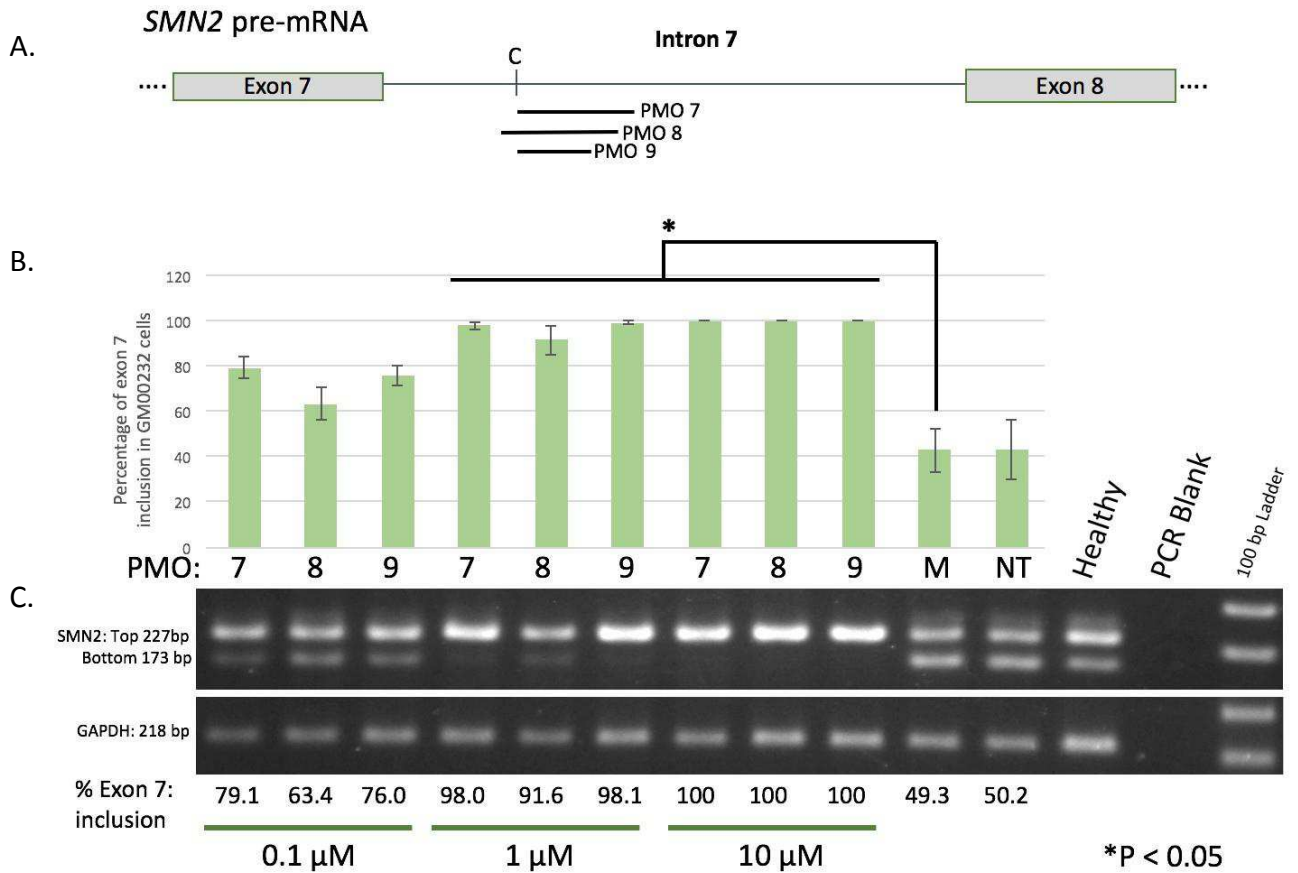


Figure 3-11: Dose-dependent analysis showing exon 7 inclusion efficacy of ISS-N1 targeting PMOs in the GM00232 SMA patient fibroblasts

(A) Diagrammatic representation of PMO annealing positions along the *SMN2* pre-mRNA transcript. (B) Histogram representing representing percentage of exon 7 inclusion in GM00232 cells following a 48 hour PMO transfection period. Treatments were normalized to the non-treated control, and compared to the mock sample using one-way ANOVA analysis. Data was shown to be normal via the Shapiro-Wilk test. (C) Semi-quantitative RT-PCR analysis depicting the percentage of exon 7 inclusion post transfection. (M: mock control; NT: non-treated control).

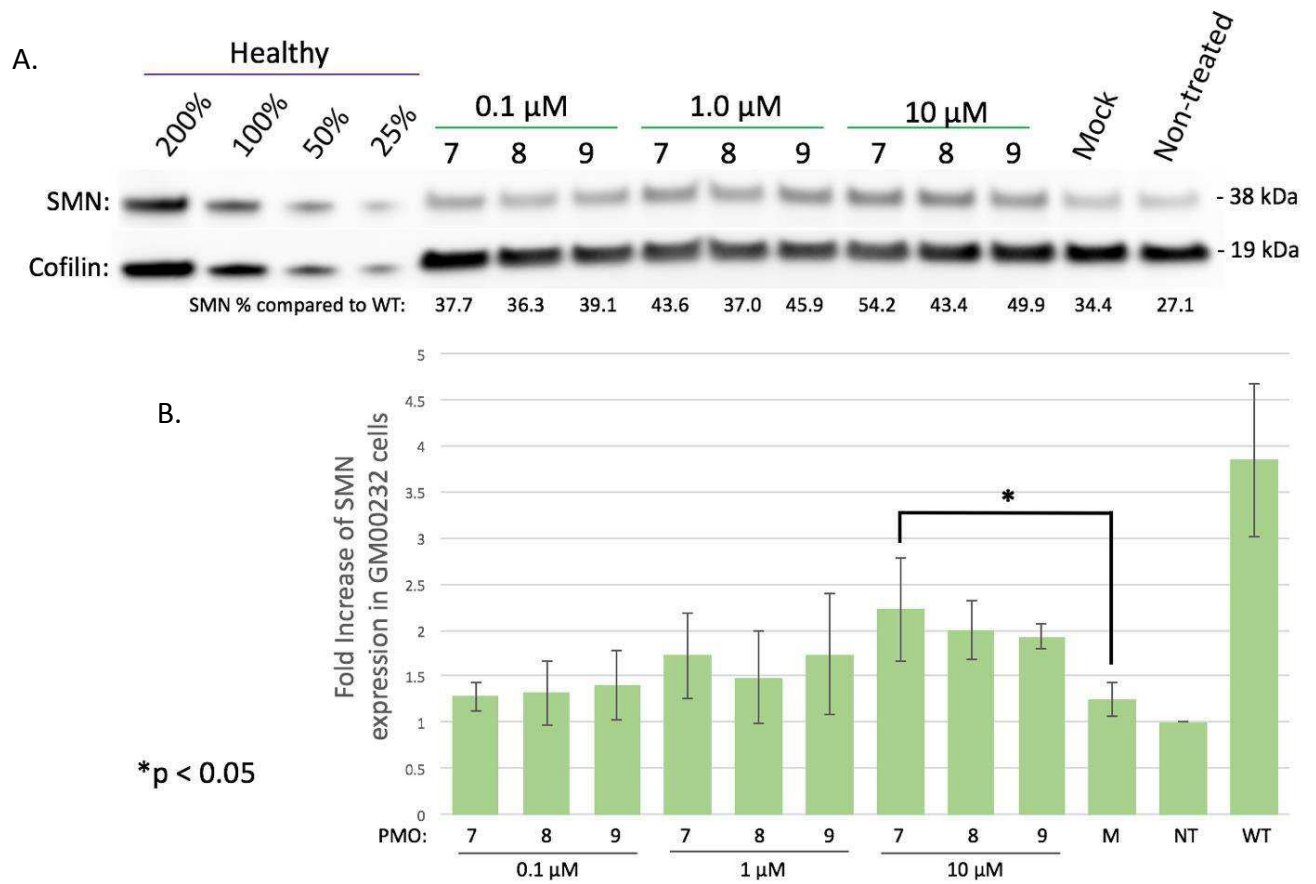


Figure 3-12: Dose-dependent analysis testing the ability of PMOs targeting ISS-N1 to promote SMN protein production in GM00232 SMA patient fibroblasts

(A) Western blot analysis of SMN protein quantity relative to healthy controls. (B) Histogram representing fold increase of SMN protein production in GM00232 fibroblasts following a 48 hour PMO transfection period. Treatments were normalized to the non-treated control, and compared to the mock sample using one-way ANOVA analysis. Data was shown to be normal via the Shapiro-Wilk test. (M: mock control; NT: non-treated control; WT: healthy control).

and non-treated samples. Z-stacking using confocal microscopy confirmed that the visible nuclear gems are within the nucleus.

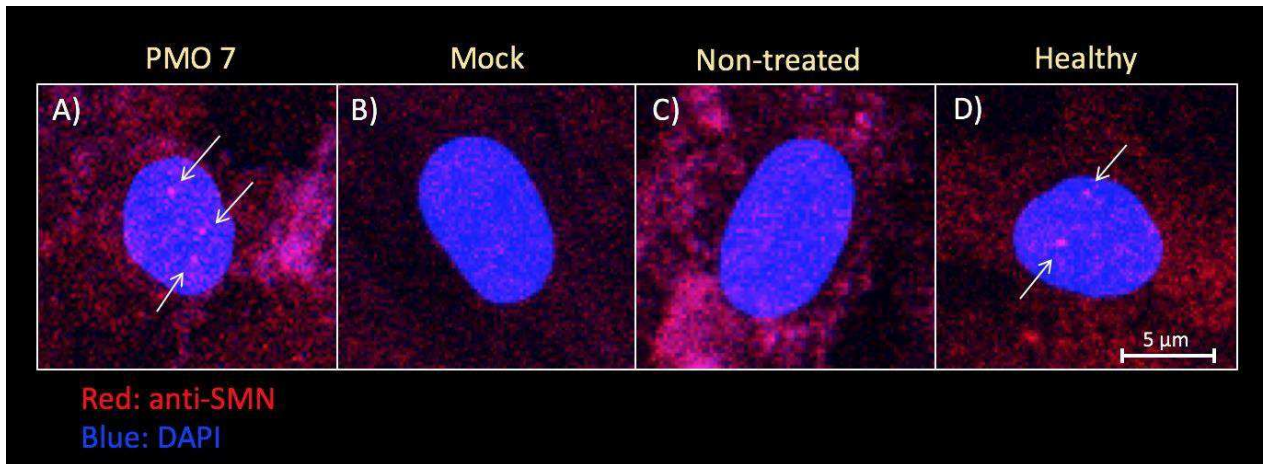


Figure 3-13: Antisense therapy using PMO chemistry recovers nuclear gem phenotype in SMA patient cell lines.

(A) Human SMA fibroblasts (GM03813) treated with 10 μ M PMO 7. Arrows indicate nuclear gem localization within the nucleus. (B). Mock PMO treatment. No visible nuclear gems (C) Non-treated GM03813 SMA fibroblasts. No visible nuclear gems were present. (D) Non-treated healthy cells. Arrows indicate nuclear gem localization within the nucleus. Results are preliminary, based on one successful round of immunocytochemistry.

CHAPTER 4

Effect of novel splice switching LNA-based antisense oligonucleotides in SMA patient cells

All data collected in this chapter was done with the help of BIOL 499 student Nicole McRorie

4.1 Background

The LNA chemistry is another class of nucleic acid analog that has both high affinity and specificity for its complementary DNA or RNA target. Other benefits of LNAs are that they have an excellent aqueous solubility, high stability, and their toxicity in biological systems is relatively low (Jepsen *et al.* 2004). As with the PMO experiments, I set out to develop a set of novel antisense oligonucleotides capable of exon 7 inclusion and subsequent “knock-up” of SMN protein. A recent publication showed that integrating DNA bases in an alternating fashion with LNA bases improves the ASOs ability to affect splicing (Shimo *et al.* 2014). Unlike PMOs, LNAs retain the classic negative charge seen in the RNA backbone which gives them more freedom to cross biological barriers. LNAs are also used in research at much lower concentrations than PMOs, which may make any future treatment more affordable.

To build off of the success of the PMO data, in this section, I examined the effect of newly designed LNA and LNA/DNA hybrid sequences targeting the ISS-N1 splice silencer. Although the screening is much narrower, the overall objective remains the same: to identify the most effective antisense treatment for SMA. Each of the LNA sequences was examined using the online BLAST (<http://blast.ncbi.nlm.nih.gov/Blast.cgi>) software to check for any potential negative off-target effects, none of which presented any reason for concern. Unlike with PMO work, LNAs have seen little use in SMA research. Designing an LNA-based therapy which can successfully ameliorate the SMA phenotype in a severe mouse model would be a big step in this field of research.

4.2 Results: Novel LNA-based ASO screening

LNAs screening at multiple transfection concentrations

Novel LNAs were tested at multiple transfection amounts to determine an optimal concentration where efficacy between LNAs is observable. Human patient SMA fibroblasts (GM03813) were transfected with LNA 1-8 at 200 nM, 100 nM, 50 nM, 25 nM, 5 nM and 1 nM [Figure 4-1]. LNAs were co-transfected with Lipofectamine RNAiMAX reagent for 48 hours. LNA 1-5 all showed complete exon 7 inclusion at transfections ranging from 25 nM up to 200 nM. 1 nM transfection failed to produce different results from the mock and non-treated samples. 5 nM transfections retained lower bands a lower band in all of the samples, which allows for quantification of efficacy so I could determine the most effective LNA for treating SMA cells.

Screening for the optimal LNA using semi-quantitative RT-PCR

Once the optimal transfection level was established, I wanted to statistically evaluate the efficacy of each individual LNA sequence. Human patient SMA fibroblasts (GM03813) were transfected with LNA 1-8 at 5 nM. Semi-quantitative RT-PCR was to determine whether the LNA-based antisense oligonucleotides are able to induce exon 7 inclusion at a statistically significant level compared to the mock sample [Figure 4-2]. Kruskal–Wallis analysis shows that LNA 1 is able to reliably increase exon 7 inclusion in *SMN2* mRNA ($p < 0.05$).

Western blot analysis reveals the importance of transfection concentration in patient SMA fibroblasts.

After confirming the effect of LNAs of exon 7 inclusion, I wanted to see if that change translates into production of full-length SMN protein. Human SMA fibroblasts (GM03813) were transfected with 5 nM of each LNA for 48 hours. Results indicate the length of LNA plays a role in how effective it is in producing full-length I protein product [Figure 4-3]. LNA 1 (30 bp) shows an increase in full-length SMN production across all biological replicates, resulting in a high level of statistical confidence ($p < 0.005$). LNAs 2 and 3 (18 bp) also increased the amount of SMN protein with high confidence. ($p < 0.01$). LNA 5 (13 bp), although not as statistically strong as the other treatments ($p < 0.05$), may be a more viable candidate for *in vivo* trials due to its shorter length. I also tested LNA efficacy with 25 nM transfections, as early RNA screening showed full exon 7 inclusion. It was surprising to see that not only were the LNAs less effective (only LNA 3 attained statistical significance ($p < 0.05$)) than in the 5 nM transfections, LNA 1 produced a new band detectable by anti-SMN antibodies around the 34 kDa mark. This result indicates that at the 25 nM levels the LNAs may have an adverse toxic effect that requires further investigation.

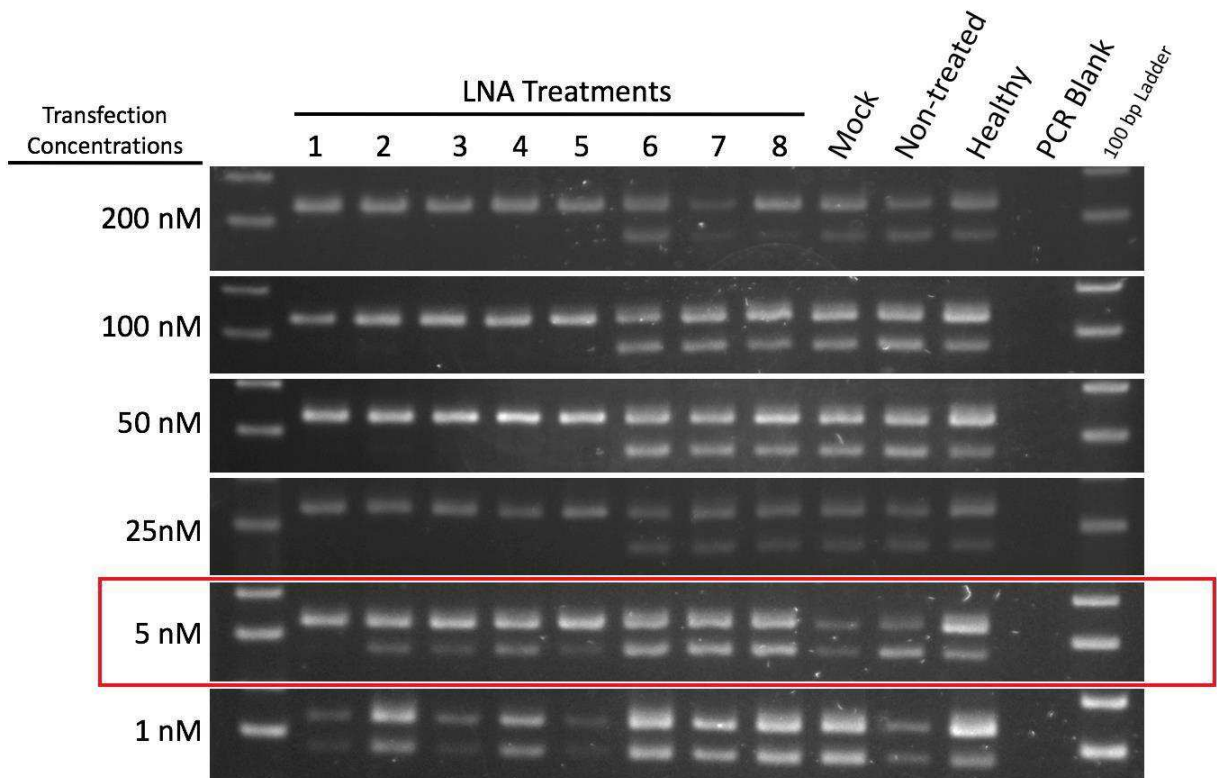
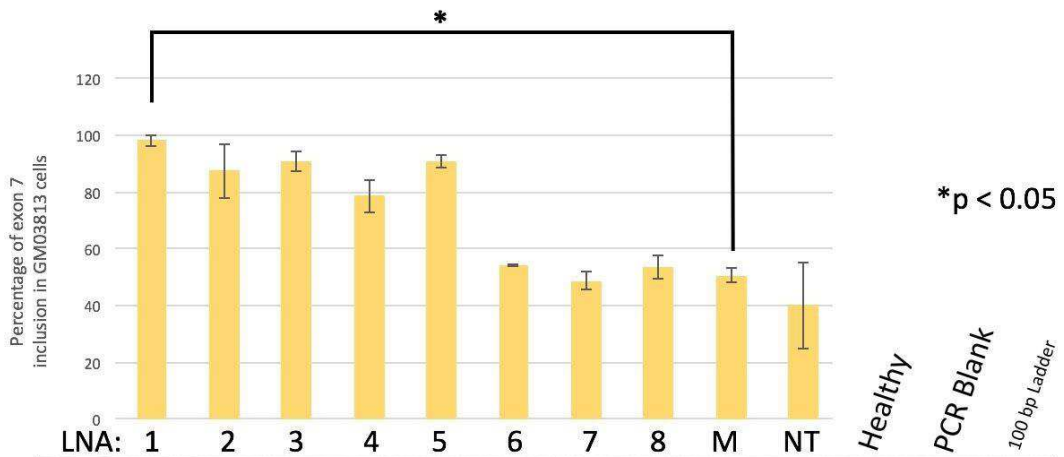


Figure 4-1: Novel LNAs screened across multiple concentration levels.

Semi-quantitative RT-PCR analysis showing exon 7 incorporation in post-transcriptional *SMN2* mRNA induced by novel LNA-based oligomers. Human patient SMA fibroblasts (GM03813) were transfected with novel LNAs 1-8. (co-transfected with Lipofectamine RNAiMAX). The splicing effect was determined 48 hours after transfection. Total RNA was amplified with *SMN2* specific primers. Transfection levels at 5 nM resulted in lower bands in all treatments, which allows for differentiation in treatment efficiency among LNA sequences.

A.



B.

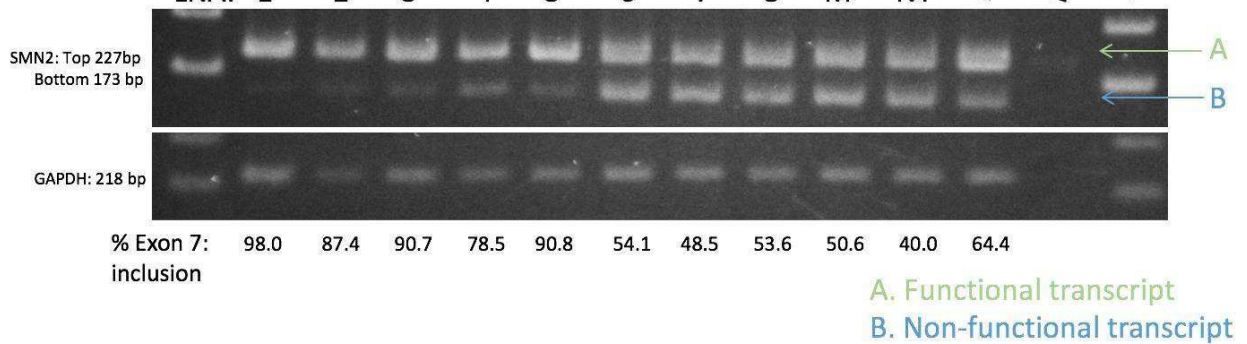


Figure 4-2: Efficacy of novel LNA antisense oligonucleotides to induce exon 7 inclusion in SMA patient cells.

(A) Histogram representing representing percentage of exon 7 inclusion in GM03813 cells following a 48 hour 5 nM LNA transfection period. Data obtained from treatment results was non-parametric. A sum of ranks (Kruskal-Wallis test) was done to rank treatment exon 7 inclusion efficacy. (B) Semi-quantitative RT-PCR analysis depicting the percentage of exon 7 inclusion post transfection. (M: mock control; NT: non-treated control)

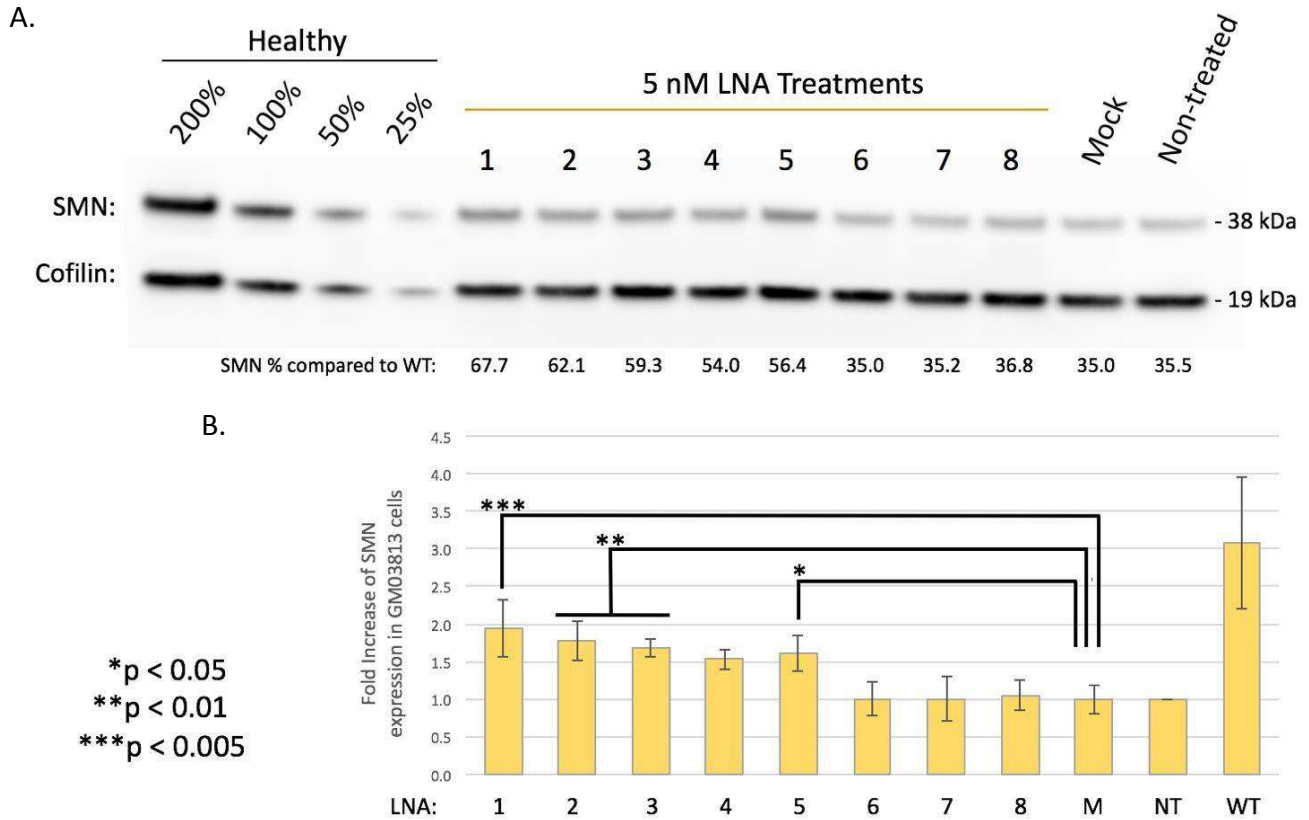


Figure 4-3: Efficacy of novel LNA antisense oligonucleotides to promote full-length SMN protein production in SMA patient cells.

(A) Western blot analysis of SMN protein quantity relative to healthy controls. (B) Histogram representing fold increase of SMN protein production in GM03813 fibroblasts following a 48 hour 5 nM LNA transfection. Treatments were normalized to the non-treated control, and compared to the mock sample using one-way ANOVA analysis. Data was shown to be normal via the Shapiro-Wilk test. (M: mock control; NT: non-treated control; WT: healthy control).

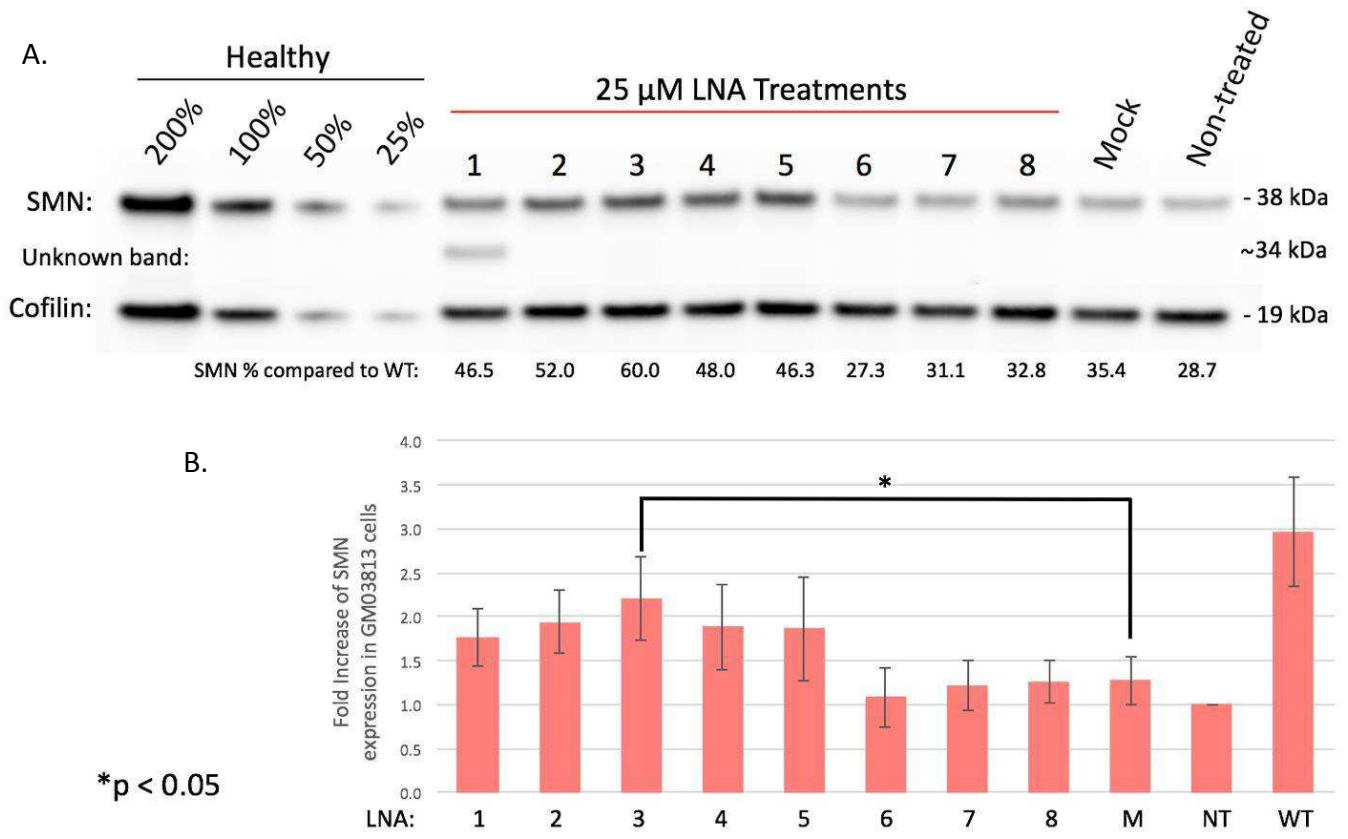


Figure 4-4: 25 nM transfections reduce efficacy of LNAs to produce SMN protein production in SMA patient cells.

(A) Western blot analysis of SMN protein quantity relative to healthy controls. LNA 1 produces a new band when transfected at 25 nM (B) Histogram representing fold increase of SMN protein production in GM03813 fibroblasts following a 48 hour 25 nM LNA transfection. Treatments were normalized to the non-treated control, and compared to the mock sample using one-way ANOVA analysis. Data was shown to be normal via the Shapiro-Wilk test. (M: mock control; NT: non-treated control; WT: healthy control).

Effect of LNAs of patient SMA fibroblasts nuclear gem phenotype

To check if LNAs are capable of restoring nuclear gem phenotype, patient SMA fibroblasts (GM03813) were transfected with 5 nM of LNA 1, 3 and 5 for 48 hours. Preliminary immunocytochemistry data suggests that none of the treated samples showed distinct nuclear gem localizations in the nuclei as seen in the healthy control cells. All treated samples appeared similar to the mock and non-treated controls [Figure 4-5]. Further optimization may be needed to see recovery of phenotype after LNA treatment.

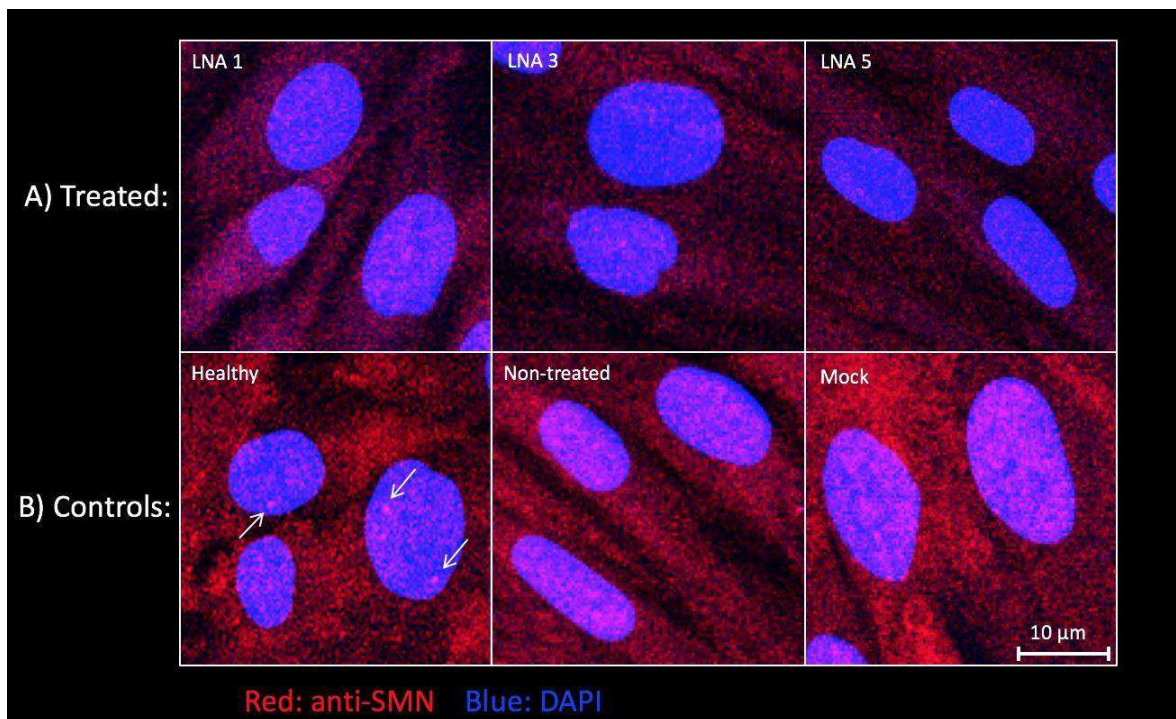


Figure 4-5: LNAs 1, 3 and 5 fail to restore nuclear gem phenotype in patient SMA fibroblasts.

(A) Patient SMA fibroblasts transfected with LNA 1, 3 and 5 at 5 nM for 48 hours. Red staining represents SMN protein, nuclei stained with blue DAPI. None of the treated samples showed any difference between mock and non-treated conditions, as they all lacked distinct nuclear gem bodies. (B) Healthy, mock and non-treated control cells. Healthy control cells contained nuclear gems localized in the nucleus indicated by the white arrows.

CHAPTER 5

Discussion

The application of antisense therapy in SMA

The use of antisense therapy for spinal muscular atrophy is quite unique, as it aims to increase the amount of protein produced rather than to induce a knockdown effect. What makes it truly different is that it does not target the gene at fault, or an upstream/downstream target of that gene. Deficiency in SMN protein, produced primarily by the *SMN1* gene, is the direct cause of SMA. The *SMN2* gene evolved from an inverted duplication of a 500 kb region within chromosome 5, and is unique to the human population (Saugier-Veber *et al.* 2001; Rochette *et al.* 2001). If no functional copy of the *SMN1* is present, patients become reliant on their *SMN2* gene for SMN production. Due to an inherent C-to-T transition within the gene that leads to a change in splicing, *SMN2* is only capable of producing approximately 10% functional SMN protein relative to *SMN1*. Naturally, *SMN2* became a highly sought after therapeutic target.

The scientific community agrees that *SMN2* can be made to produce more functional full-length SMN protein and, therefore is a good therapeutic target for treating SMA. The current question is: “What is the best method of achieving this goal”? Using antisense therapy to target silencers along the *SMN2* pre-mRNA to alter how it will be spliced continues to be thoroughly investigated, particularly within the ISS-N1 silencer region.

The foundation of this project was to design novel antisense oligonucleotides targeting various silencers along different regions within the *SMN2* gene, hinging on the hypothesis that longer ASOs may be more effective at increasing the amount of functional SMN protein. Once I determined the optimal target site, I tested multiple ASO chemistries to identify which is most suitable for treatment. The PMO chemistry was chosen for screening our sequences, as it was

relatively new to the SMA field. PMOs were promising as they were biologically stable, had a high specificity to target pre-mRNA and showed no signs of toxicity in *in vivo* mouse experiments (Zhou *et al.* 2013).

Initial PMO screening shows ISS-N1 is the most suitable target site for PMOs.

In this study, my colleagues and I designed several new PMOs targeting four different regions along the *SMN2* pre-mRNA, along with several PMO sequences previously shown to be effective. In order to increase SMN quantity, I first needed to correct RNA splicing so that full-length *SMN2* transcript could be produced. I used semi-quantitative RT-PCR to evaluate the percentage of the *SMN2* transcript containing exon 7 after each PMO treatment. PMOs targeting Element-1 were designed to cover a portion of the silencer, so that its influence on the spliceosomal machinery would be weakened or completely suppressed. These sequences were made based on previous work done using the 2'-O-methyl with a phosphorothioate backbone (2'-O-MePS) antisense chemistry (Miyajima *et al.* 2002). It was interesting to see that these PMOs had an inverse effect compared to what I expected. This is seen most prevalently in the PMO 3 treatment, where compared to the mock and non-treated controls, the amount of full-length *SMN2* post-transcriptional mRNA was reduced. One possibility is that the change in antisense chemistry may play a role in the ASO function, although reversing the effect is quite unlikely. Another possibility is that the larger size of the PMO chemistry may have a steric effect where it prevents the spliceosomal machinery from being able to incorporate exon 7. Although PMO 3 is shorter in length than PMOs 1 and 2, its position targets a more downstream area

closer to exon 7 itself. Sequences that lie closer to exon acceptor sites fail to induce exon 7 inclusion.

This idea is supported by the PMO 4, 5 and 6 results which target exon 7 directly. These PMOs were designed to position themselves close to the 3' end of exon 7 to promote the exons inclusion into the mature *SMN2* transcript. The C-to-T transition mutation region on exon 7 was not targeted because the transcription regulator Sam68 binds to that region, making ASO hybridization within that region unfavorable (Pedrotti *et al.* 2010). PMO 3, the longest of the 3 PMOs targeting exon 7 had the most obvious effect on preventing the inclusion of exon 7. These screening results indicate that if you want to successfully induce the inclusion of an exon, you cannot place the ASO too close to acceptor or donor sites recognized by the spliceosome. This becomes more evident in DMD research, where in order to promote exon skipping, many of the successful ASO treatments lay across the acceptor or donor site region (Mendell *et al.* 2016).

The next region that was targeted was the ISS-N1 intronic splice silencer. All three PMOs (PMO 7, 8 and 9) that targeted that location induced complete incorporation of exon 7 into the final *SMN2* transcripts. As no bottom bands were observable, it indicates that not only are these PMOs 100% effective, but also that the transfection efficacy was extremely high. As this RNA screening result was replicated three times, the results for PMO 1-6 can be attributed to the ineffectiveness of the sequence/chemistry itself rather than the inability of the ASO to get to its target. PMOs 10 and 11 were designed with the same line of thinking as the PMOs targeting exon 7, and failed at showing any difference from the mock and non-treated controls.

Hybrid and cocktail PMO screening

Two alternative strategies I tested were cocktail PMOs and hybrid PMOs. The cocktail PMO treatments were designed to incorporate the use of smaller sequences working in tandem to induce exon 7 inclusion, facilitating the production of full-length *SMN2* mRNA. The first set of PMO cocktail (PMO 12 and 13) showed an increase in exon 7 inclusion efficacy compared to mock samples when tested individually and together. It is important to note that cocktail treatment contained 10 μ M of each PMO, so the exon 7 inclusion effect may be additive rather than the two components working synergistically. The second cocktail set (PMO 15 and 16) did not show any promising results. As previously mentioned, the position of PMO 15 is very close to the exon 7 splice donor site, and may be contributing to the exclusion of exon 7. Both individual and combined treatments showed unfavorable results. PMO 14 was designed to target two positions at once, while connecting two sections with non-complementary bases. The effect of this strategy appears to be unfavorable, but that is most likely due to its close position on the exon 7 splice donor site.

The hybrid PMOs were designed to target Element-1 and ISS-N1 simultaneously. Each PMO was made so that half the sequence hybridized to Element-1, while the other hybridized to the ISS-N1 silencer. The goal was to develop a single treatment capable of suppressing both silencers, allowing for an additive effect to induce exon 7 inclusion. The portion of the PMOs that hybridized to ISS-N1 all began at the -10 cytosine position and continues downstream. As the previous screening results showed that PMOs targeting Element-1 directly were ineffective, I instead designed the sequence to flank the silencer as done successfully in previous research done by the Lorson group (Osman *et al.* 2014). In their study they designed a hybrid PMO

flanking both ends of the Element-1 silencer. I ordered this sequence as a potential positive control (PMO 21). Based on the screening results I concluded that the hybrid PMOs would be ineffective, as 10 μ M transfections were not able to induce 100% exon 7 inclusion I previously observed. Although PMO 21 appeared to be effective when used *in vivo* by the Lorson group (Osman *et al.* 2014), in my experiment they failed to induce any sort of effect on the patient cells, with results that appeared similar to the mock and non-treated controls. This leads us to believe that the sequences flanking Element-1 are not contributing the treatment effect. Most likely, PMO 17-20 have an effect on exon 7 inclusion due the portion complementary to the ISS-N1 region, but they are not as effective as PMOs 7-9 because the complementary region is shorter, and it is possible the extra Element-1 targeting region further weakens its effect.

Identifying efficacy of SMN protein “knock-up” at varying transfection concentrations

Achieving high levels of exon 7 inclusion would not be beneficial if that result didn't translate to a subsequent increase in full-length SMN protein production. I followed up on my original RT-PCR screening experiment with an identical experiment to identify SMN protein expression level. The Western blot results supported the data obtained from RT-PCR screening, showing that PMO 7, 8 and 9 do indeed increase SMN protein production by a large margin relative to all other treatments. Follow up protein analysis was not done for the cocktail and hybrid PMO screens, as they were not as effective as PMO 7, 8 and 9.

Before moving forward, I looked at the effect of my most successful PMOs from the screening at reduced transfection concentrations. I chose 1 μ M, 3 μ M and 5 μ M as my transfection amounts, and carried out the subsequent RT-PCR and Western blot experiments.

Results indicated that even at these lower concentrations the PMOs were still quite effective. An interesting observation was that PMO 7 was more effective relative to PMO 8 and 9 as the concentrations were increased. The PMOs co-transfection with EndoPorter ensures that the PMOs get past the cell membrane via endocytosis, however, longer PMOs may not be able to pass through the nuclear membrane as readily as shorter ones. This may mean that the longer sequence of PMO 7 may be more effective for antisense therapy once it reaches its destination. PMOs 7-9 were also tested at even lower concentrations (data not shown) to see at which level the treatments became ineffective. These results were used to set the transfection ranges to the dose-dependent experiments.

PMO 7, 8 and 9 induce exon 7 inclusion and increased SMN production in multiple SMA patient cell lines

To test the efficacy of our newly designed PMOs (PMO 7 and 8), and the PMO version of a sequence currently in clinical trials (PMO 9), I performed a dose-dependent transfection analysis set at 0.1 μ M, 1.0 μ M and 10 μ M. I tested the effect of these three PMOs in three different SMA patient fibroblast cell lines. The concentration range was chosen based on my previous observations. All cell lines tested came from patients clinically diagnosed with type I SMA. The first set of dose-dependent analyses were done on type I GM03813 SMA fibroblasts that contain two copies of the *SMN2* gene. Transfections at 10 μ M showed a significant increase in both exon 7 inclusion and SMN protein production for all three PMOs. At the mRNA level it was clear that PMO transfection at 1 μ M was still very effective, however, this result did not translate into a significant increase in SMN protein production over the mock treated

samples. Based on the results obtained from this cell line, I concluded that all three PMOs are capable of inducing exon 7 inclusion and a subsequent increase in SMN protein production when there is a sufficient concentration of PMO in the transfection. A limitation to the data obtained from this set of results is that I could not differentiate between the efficacy of the PMOs within the treatment group.

The second set of dose-dependent analyses was done on type I GM09677 SMA fibroblasts, which also contain two copies of the *SMN2* gene. Data from these experiments proved to be more informative. Not only were there statistical differences at 1.0 μ M transfections in the Western blot analysis, but also within the 10 μ M treatment group. In the 1.0 μ M transfections, both PMO 7 and 9 resulted in a statistically significant increase in SMN protein. This is an important result when considering future *in vivo* studies, as the goal is to use the minimum amount of drug to ameliorate disease symptoms. The 10 μ M treatments showed that PMO 7 had a much higher confidence with a p-value below 0.01. This result supports my hypothesis that longer PMOs may more effective at blocking silencer effects, as we have more confidence in the PMO 7 effects. Both PMO 8 and 9 showed statistical significance as will with a p-value less than 0.05.

The third set of dose-dependent analyses was done on type I GM00232 SMA fibroblasts, which contain only one copy of the *SMN2* gene. The results obtained from RT-PCR analysis were similar to that of the previous cell lines, however, the Western blot analysis indicates that the treatments are less effective when there are fewer copies of *SMN2* present. As the PMOs have fewer targets to treat, it is not possible to produce the same amount of SMN protein “knock-up” as seen when there are more copies of *SMN2*. 1.0 μ M treatments showed no statistically

significant increase in SMN protein production. The results from the 10 μ M treatments support my hypothesis in that a long PMO is more capable of masking the silencer effect, as PMO 7 alone displayed a statistically significant effect on increasing SMN protein production, while all other treatments failed to do so.

In summary, all three PMOs tested are capable of inducing exon 7 inclusion, and significantly increasing the amount of full-length SMN product given there are sufficient therapeutic targets. In cell lines GM03813 and GM09677 I saw that there is variance in treatment effectiveness. While PMO treatments in the GM03813 at 1.0 μ M did not produce significant results ($p > 0.05$), in the GM09677 both PMO 7 and 9 both resulted in a visible increase in protein production. The GM03813 cells however, did respond more to the PMO treatments at 10 μ M as they all obtained a significant result with a p-value less than 0.01, while in the GM09677 cells line only PMO 7 achieved a significant increase. Results from the GM00232 cell line implies that *SMN2* copy number may directly affect treatment efficacy. As more *SMN2* transcript are present, there are more therapeutic targets for the PMOs to hybridize to. Patients with more *SMN2* copies would be expected to respond better to PMO treatments. Importantly, PMO 7 was the only candidate drug capable of producing a significant difference in protein production in a cell line with one *SMN2* copy. If trying to design a drug that can be used for therapy in the greatest number of patients, PMO 7 is the strongest candidate.

Evaluation of novel splice-switching LNA/DNA mixmers targeting ISS-N1

In this study, I also sought to evaluate the efficacy of novel splice-switching LNA/DNA mixmer antisense oligonucleotides. Based on the PMO screening results, I designed new LNAs

to target the ISS-N1 intronic splice silencer starting at the -10 cytosine position end extending downstream. I designed LNAs at varying lengths, with a variety of different LNA and DNA positions. This was done because recently it was reported that activity of LNA/DNA mixmer ASOs was higher than a purely LNA-based sequence (Shimo *et al.* 2014). All LNAs designed were modified to contain a phosphorothioated backbone, as previous work done in our lab showed LNAs without the phosphorothioation have no effect on exon 7 inclusion, most likely due to degradation by endonucleases (data not shown).

First I identified which LNAs were capable of inducing exon 7 inclusion, and then determine which concentration was optimal to evaluate the efficacy of exon 7 inclusion within the group. I initially began my transfections at 200 nM, and lowered the concentration systematically until I reached a level where you could see two visible bands in each lane. At 5 nM I were able to see bottom bands appear in for every treatment, and proceeded to run statistical analysis at this concentration. Semi-quantitative RT-PCR data obtained resulted in a non-parametric data set, however Kruskal-Wallis analysis showed that LNA 1 achieved a significant increase in exon 7 inclusion. Significant results with LNAs at a 5 nM concentration have not previous been reported.

The second objective was to check if the exon 7 inclusion translated into an increase in full-length SMN protein production. I measured SMN protein levels after transfections with 5 nM, as well as 25 nM of the LNAs, because even though transfections at this level induced 100% exon 7 inclusion, I predicted that I could observe a difference in SMN “knock-up” as seen with the PMO results. The 5 nM treatments showed that as the length of the LNA/DNA mixmer increases, there is an increase in full-length SMN protein product. The the treatment with the

that resulted in most confidence was LNA 1, which yielded a statistically significant increase in SMN protein with a p-value less than 0.005. This result supports my original hypothesis that longer ASO sequences are more effective than shorter ones. At the 25 nM transfections, I saw the effectiveness of the LNAs reduced dramatically. This is possibly due to oversaturation of LNA to target sites, leading to toxicity. LNA toxicity is revolved around its high affinity towards RNA. If too much treatment is present, it is possible they interfere with the mRNA translation, resulting in less full-length SMN product produced. A new observation I saw with this experiment is the detection of a new band at ~34 kDa. In this project it is reported for the first time that at higher concentrations, a 30 bp LNA/DNA mixmer is capable of inducing alternate splicing effects when targeting the ISS-N1 silencer. The identity of the new band has not been confirmed, however, I speculate that it may be an alternate SMN splice form that does not contain intron 6. Interestingly, none of the other LNAs transfected at 25 nM produced this effect. If this was a result of the LNA covering a critical point downstream, I would have expected the 30 bp PMOs reproduce this effect, however that observation was not made. Further experimentation is needed to identify the new band, as well as to determine what properties of LNA 1 cause its formation.

Restoring the nuclear gem phenotype in SMA fibroblasts

As I previously tested to see if exon 7 inclusion leads to an increase in full-length SMN protein production, I was also interested in whether an increase in protein production restored the nuclear gem localization in SMA fibroblast nuclei, as seen in healthy cells. Nuclear gems are a marker of cell health, and are not present in cells with insufficient SMN protein (Ebert *et al.*

2009). They represent SMN complex localization to the Cajal bodies within nuclei. While the absence of nuclear gems appears to be non-consequential for fibroblasts, a recent study revealed the importance of nuclear gems in motor neuron survival (Tsuiji *et al.* 2013). In the study I was able to observe nuclear gems in the healthy control, however they were not present in the SMA cell lines. I tested the most effective PMO and LNA treatments to see if it was possible to restore the nuclear gem phenotype in SMA patient fibroblast.

To determine if PMOs could restore nuclear gems, I transfected GM03813 SMA fibroblasts with 10 μ M of PMO 7. Cells were stained with anti-SMN antibody and DAPI to check if the nuclear gems localized to within the nucleus. My preliminary data shows that PMO 7 is capable of restoring the nuclear gems in the fibroblasts. More optimization for the immunocytochemistry experiments is needed, as this result was only seen in one out of three rounds. Different transfection and fixation methods may result in better reproducibility of the experiment.

I also sought to identify whether LNA treatments at 5 nM would restore nuclear gems in SMA patient fibroblasts, as this concentration produced very promising Western blot results. GM03813 fibroblasts were stained with anti-SMN antibody and DAPI to check if the nuclear gems localized to within the nucleus. After three rounds of experiments, I could not find any evidence of nuclear gems in treated SMA cells. One concern that a 48-hour transfection period was too long, and resulted in toxicity at the molecular level, as cell morphology looked normal. Toxicity can arise from the LNAs themselves, or possibly the transfection reagent, which further indicates more optimization for the transfection protocol is needed. Another factor that could lead to the negative results could be the fixation method, as seen with the PMO trials. Further

protocol optimization for immunocytochemistry should be conducted before I could rule out the LNAs ability to restore nuclear gems.

Conclusions and future directions

In this study, I investigated several targeting strategies and two different ASO chemistries with potential to improve current antisense-based treatments in SMA studies. My findings reveal that of all the sites I tested, the ISS-N1 splice silencer is the most suitable target location for antisense therapy for inducing exon 7 inclusion in post-transcriptional *SMN2* mRNA which ultimately leads to an increase in full-length SMN protein production. I demonstrated the importance of both PMO length and position when targeting a silencer. PMO 7 and 9 both begin at the -10 cytosine start site, however, PMO 7 showed greater efficacy in two out of three cell lines tested. Likewise, it is evident that PMO 7 is more effective than PMO 8 even though both are 30 bases long. The difference in their efficacy is due to the position, and even though PMO 8 begins only one base upstream, the effect is quite evident.

I also investigated the efficacy of LNA/DNA mixmer ASOs targeting the ISS-N1 silencer site. In this study, I showed the importance of not only length and chemistry, but treatment quantity as well. Transfections at 5 nM supported my hypothesis that longer ASOs are more effective at both the RNA and protein level. However, SMN protein analysis following a 25 nM transfection revealed that too much of the treatment results in a diminished effect of the treatment, most likely due to cell toxicity.

For both the PMOs and LNAs, it is evident that the immunocytochemistry experiments done to visualize nuclear gems need further optimization to improve both viability and

replicability. In the 10 μ M trial with PMO 7, only one out of three biological rounds resulted in a recovery of phenotype. Though the data at this point is considered preliminary, it is a promising starting point as it falls in line with current literature. As for the LNA trials I was not able to see any positive results. Potential areas that may improve the outcome of future experiments are transfection time and transfection concentrations (of both LNAs and transfection reagents). In addition the fixation methods may need to be further optimized by experimenting with different fixation reagents and conditions.

The clearest direction for future experiments is to test our most effective ASOs in an *in vivo* SMA mouse model. SMA mouse models have a distinct advantage in that they all contain one or more copies of the human *SMN2* transgene. Over the past year I worked on developing an SMA mouse *in vivo* protocol, and my lab has begun breeding mice for future experiments. We began with the FVB.Cg-Smn1^{tm1Hung} Tg(SMN2)2Hung/J mouse line from Jackson laboratories which contain one copy of the mouse *Smn* gene and one copy of the human *SMN2* transgene. Using an FVB background wildtype, we plan on establishing both a moderate (*Smn*^{-/-}; *SMN2*^{+/+}), and severe (*Smn*^{-/-}; *SMN2*^{+/-}) SMA mice to test our ASOs on. We plan on testing PMO 7 to evaluate the efficacy of a 30 bp PMO sequence, as well as PMO 9 for comparison because its sequence is currently in human clinical trials in the 2'MOE chemistry. We will also test LNA 1, 3 and 5 to evaluate which is most effective at ameliorating the SMA phenotype in the mice, as currently no mouse experiments containing LNA/DNA mixmers have been published. Although longer ASOs are more effective *in vitro* based on my results, they may not be able to compete with shorter ASOs *in vivo*. In both animal trials and human clinical trials, ASOs are injected at

molecular weight per bodyweight of the subject rather than molarity, so shorter ASOs will effectively have more functional units than longer ASOs.

To evaluate the ASO efficacy we will compare life span of treated versus non-treated mice using the Kaplan-Meier survival analysis. We will also perform functional analysis such as grip strength test, rotarod, and up-right test. Molecular analysis will be done to evaluate the formation of neuromuscular junctions, as they are not well developed in SMA mice, along with Western blot analysis to check for SMN protein “knock-up”. Though it is still uncertain what amount of SMN protein is needed to derive a normal phenotype, however, a recent mouse study revealed that as little as 50% recovery led to proper muscle development (Iyer *et al.* 2015). Just as with the SMA disease phenotype, the treatment effects may have a wide spectrum where different amounts of SMN recovery may be beneficial to some but not for others.

In summary, I have identified several novel ASOs capable of restoring exon 7 inclusion and increasing full-length SMN protein production in SMA patient cell lines. In the future my lab will test these ASOs *in vivo* in both a moderate and severe mouse line to determine if they can prevent symptoms or even restore a healthy phenotype in these mice. Based on the preclinical *in vivo* results, I hope to implement our drugs for testing in human clinical trials to potentially be a safer and more effective alternative to drugs currently undergoing investigation.

REFERENCES

- Akten, B., Kye, M. J., Hao le, T., Wertz, M. H., Singh, S., Nie, D., . . . Sahin, M. (2011). Interaction of survival of motor neuron (SMN) and HuD proteins with mRNA cpg15 rescues motor neuron axonal deficits. *Proc Natl Acad Sci U S A*, *108*(25), 10337-10342. doi: 10.1073/pnas.1104928108
- Amantana, A., & Iversen, P. L. (2005). Pharmacokinetics and biodistribution of phosphorodiamidate morpholino antisense oligomers. *Curr Opin Pharmacol*, *5*(5), 550-555. doi: 10.1016/j.coph.2005.07.001
- Avila, A. M., Burnett, B. G., Taye, A. A., Gabanella, F., Knight, M. A., Hartenstein, P., . . . Sumner, C. J. (2007). Trichostatin A increases SMN expression and survival in a mouse model of spinal muscular atrophy. *J Clin Invest*, *117*(3), 659-671. doi: 10.1172/JCI29562
- Baccon, J., Pellizzoni, L., Rappsilber, J., Mann, M., & Dreyfuss, G. (2002). Identification and characterization of Gemin7, a novel component of the survival of motor neuron complex. *J Biol Chem*, *277*(35), 31957-31962. doi: 10.1074/jbc.M203478200
- Badros, A. Z., Goloubeva, O., Rapoport, A. P., Ratterree, B., Gahres, N., Meisenberg, B., . . . Fenton, R. G. (2005). Phase II study of G3139, a Bcl-2 antisense oligonucleotide, in combination with dexamethasone and thalidomide in relapsed multiple myeloma patients. *J Clin Oncol*, *23*(18), 4089-4099. doi: 10.1200/JCO.2005.14.381
- Baioni, M. T., & Ambiel, C. R. (2010). Spinal muscular atrophy: diagnosis, treatment and future prospects. *J Pediatr (Rio J)*, *86*(4), 261-270. doi: doi:10.2223/JPED.1988
- Battle, D. J., Kasim, M., Yong, J., Lotti, F., Lau, C. K., Mouaikel, J., . . . Dreyfuss, G. (2006). The SMN complex: an assembly machine for RNPs. *Cold Spring Harb Symp Quant Biol*, *71*, 313-320. doi: 10.1101/sqb.2006.71.001

- Baughan, T. D., Dickson, A., Osman, E. Y., & Lorson, C. L. (2009). Delivery of bifunctional RNAs that target an intronic repressor and increase SMN levels in an animal model of spinal muscular atrophy. *Hum Mol Genet*, *18*(9), 1600-1611. doi: 10.1093/hmg/ddp076
- Bo, X., & Wang, S. (2005). TargetFinder: a software for antisense oligonucleotide target site selection based on MAST and secondary structures of target mRNA. *Bioinformatics*, *21*(8), 1401-1402. doi: 10.1093/bioinformatics/bti211
- Brkusanin, M., Kosac, A., Jovanovic, V., Pesovic, J., Brajuskovic, G., Dimitrijevic, N., . . . Savic-Pavicevic, D. (2015). Joint effect of the SMN2 and SERF1A genes on childhood-onset types of spinal muscular atrophy in Serbian patients. *J Hum Genet*, *60*(11), 723-728. doi: 10.1038/jhg.2015.104
- Buhler, D., Raker, V., Luhrmann, R., & Fischer, U. (1999). Essential role for the tudor domain of SMN in spliceosomal U snRNP assembly: implications for spinal muscular atrophy. *Hum Mol Genet*, *8*(13), 2351-2357.
- Cali, F., Ruggeri, G., Chiavetta, V., Scuderi, C., Bianca, S., Barone, C., . . . Musumeci, S. (2014). Carrier screening for spinal muscular atrophy in Italian population. *J Genet*, *93*(1), 179-181.
- Cantarero, L., Sanz-Garcia, M., Vinograd-Byk, H., Renbaum, P., Levy-Lahad, E., & Lazo, P. A. (2015). VPK1 regulates Cajal body dynamics and protects coilin from proteasomal degradation in cell cycle. *Sci Rep*, *5*, 10543. doi: 10.1038/srep10543
- Carre, A., & Empey, C. (2016). Review of Spinal Muscular Atrophy (SMA) for Prenatal and Pediatric Genetic Counselors. *J Genet Couns*, *25*(1), 32-43. doi: 10.1007/s10897-015-9859-z

- Cartegni, L., & Krainer, A. R. (2002). Disruption of an SF2/ASF-dependent exonic splicing enhancer in SMN2 causes spinal muscular atrophy in the absence of SMN1. *Nat Genet*, 30(4), 377-384. doi: 10.1038/ng854
- Chan, J. H., Lim, S., & Wong, W. S. (2006). Antisense oligonucleotides: from design to therapeutic application. *Clin Exp Pharmacol Physiol*, 33(5-6), 533-540. doi: 10.1111/j.1440-1681.2006.04403.x
- Charroux, B., Pellizzoni, L., Perkinson, R. A., Shevchenko, A., Mann, M., & Dreyfuss, G. (1999). Gemin3: A novel DEAD box protein that interacts with SMN, the spinal muscular atrophy gene product, and is a component of gems. *J Cell Biol*, 147(6), 1181-1194.
- Crooke, S. T. (2000). Progress in antisense technology: the end of the beginning. *Methods Enzymol*, 313, 3-45.
- Crooke, S. T. (2004). Progress in antisense technology. *Annu Rev Med*, 55, 61-95. doi: 10.1146/annurev.med.55.091902.104408
- Darras, B. T. (2015). Spinal muscular atrophies. *Pediatr Clin North Am*, 62(3), 743-766. doi: 10.1016/j.pcl.2015.03.010
- Deyle, D. R., & Russell, D. W. (2009). Adeno-associated virus vector integration. *Curr Opin Mol Ther*, 11(4), 442-447.
- Dominguez, E., Marais, T., Chatauret, N., Benkhalifa-Ziyyat, S., Duque, S., Ravassard, P., . . . Barkats, M. (2011). Intravenous scAAV9 delivery of a codon-optimized SMN1 sequence rescues SMA mice. *Hum Mol Genet*, 20(4), 681-693. doi: 10.1093/hmg/ddq514

- Ebert, A. D., Yu, J., Rose, F. F., Jr., Mattis, V. B., Lorson, C. L., Thomson, J. A., & Svendsen, C. N. (2009). Induced pluripotent stem cells from a spinal muscular atrophy patient. *Nature*, *457*(7227), 277-280. doi: 10.1038/nature07677
- Eckstein, F. (2000). Phosphorothioate oligodeoxynucleotides: what is their origin and what is unique about them? *Antisense Nucleic Acid Drug Dev*, *10*(2), 117-121. doi: 10.1089/oli.1.2000.10.117
- Enwerem, II, Wu, G., Yu, Y. T., & Hebert, M. D. (2015). Cajal body proteins differentially affect the processing of box C/D scaRNPs. *PLoS One*, *10*(4), e0122348. doi: 10.1371/journal.pone.0122348
- Etzerodt, M., Vignali, R., Ciliberto, G., Scherly, D., Mattaj, I. W., & Philipson, L. (1988). Structure and expression of a *Xenopus* gene encoding an snRNP protein (U1 70K). *EMBO J*, *7*(13), 4311-4321.
- Fallini, C., Bassell, G. J., & Rossoll, W. (2012). Spinal muscular atrophy: the role of SMN in axonal mRNA regulation. *Brain Res*, *1462*, 81-92. doi: 10.1016/j.brainres.2012.01.044
- Fallini, C., Zhang, H., Su, Y., Silani, V., Singer, R. H., Rossoll, W., & Bassell, G. J. (2011). The survival of motor neuron (SMN) protein interacts with the mRNA-binding protein HuD and regulates localization of poly(A) mRNA in primary motor neuron axons. *J Neurosci*, *31*(10), 3914-3925. doi: 10.1523/JNEUROSCI.3631-10.2011
- Fan, L., & Simard, L. R. (2002). Survival motor neuron (SMN) protein: role in neurite outgrowth and neuromuscular maturation during neuronal differentiation and development. *Hum Mol Genet*, *11*(14), 1605-1614.

- Fischer, U., Liu, Q., & Dreyfuss, G. (1997). The SMN-SIP1 complex has an essential role in spliceosomal snRNP biogenesis. *Cell*, *90*(6), 1023-1029.
- Fletcher, S., Honeyman, K., Fall, A. M., Harding, P. L., Johnsen, R. D., Steinhaus, J. P., . . . Wilton, S. D. (2007). Morpholino oligomer-mediated exon skipping averts the onset of dystrophic pathology in the mdx mouse. *Mol Ther*, *15*(9), 1587-1592. doi: 10.1038/sj.mt.6300245
- Gall, J. G., Bellini, M., Wu, Z., & Murphy, C. (1999). Assembly of the nuclear transcription and processing machinery: Cajal bodies (coiled bodies) and transcriptosomes. *Mol Biol Cell*, *10*(12), 4385-4402.
- Ganji, H., Nouri, N., Salehi, M., Aryani, O., Houshmand, M., Basiri, K., . . . Sedghi, M. (2015). Detection of intragenic SMN1 mutations in spinal muscular atrophy patients with a single copy of SMN1. *J Child Neurol*, *30*(5), 558-562. doi: 10.1177/0883073814521297
- Garbes, L., Riessland, M., Holker, I., Heller, R., Hauke, J., Trankle, C., . . . Wirth, B. (2009). LBH589 induces up to 10-fold SMN protein levels by several independent mechanisms and is effective even in cells from SMA patients non-responsive to valproate. *Hum Mol Genet*, *18*(19), 3645-3658. doi: 10.1093/hmg/ddp313
- Gray, K., Isaacs, D., Kilham, H. A., & Tobin, B. (2013). Spinal muscular atrophy type I: do the benefits of ventilation compensate for its burdens? *J Paediatr Child Health*, *49*(10), 807-812. doi: 10.1111/jpc.12386
- Gubitz, A. K., Mourelatos, Z., Abel, L., Rappsilber, J., Mann, M., & Dreyfuss, G. (2002). Gemin5, a novel WD repeat protein component of the SMN complex that binds Sm proteins. *J Biol Chem*, *277*(7), 5631-5636. doi: 10.1074/jbc.M109448200

- Hamm, J., Darzynkiewicz, E., Tahara, S. M., & Mattaj, I. W. (1990). The trimethylguanosine cap structure of U1 snRNA is a component of a bipartite nuclear targeting signal. *Cell*, *62*(3), 569-577.
- Harada, Y., Sutomo, R., Sadewa, A. H., Akutsu, T., Takeshima, Y., Wada, H., . . . Nishio, H. (2002). Correlation between SMN2 copy number and clinical phenotype of spinal muscular atrophy: three SMN2 copies fail to rescue some patients from the disease severity. *J Neurol*, *249*(9), 1211-1219. doi: 10.1007/s00415-002-0811-4
- Hedlund, E. (2011). The protective effects of beta-lactam antibiotics in motor neuron disorders. *Exp Neurol*, *231*(1), 14-18. doi: 10.1016/j.expneurol.2011.06.002
- Hsieh-Li, H. M., Chang, J. G., Jong, Y. J., Wu, M. H., Wang, N. M., Tsai, C. H., & Li, H. (2000). A mouse model for spinal muscular atrophy. *Nat Genet*, *24*(1), 66-70. doi: 10.1038/71709
- Hua, Y., Sahashi, K., Rigo, F., Hung, G., Horev, G., Bennett, C. F., & Krainer, A. R. (2011). Peripheral SMN restoration is essential for long-term rescue of a severe spinal muscular atrophy mouse model. *Nature*, *478*(7367), 123-126. doi: 10.1038/nature10485
- Hua, Y., Vickers, T. A., Baker, B. F., Bennett, C. F., & Krainer, A. R. (2007). Enhancement of SMN2 exon 7 inclusion by antisense oligonucleotides targeting the exon. *PLoS Biol*, *5*(4), e73. doi: 10.1371/journal.pbio.0050073
- Hubers, L., Valderrama-Carvajal, H., Laframboise, J., Timbers, J., Sanchez, G., & Cote, J. (2011). HuD interacts with survival motor neuron protein and can rescue spinal muscular atrophy-like neuronal defects. *Hum Mol Genet*, *20*(3), 553-579. doi: 10.1093/hmg/ddq500

- Iyer, C. C., McGovern, V. L., Murray, J. D., Gombash, S. E., Zaworski, P. G., Foust, K. D., . . . Burghes, A. H. (2015). Low levels of Survival Motor Neuron protein are sufficient for normal muscle function in the SMNDelta7 mouse model of SMA. *Hum Mol Genet*, *24*(21), 6160-6173. doi: 10.1093/hmg/ddv332
- Jady, B. E., Richard, P., Bertrand, E., & Kiss, T. (2006). Cell cycle-dependent recruitment of telomerase RNA and Cajal bodies to human telomeres. *Mol Biol Cell*, *17*(2), 944-954. doi: 10.1091/mbc.E05-09-0904
- Jepsen, J. S., Sorensen, M. D., & Wengel, J. (2004). Locked nucleic acid: a potent nucleic acid analog in therapeutics and biotechnology. *Oligonucleotides*, *14*(2), 130-146. doi: 10.1089/1545457041526317
- Kashima, T., & Manley, J. L. (2003). A negative element in SMN2 exon 7 inhibits splicing in spinal muscular atrophy. *Nat Genet*, *34*(4), 460-463. doi: 10.1038/ng1207
- Kolb, S. J., Battle, D. J., & Dreyfuss, G. (2007). Molecular functions of the SMN complex. *J Child Neurol*, *22*(8), 990-994. doi: 10.1177/0883073807305666
- Kroiss, M., Schultz, J., Wiesner, J., Chari, A., Sickmann, A., & Fischer, U. (2008). Evolution of an RNP assembly system: a minimal SMN complex facilitates formation of UsnRNPs in *Drosophila melanogaster*. *Proc Natl Acad Sci U S A*, *105*(29), 10045-10050. doi: 10.1073/pnas.0802287105
- Kurreck, J. (2003). Antisense technologies. Improvement through novel chemical modifications. *Eur J Biochem*, *270*(8), 1628-1644.
- Kurreck, J., Wyszko, E., Gillen, C., & Erdmann, V. A. (2002). Design of antisense oligonucleotides stabilized by locked nucleic acids. *Nucleic Acids Res*, *30*(9), 1911-1918.

- Lafarga, M., Casafont, I., Bengoechea, R., Tapia, O., & Berciano, M. T. (2009). Cajal's contribution to the knowledge of the neuronal cell nucleus. *Chromosoma*, *118*(4), 437-443. doi: 10.1007/s00412-009-0212-x
- Lee, J. J., & Yokota, T. (2013). Antisense therapy in neurology. *J Pers Med*, *3*(3), 144-176. doi: 10.3390/jpm3030144
- Li, D. K., Tisdale, S., Lotti, F., & Pellizzoni, L. (2014). SMN control of RNP assembly: from post-transcriptional gene regulation to motor neuron disease. *Semin Cell Dev Biol*, *32*, 22-29. doi: 10.1016/j.semcdb.2014.04.026
- Liang, X. H., Liu, L., & Michaeli, S. (2001). Identification of the first trypanosome H/ACA RNA that guides pseudouridine formation on rRNA. *J Biol Chem*, *276*(43), 40313-40318. doi: 10.1074/jbc.M104488200
- Liu, Q., & Dreyfuss, G. (1996). A novel nuclear structure containing the survival of motor neurons protein. *EMBO J*, *15*(14), 3555-3565.
- Mann, C. J., Honeyman, K., McClorey, G., Fletcher, S., & Wilton, S. D. (2002). Improved antisense oligonucleotide induced exon skipping in the mdx mouse model of muscular dystrophy. *J Gene Med*, *4*(6), 644-654. doi: 10.1002/jgm.295
- Mattis, V. B., Rai, R., Wang, J., Chang, C. W., Coady, T., & Lorson, C. L. (2006). Novel aminoglycosides increase SMN levels in spinal muscular atrophy fibroblasts. *Hum Genet*, *120*(4), 589-601. doi: 10.1007/s00439-006-0245-7
- McWhorter, M. L., Monani, U. R., Burghes, A. H., & Beattie, C. E. (2003). Knockdown of the survival motor neuron (Smn) protein in zebrafish causes defects in motor axon outgrowth and pathfinding. *J Cell Biol*, *162*(5), 919-931. doi: 10.1083/jcb.200303168

- Meister, G., Eggert, C., Buhler, D., Brahms, H., Kambach, C., & Fischer, U. (2001). Methylation of Sm proteins by a complex containing PRMT5 and the putative U snRNP assembly factor pICln. *Curr Biol*, *11*(24), 1990-1994.
- Meister, G., Eggert, C., & Fischer, U. (2002). SMN-mediated assembly of RNPs: a complex story. *Trends Cell Biol*, *12*(10), 472-478.
- Mendell, J. R., Goemans, N., Lowes, L. P., Alfano, L. N., Berry, K., Shao, J., . . . Telethon Foundation, D. M. D. I. N. (2016). Longitudinal effect of eteplirsen versus historical control on ambulation in Duchenne muscular dystrophy. *Ann Neurol*, *79*(2), 257-271. doi: 10.1002/ana.24555
- Menke, L. A., Poll-The, B. T., Clur, S. A., Bilardo, C. M., van der Wal, A. C., Lemmink, H. H., & Cobben, J. M. (2008). Congenital heart defects in spinal muscular atrophy type I: a clinical report of two siblings and a review of the literature. *Am J Med Genet A*, *146A*(6), 740-744. doi: 10.1002/ajmg.a.32233
- Miyajima, H., Miyaso, H., Okumura, M., Kurisu, J., & Imaizumi, K. (2002). Identification of a cis-acting element for the regulation of SMN exon 7 splicing. *J Biol Chem*, *277*(26), 23271-23277. doi: 10.1074/jbc.M200851200
- Monani, U. R. (2005). Spinal muscular atrophy: a deficiency in a ubiquitous protein; a motor neuron-specific disease. *Neuron*, *48*(6), 885-896. doi: 10.1016/j.neuron.2005.12.001
- Monani (1), U. R., Coover, D. D., & Burghes, A. H. (2000). Animal models of spinal muscular atrophy. *Hum Mol Genet*, *9*(16), 2451-2457.
- Monani (2), U. R., Sendtner, M., Coover, D. D., Parsons, D. W., Andreassi, C., Le, T. T., . . . Burghes, A. H. (2000). The human centromeric survival motor neuron gene (SMN2)

- rescues embryonic lethality in *Smn(-/-)* mice and results in a mouse with spinal muscular atrophy. *Hum Mol Genet*, 9(3), 333-339.
- Moosa, A., & Dubowitz, V. (1973). Spinal muscular atrophy in childhood. Two clues to clinical diagnosis. *Arch Dis Child*, 48(5), 386-388.
- Narver, H. L., Kong, L., Burnett, B. G., Choe, D. W., Bosch-Marce, M., Taye, A. A., . . . Sumner, C. J. (2008). Sustained improvement of spinal muscular atrophy mice treated with trichostatin A plus nutrition. *Ann Neurol*, 64(4), 465-470. doi: 10.1002/ana.21449
- Naryshkin, N. A., Weetall, M., Dakka, A., Narasimhan, J., Zhao, X., Feng, Z., . . . Metzger, F. (2014). Motor neuron disease. SMN2 splicing modifiers improve motor function and longevity in mice with spinal muscular atrophy. *Science*, 345(6197), 688-693. doi: 10.1126/science.1250127
- Nelson, M. H., Stein, D. A., Kroeker, A. D., Hatlevig, S. A., Iversen, P. L., & Moulton, H. M. (2005). Arginine-rich peptide conjugation to morpholino oligomers: effects on antisense activity and specificity. *Bioconjug Chem*, 16(4), 959-966. doi: 10.1021/bc0501045
- Nizzardo, M., Simone, C., Salani, S., Ruepp, M. D., Rizzo, F., Ruggieri, M., . . . Corti, S. (2014). Effect of combined systemic and local morpholino treatment on the spinal muscular atrophy Delta7 mouse model phenotype. *Clin Ther*, 36(3), 340-356 e345. doi: 10.1016/j.clinthera.2014.02.004
- Ogg, S. C., & Lamond, A. I. (2002). Cajal bodies and coilin--moving towards function. *J Cell Biol*, 159(1), 17-21. doi: 10.1083/jcb.200206111
- Osman, E. Y., Miller, M. R., Robbins, K. L., Lombardi, A. M., Atkinson, A. K., Brehm, A. J., & Lorson, C. L. (2014). Morpholino antisense oligonucleotides targeting intronic repressor

- Element1 improve phenotype in SMA mouse models. *Hum Mol Genet*, 23(18), 4832-4845. doi: 10.1093/hmg/ddu198
- Passini, M. A., Bu, J., Roskelley, E. M., Richards, A. M., Sardi, S. P., O'Riordan, C. R., . . . Cheng, S. H. (2010). CNS-targeted gene therapy improves survival and motor function in a mouse model of spinal muscular atrophy. *J Clin Invest*, 120(4), 1253-1264. doi: 10.1172/JCI41615
- Paushkin, S., Gubitz, A. K., Massenet, S., & Dreyfuss, G. (2002). The SMN complex, an assemblysome of ribonucleoproteins. *Curr Opin Cell Biol*, 14(3), 305-312.
- Pedrotti, S., Bielli, P., Paronetto, M. P., Ciccocanti, F., Fimia, G. M., Stamm, S., . . . Sette, C. (2010). The splicing regulator Sam68 binds to a novel exonic splicing silencer and functions in SMN2 alternative splicing in spinal muscular atrophy. *EMBO J*, 29(7), 1235-1247. doi: 10.1038/emboj.2010.19
- Pellizzoni, L. (2007). Chaperoning ribonucleoprotein biogenesis in health and disease. *EMBO Rep*, 8(4), 340-345. doi: 10.1038/sj.embor.7400941
- Pellizzoni, L., Charroux, B., Rappsilber, J., Mann, M., & Dreyfuss, G. (2001). A functional interaction between the survival motor neuron complex and RNA polymerase II. *J Cell Biol*, 152(1), 75-85.
- Pellizzoni, L., Yong, J., & Dreyfuss, G. (2002). Essential role for the SMN complex in the specificity of snRNP assembly. *Science*, 298(5599), 1775-1779. doi: 10.1126/science.1074962

- Porensky, P. N., Mitrpant, C., McGovern, V. L., Bevan, A. K., Foust, K. D., Kaspar, B. K., . . . Burghes, A. H. (2012). A single administration of morpholino antisense oligomer rescues spinal muscular atrophy in mouse. *Hum Mol Genet*, *21*(7), 1625-1638. doi: 10.1093/hmg/ddr600
- Prior, T. W., Snyder, P. J., Rink, B. D., Pearl, D. K., Pyatt, R. E., Mihal, D. C., . . . Garner, S. (2010). Newborn and carrier screening for spinal muscular atrophy. *Am J Med Genet A*, *152A*(7), 1608-1616. doi: 10.1002/ajmg.a.33474
- Raker, V. A., Hartmuth, K., Kastner, B., & Luhrmann, R. (1999). Spliceosomal U snRNP core assembly: Sm proteins assemble onto an Sm site RNA nonanucleotide in a specific and thermodynamically stable manner. *Mol Cell Biol*, *19*(10), 6554-6565.
- Riessland, M., Ackermann, B., Forster, A., Jakubik, M., Hauke, J., Garbes, L., . . . Wirth, B. (2010). SAHA ameliorates the SMA phenotype in two mouse models for spinal muscular atrophy. *Hum Mol Genet*, *19*(8), 1492-1506. doi: 10.1093/hmg/ddq023
- Rochette, C. F., Gilbert, N., & Simard, L. R. (2001). SMN gene duplication and the emergence of the SMN2 gene occurred in distinct hominids: SMN2 is unique to Homo sapiens. *Hum Genet*, *108*(3), 255-266.
- Rose, F. F., Jr., Mattis, V. B., Rindt, H., & Lorson, C. L. (2009). Delivery of recombinant follistatin lessens disease severity in a mouse model of spinal muscular atrophy. *Hum Mol Genet*, *18*(6), 997-1005. doi: 10.1093/hmg/ddn426
- Rossoll, W., & Bassell, G. J. (2009). Spinal muscular atrophy and a model for survival of motor neuron protein function in axonal ribonucleoprotein complexes. *Results Probl Cell Differ*, *48*, 289-326. doi: 10.1007/400_2009_4

- Rossoll, W., Jablonka, S., Andreassi, C., Kroning, A. K., Karle, K., Monani, U. R., & Sendtner, M. (2003). Smn, the spinal muscular atrophy-determining gene product, modulates axon growth and localization of beta-actin mRNA in growth cones of motoneurons. *J Cell Biol*, *163*(4), 801-812. doi: 10.1083/jcb.200304128
- Russman, B. S. (2007). Spinal muscular atrophy: clinical classification and disease heterogeneity. *J Child Neurol*, *22*(8), 946-951. doi: 10.1177/0883073807305673
- Samarsky, D. A., Fournier, M. J., Singer, R. H., & Bertrand, E. (1998). The snoRNA box C/D motif directs nucleolar targeting and also couples snoRNA synthesis and localization. *EMBO J*, *17*(13), 3747-3757. doi: 10.1093/emboj/17.13.3747
- Satkauskas, S., & Bagnard, D. (2007). Local protein synthesis in axonal growth cones: what is next? *Cell Adh Migr*, *1*(4), 179-184.
- Saugier-veber, P., Drouot, N., Lefebvre, S., Charbonnier, F., Vial, E., Munnich, A., & Frebourg, T. (2001). Detection of heterozygous SMN1 deletions in SMA families using a simple fluorescent multiplex PCR method. *J Med Genet*, *38*(4), 240-243.
- Selenko, P., Sprangers, R., Stier, G., Buhler, D., Fischer, U., & Sattler, M. (2001). SMN tudor domain structure and its interaction with the Sm proteins. *Nat Struct Biol*, *8*(1), 27-31. doi: 10.1038/83014
- Shimo, T., Tachibana, K., Saito, K., Yoshida, T., Tomita, E., Waki, R., . . . Obika, S. (2014). Design and evaluation of locked nucleic acid-based splice-switching oligonucleotides in vitro. *Nucleic Acids Res*, *42*(12), 8174-8187. doi: 10.1093/nar/gku512

- Shpargel, K. B., & Matera, A. G. (2005). Gemin proteins are required for efficient assembly of Sm-class ribonucleoproteins. *Proc Natl Acad Sci U S A*, *102*(48), 17372-17377. doi: 10.1073/pnas.0508947102
- Singh, N. K., Singh, N. N., Androphy, E. J., & Singh, R. N. (2006). Splicing of a critical exon of human Survival Motor Neuron is regulated by a unique silencer element located in the last intron. *Mol Cell Biol*, *26*(4), 1333-1346. doi: 10.1128/MCB.26.4.1333-1346.2006
- Singh, N. N., Hollinger, K., Bhattacharya, D., & Singh, R. N. (2010). An antisense microwalk reveals critical role of an intronic position linked to a unique long-distance interaction in pre-mRNA splicing. *RNA*, *16*(6), 1167-1181. doi: 10.1261/rna.2154310
- Singh, N. N., Shishimorova, M., Cao, L. C., Gangwani, L., & Singh, R. N. (2009). A short antisense oligonucleotide masking a unique intronic motif prevents skipping of a critical exon in spinal muscular atrophy. *RNA Biol*, *6*(3), 341-350.
- Sotelo-Silveira, J. R., Calliari, A., Kun, A., Koenig, E., & Sotelo, J. R. (2006). RNA trafficking in axons. *Traffic*, *7*(5), 508-515. doi: 10.1111/j.1600-0854.2006.00405.x
- Sun, X., Marque, L. O., Corder, Z., Pruitt, J. L., Bhat, M., Li, P. P., . . . Rudnicki, D. D. (2014). Phosphorodiamidate morpholino oligomers suppress mutant huntingtin expression and attenuate neurotoxicity. *Hum Mol Genet*, *23*(23), 6302-6317. doi: 10.1093/hmg/ddu349
- Swanger, S. A., & Bassell, G. J. (2011). Making and breaking synapses through local mRNA regulation. *Curr Opin Genet Dev*, *21*(4), 414-421. doi: 10.1016/j.gde.2011.04.002
- Terns, M. P., & Terns, R. M. (2001). Macromolecular complexes: SMN--the master assembler. *Curr Biol*, *11*(21), R862-864.

- Touznik, A., Lee, J. J., & Yokota, T. (2014). New developments in exon skipping and splice modulation therapies for neuromuscular diseases. *Expert Opin Biol Ther*, *14*(6), 809-819. doi: 10.1517/14712598.2014.896335
- Tsuiji, H., Iguchi, Y., Furuya, A., Kataoka, A., Hatsuta, H., Atsuta, N., . . . Yamanaka, K. (2013). Spliceosome integrity is defective in the motor neuron diseases ALS and SMA. *EMBO Mol Med*, *5*(2), 221-234. doi: 10.1002/emmm.201202303
- Vester, B., & Wengel, J. (2004). LNA (locked nucleic acid): high-affinity targeting of complementary RNA and DNA. *Biochemistry*, *43*(42), 13233-13241. doi: 10.1021/bi0485732
- von Gontard, A., Zerres, K., Backes, M., Laufersweiler-Plass, C., Wendland, C., Melchers, P., . . . Rudnik-Schoneborn, S. (2002). Intelligence and cognitive function in children and adolescents with spinal muscular atrophy. *Neuromuscul Disord*, *12*(2), 130-136.
- Wan, L., Battle, D. J., Yong, J., Gubitza, A. K., Kolb, S. J., Wang, J., & Dreyfuss, G. (2005). The survival of motor neurons protein determines the capacity for snRNP assembly: biochemical deficiency in spinal muscular atrophy. *Mol Cell Biol*, *25*(13), 5543-5551. doi: 10.1128/MCB.25.13.5543-5551.2005
- Wang, D. O., Martin, K. C., & Zukin, R. S. (2010). Spatially restricting gene expression by local translation at synapses. *Trends Neurosci*, *33*(4), 173-182. doi: 10.1016/j.tins.2010.01.005
- Wang, H. Y., Yang, Y. H., & Jong, Y. J. (2013). Correlations between change scores of measures for muscle strength and motor function in individuals with spinal muscular atrophy types 2 and 3. *Am J Phys Med Rehabil*, *92*(4), 335-342.

- Warfield, K. L., Swenson, D. L., Olinger, G. G., Nichols, D. K., Pratt, W. D., Blouch, R., . . . Bavari, S. (2006). Gene-specific countermeasures against Ebola virus based on antisense phosphorodiamidate morpholino oligomers. *PLoS Pathog*, *2*(1), e1. doi: 10.1371/journal.ppat.0020001
- Weinstein, L. B., & Steitz, J. A. (1999). Guided tours: from precursor snoRNA to functional snoRNP. *Curr Opin Cell Biol*, *11*(3), 378-384. doi: 10.1016/S0955-0674(99)80053-2
- Will, C. L., & Luhrmann, R. (2001). Spliceosomal UsnRNP biogenesis, structure and function. *Curr Opin Cell Biol*, *13*(3), 290-301.
- Wirth, B., Brichta, L., Schrank, B., Lochmuller, H., Blick, S., Baasner, A., & Heller, R. (2006). Mildly affected patients with spinal muscular atrophy are partially protected by an increased SMN2 copy number. *Hum Genet*, *119*(4), 422-428. doi: 10.1007/s00439-006-0156-7
- Wu, H., Lima, W. F., Zhang, H., Fan, A., Sun, H., & Crooke, S. T. (2004). Determination of the role of the human RNase H1 in the pharmacology of DNA-like antisense drugs. *J Biol Chem*, *279*(17), 17181-17189. doi: 10.1074/jbc.M311683200
- Zerres, K., & Davies, K. E. (1999). 59th ENMC International Workshop: Spinal Muscular Atrophies: recent progress and revised diagnostic criteria 17-19 April 1998, Soestduinen, The Netherlands. *Neuromuscul Disord*, *9*(4), 272-278.
- Zerres, K., Rudnik-Schoneborn, S., Forrest, E., Lusakowska, A., Borkowska, J., & Hausmanowa-Petrusewicz, I. (1997). A collaborative study on the natural history of childhood and juvenile onset proximal spinal muscular atrophy (type II and III SMA): 569 patients. *J Neurol Sci*, *146*(1), 67-72.

Zhang, Z., Lotti, F., Dittmar, K., Younis, I., Wan, L., Kasim, M., & Dreyfuss, G. (2008). SMN deficiency causes tissue-specific perturbations in the repertoire of snRNAs and widespread defects in splicing. *Cell*, *133*(4), 585-600. doi: 10.1016/j.cell.2008.03.031

Zhou, H., Janghra, N., Mitrapant, C., Dickinson, R. L., Anthony, K., Price, L., . . . Muntoni, F. (2013). A novel morpholino oligomer targeting ISS-N1 improves rescue of severe spinal muscular atrophy transgenic mice. *Hum Gene Ther*, *24*(3), 331-342. doi: 10.1089/hum.2012.211

Zhou, H., Meng, J., Marrosu, E., Janghra, N., Morgan, J., & Muntoni, F. (2015). Repeated low doses of morpholino antisense oligomer: an intermediate mouse model of spinal muscular atrophy to explore the window of therapeutic response. *Hum Mol Genet*, *24*(22), 6265-6277. doi: 10.1093/hmg/ddv329